DEVELOPMENT OF A MEMS DEVICE TO CONTINUOUSLY MONITOR GLAUCOMA

By
Smitha Shankar

Submitted for fulfilment of degree
in Masters of Engineering by Research

RMIT University
SET Portfolio
School of Electrical and Computer Engineering

March 2006

DECLARATION

To the best of my knowledge, all work appearing in this dissertation, except for that which has been duly acknowledged, is that of the candidate alone. This work has not been submitted previously, in whole part, to qualify for any other academic award. The content of this thesis is the result of the work that has been completed since the official commencement date of the approved research program. Any editorial work, carried out by a third party, has been duly acknowledged.

Smitha Shankar

Title: DEVELOPMENT OF A MEMS DEVICE TO CONTINUOUSLY MONITOR GLAUCOMA

Author: Smitha Shankar

Summary of Thesis

This thesis investigates the development of a MEMS (microelectromechanical system) device which can be implanted in the eye to continuously monitor glaucoma conditions. The thesis commences with a brief introduction to glaucoma and the problems associated with current treatment methods. A mathematical model of the intraocular pressure (IOP) dynamics of the eye is then used to analyse how IOP measurements could be utilised to internally indicate a change in the level of severity of glaucoma using a MEMS device. Finite element method analyses are then used to determine the electro-mechanical requirements of a MEMS pressure sensor that would be capable of continuously monitoring glaucoma from within the eye. The results from both the investigations are then combined mathematically in a model to estimate the electronic response that would be obtained from an implantable micro system comprising a MEMS device to increase the pressure within the eye, a pressure sensor and processing electronics. The mathematical model of the micro system was tested for normal and adverse operating conditions to estimate the output corresponding to various levels of IOP in a person's eye. An overview of the powering, fabrication, biocompatibility and packaging details of the MEMS glaucoma monitoring system has also been provided in the thesis. Finally, it is concluded that it will be possible to monitor glaucoma continuously from within the eye using a MEMS device.

“This thesis is dedicated to the loving memories of my mother Dr. V. Sneha Latha and my brother Ashwin”.

- Smitha.

ACKNOWLEDGEMENTS

I wish to thank my family for the support and encouragement they have provided me with since the time I begun my Masters. I was accepted into the School of Electrical and Computer Engineering at RMIT University as a Masters (Research) student in July 2003.

I would like to thank Prof. Ian Bates for having provided me with the opportunity for working on this exciting MEMS project. Dr. Jason Chaffey was appointed as my second supervisor when I started on the project, he has since remained a great source of help and encouragement and his support and interest in my project have continued even after he relocated to Adelaide in 2004. Prof. Mike Austin was appointed as my first supervisor by the school. He has helped me tremendously with my writing, has been extremely cooperative and offered me his assistance and support at all times.

I have been a part of the AECM team headed by Prof. Ian Bates, since I started and have benefited greatly by his guidance, support and vision for my project. Working with him has been a very enriching and rewarding experience. I cannot thank Lynda Gilbert enough for her patience and all the assistance she has provided me with over the last two years. My team members Sanchitha Fernando and Tim Walker have been extremely generous with their time and have made significant technical contributions to my work. Andrej Mikhailovsjki, Manvinder Singh, Dr Arun Sharma, Keerthy Silva, Xing Liu, Lu Miao, Zhong Li, Surendran Devadoss and Dr Vijaya Mathe, the remaining AECM team members and the ones before them have all been very friendly and helpful during my time here. A special word of thanks to Dr.Arvind Sinha and Axel Schauenburg, Sir Lawrence Wackett Centre, Aerospace and Systems Engineering, RMIT and to Miss Kesha Rana and Mr Daud Channa for their support. I will always cherish the friendships that have been formed and the time spent at RMIT.

ABSTRACT

The objective of this thesis was to investigate the development of microelectromechanical system (MEMS) which can be implanted in the eye to provide continuous monitoring of glaucoma conditions. Current glaucoma monitoring involves taking laboratory based intra ocular pressure (IOP) measurements. The measurement of intraocular fluid flow and IOP parameters related to blockage formation in the eye require to be continuously monitored in Glaucoma. Making blockage related information available to patients could indicate the conditions leading to a blockage and help to improve glaucoma treatment and reduce the risk of permanent blindness.

The specific aim of this research was to develop an implantable micro device capable of responding to the blockage of fluid flow in the eye. A mathematical model of the IOP dynamics in the eye, incorporating the IOP exponential decay phenomenon, was used to study the pressure changes that will occur in the eye due to glaucoma during external measurements. The mathematical model helped to analyse the principle behind IOP measurement and was extended to internal measurements by analysing time-based changes of variables integral to the process, such as eye rigidity, size, pressure, volume etc. The mathematical simulations helped to determine the physical requirements of an implantable micro device capable of increasing the IOP temporarily for the duration of a measurement. Finite element method analyses were conducted to determine the dimensions of a MEMS pressure sensor that could respond mechanically to the pressure changes initiated inside the eye by the micro device and convert the responses to electrically measurable units. The pressure resolution required of the MEMS pressure sensor was learned from the investigations and the electrical output indicative of the extent of glaucoma in an eye was also calculated.

Integrating the intraocular dynamics and the MEMS pressure sensor responses constituted a mathematical model of the implantable micro system. The micro system model was tested for normal and adverse eye operating conditions to estimate the output based on various internal IOP measurements. The output that would be obtained from the implantable micro system was compared to responses from external measurements and found to be comparable. An overview of a comprehensive MEMS monitoring

system including the micro device to increase the pressure within the eye, a MEMS pressure sensor, and powering and signal conditioning electronics was provided. A description of the technologies that could be used for the fabrication and packaging of the device and the sensor was also included at the end of the thesis along with a discussion on bio-compatibility and implanting issues.

Thus the feasibility of combining a micro device and a micro sensor with powering and signal conditioning electronics to create an implantable MEMS system that can make continuous measurements which can indicate the onset of or an increase in blockage of the eye of a person with glaucoma is presented in the thesis.

A paper titled “A MEMS Glaucoma Monitoring Device” has been published in the International Society for Optical Engineering (SPIE) Journal and a poster paper was presented at the SPIE International Symposium for Micro and Nano Materials held at the University of Technology in Sydney, December 11-15, 2004.

CONTENTS

6. Testing of the MEMS System

7. Review of Technology for Fabrication and Packaging

List of Figures

List of Tables

List of Abbreviations

- IOP - Intraocular Pressure
- MEMS - Microelectromechanicalsystems
- C_f - The symbol denotes Outflow Facility in the eye
- R- The symbol denotes Resistance to fluid outflow from the eye
- ANSYS - Abbreviation for Finite Element Method Analysis software
- FEM - Finite Element method
- mm - Milimetre
- mV- Millivolt
- kPa - kilo Pascal
- kJ - kilo Joule
- mmHg - Millimetre of Mercury
- T_v - Symbol to denote the time at which volume change is started in the simulation.
- T_v on - Symbol to denote the time during which volume change must be maintained in the simulation.
- d_{on} - Symbol to denote the time at which volume change effect is minimum in the simulation.
- IOP diff - Symbol to denote the time during which there is maximum change in the rate of fall of IOP in the simulation.
- Alarm min - Symbol to indicate that high priority alarm must be issued by the system
- Alarm min - Symbol to indicate that normal priority alarm must be issued by the system
- No alarm - Symbol to indicate that no alarm needs to be issued by the system
- Press fall max - Symbol to denote the time during which IOP fall is maximum in the simulation
- Volt Diff max - Symbol to denote the time during which there is maximum difference in the voltage output of the sensor in the simulation
- IPMC - Ionic Polymer Metal composite

- LIGA - German acronym for X-ray Lithography (X-ray-**Li**thographie: Electroplating – **Ga**lvanoformung)
- CMOS - Complementary metal oxide semiconductor
- ASIC - Application specific integrated circuit
- LC – Inductance, Capacitance
- DC - Direct Current
- RF - Radio Frequency
- µl - Microlitre
- µm - Micrometre
- kΩ - Kilo ohms
- $\sigma_{l,t}$ - longitudinal and transverse stresses
- T_x - In plane forces along x axis
- T_y - In plane forces along y axis

1 Introduction

1.1 Motivation

It has been estimated that at least 65 million people worldwide are affected by glaucoma. Of this number, at least 3 million people are permanently blind [1]. Glaucoma has been recorded in literature to be the third leading cause of irreversible blindness in adults [2]. The risk of going blind from the disease is more likely in developing countries in comparison to developed countries [3]. It has been recorded adults over 40 with a history of heart disease, diabetes or a family history of eye disease, run a higher risk of developing glaucoma and therefore the ageing population of a country generally forms the target group for this disease [4]. Glaucoma is also known to occur as a congenital condition [5].

The major symptoms of glaucoma are elevated intra ocular pressure (IOP), optic disc cupping, optic nerve damage and visual field loss [6]. The disease occurs when the drainage of fluid (aqueous humor) that flows continuously within the eye is obstructed. Fluid flow obstruction causes IOP to rise. An increase in IOP is associated with destruction of the optic nerve and is responsible for the occurrence of irreversible vision loss in human beings [7]. There is no cure for this pathological condition, however, it can be controlled upon detection of onset and managed by life-long monitoring of symptoms using pharmacologic agents [8].

While monitoring and control of elevated IOP is the widely adopted method of treating glaucoma, there have been records of the disease progressing under normal IOP levels as in the case of normal tension glaucoma [9]. The deterioration of the condition is not noticeable until a sudden significant vision loss is reported, or a progressive worsening of the symptoms is observed. The loss of vision is not accompanied by pain or discomfort and there is the risk of the condition deteriorating even when being treated, unless frequent and timely monitoring of IOP and its symptoms is performed [10].

As current monitoring methods do not allow for any indication of onset or progression of the disease, patients are exposed to the threat of permanent blindness while under clinical management. Therefore despite the treatment and monitoring methods made available to glaucoma patients, there are risks associated, as disease progression cannot be monitored in all cases. Indicating to the patient at an early stage about impending vision loss would make possible the necessary corrective action and has led to the investigations outlined in this thesis.

1.2 Problems with monitoring Glaucoma

Monitoring the progression of glaucoma is complicated because the measurement involves detecting a change in the delicate flow-IOP equilibrium inside the eye [11]. Due to the constant change and fluctuation of flow and pressure parameters, it is difficult to continuously measure and track the parameters that contribute to the progression of the disease. It is not possible to detect the changes immediately as they develop over a period of time [12].

1.2.1 Description of the eye

In the eye, a fluid called aqueous humor is produced continuously by the ciliary bodies of the eye and flows into a hemispherical chamber called the anterior chamber, through the pupil [13]. As depicted in Figure 1.1, the cornea at the front and the iris at the back bind the anterior chamber. The clear aqueous humor fluid flows into the anterior chamber at the rate of approximately 2.5µl/min and fills up the 250 µl volume of the

anterior chamber [14]. The extremely slow flow rate of the fluid is suited to the lubrication and nourishment of the intraocular contents. The flow rate also maintains the IOP whose stability is vital for the preservation of the shape and rigidity of the eyeball. IOP is closely linked with the fluid flow rates and is also defined as the tissue pressure of the ocular contents [13].

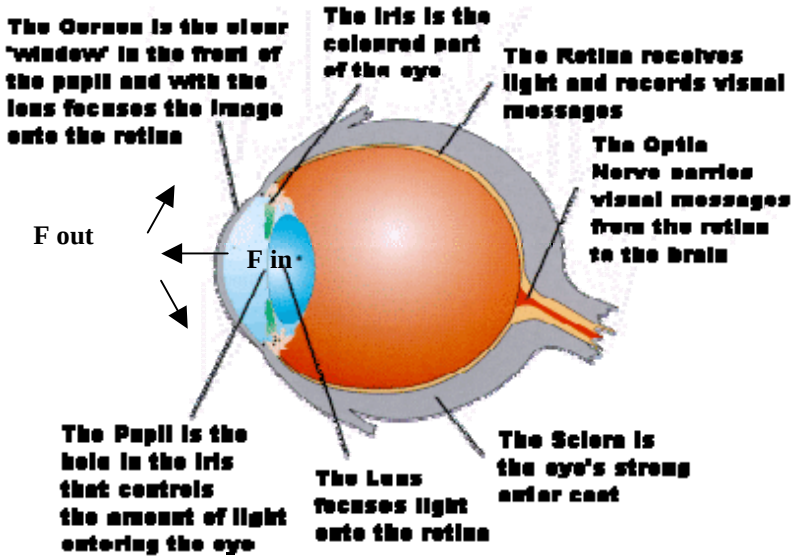

Figure 1.1 An Illustration of the structures of the eye [15]

The flow rate of aqueous humor into and out of the eye is balanced so that a stable IOP is maintained inside the eye. At equilibrium flow and pressure conditions an average IOP between 12-15mmHg is normally maintained in an eye [13].

The fluid circulates within the anterior chamber and then exits through an annular opening running along the junction of the iris and sclera called Schlemm's Canal, into a region that is made of tissue and is porous, known as the trabecular meshwork. Approximately 98% of the aqueous humor flows out through the annular opening into the trabecular meshwork and drains back into the circulatory system of the eye [16]. As the outflow of fluid occurs in a direction against gravity, most of the resistance to drainage is encountered at the outlet channels in the porous trabecular region of the eye [16].

1.2.2 How glaucoma affects the eye

When there is a resistance at the outlet regions, fluid flow is blocked and the flow-IOP equilibrium is altered [17]. Figure 1.2 below illustrates the regions at the fluid outlet where majority of the blockage occurs.

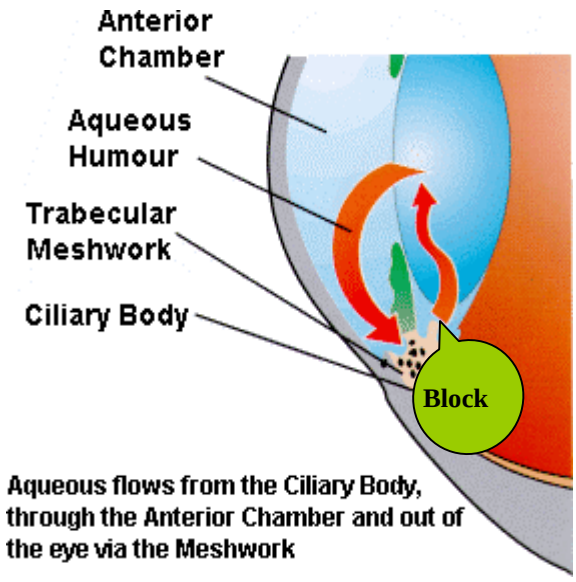

Figure 1.2 An Illustration of the fluid outflow path from the eye [15]

Some of the possible changes that could occur in the outlet region are: [18]

1. The lens blocking the fluid inlet region.
2. A rise in pressure at the exit regions.
3. A part of the lens-iris dislocating or contracting thus blocking the angle of drainage.
4. The cornea enlarging or expanding and thus blocking drainage.

The changes in the eye that prompt the blockage of fluid are known not to occur suddenly but accumulate gradually over a period of time. When a blockage occurs, IOP rises from 15 to nearly 25 mmHg. In severe cases, IOP has been recorded up to 40 mmHg and above [18].

1.2.3 Treatment of glaucoma

Doctors treating glaucoma target controlling IOP rise and maintenance of IOP within 12-15 mmHg as a means of achieving proper flow regulation [19].IOP is measured externally on a monthly basis using a tonometer in a clinic [20]. The condition is treated with a pharmacologic known as beta-blockers or adrenergic agnostics which are used to clear blockages by regulating fluid production, inlet and exit pressures to maintain an optimal IOP level [21]. IOP is prone to fluctuations and has been recorded to vary during different times of the day [22]. When chemicals fail to bring down IOP, treatment is then focused on surgical removal and correction of the structures blocking fluid drainage [18].

Apart from raised IOP, patients with glaucoma have been observed to have an increased resistance to outflow of the aqueous humor which is also expressed as facility of outflow and is an important blockage related parameter denoted by the symbol C_f. The measurement of C_f levels is linked with the detection of the onset of a blockage as they could provide a direct indication of the level of resistance to flow [23]. The value of C_f is recorded during a type of IOP measurement known as tonography, but despite its potential to reveal greater clinical information regarding the progression of the disease, it has been restricted to research purposes in recent years [24].

1.3 Objective of this work

The objective of this research is to investigate and develop a microelectromechanical system (MEMS) that can provide an indication of blockage onset in glaucoma by monitoring continuously factors that contribute to a rise in IOP.

In recent times, microelectromechanical systems (MEMS) technology has shown the potential to allow for the development of Microsystems with the capacity and efficiency required for in-situ monitoring of biological phenomenon [25]. Over the last couple of decades, several developments utilising this technology have been reported in the automotive, defence, industrial and medical instrumentation sectors [26]. For example, lab-on-chip systems, micro-total analysis systems (μ-TAS), micro-sensors, micro-actuators, micro-valves, micro-pumps, micro-dispensing units and diffuser pumps etc have been some of the recent additions to the micro system product family that find critical applications in the bio-medical research and development field [27].

Micro pressure sensors for monitoring pressure activity in the human body, micro surgical tools, grippers, tweezers for minimally invasive surgery and micro fluid dispensing units follow in the large list of some of the examples of MEMS products currently in use [28], [29].

These systems can be manufactured in bulk thus cutting production costs. The fabrication technology is largely borrowed from the IC fabrication industry, but allows for the development of new products suited to this particular application. These systems can be combined with signal processing and transmission electronics on a single–chip providing the advantage of reduction in size and bulk with the added possibility of powering through inductive coupling methods and telemetry [30].

The MEMS approach aims to provide in-situ monitoring of flow and IOP the changes as they occur when an eye is affected with glaucoma. MEMS technology will allow for the physical changes to be converted into electronically measurable quantities, storing and transmitting information to external electronic readout devices. This will enable the

patient or doctor to readily access the information when necessary and remove the need for a clinic-based measurement with the skill, time and costs involved.

As MEMS technology can lend itself to the development of miniature implantable devices, the investigations will aim at deriving the requirements of a MEMS based method that will be capable of capturing any change in the level of C_f and IOP in the eye and providing a measurable indication of that change. The investigations will aim to arrive at the requirements of a system capable of delivering such a measurement by analysing the working of the eye and the principles behind glaucoma monitoring. The work to be undertaken in this thesis will focus on:

1. Determining the factors that will be critical to making continuous C_f based IOP measurements from within the eye using a mathematical model.

2. Developing the powering, size and sensitivity requirements of a system.

3. Testing the output that will be obtained from such an implantable system.

4. Determining the fabrication and production feasibility of a MEMS implant.

This thesis is an extension of similar work undertaken by other researchers.

1.4 Overview of chapters

In Chapter 2, the literature review provides an introduction of the importance of C_f based glaucoma monitoring techniques. The principle and theory behind C_f measurements are described and the different methods of undertaking C_f measurements are explained. This chapter covers details of currently existing clinic-based IOP measurements, followed by an explanation of the alternate IOP measurement methods proposed in the literature. The use and applications of existing miniature glaucoma surgical implants is introduced and finally a discussion about recently developed MEMS IOP sensors in the literature is presented. The need to achieve a continuous C_f based IOP monitoring method is brought out at the end of the literature review.

In Chapter 3, the need for the use of a mathematical model of the eye is deduced by analysing the working of the eye and the role of the flow pressure equilibrium in C_f based IOP monitoring. A mathematical model of the eye that can capture the time based IOP activity of the eye that incorporates changes in eye volume and rigidity is introduced. The use of the model is validated by comparing the IOP output to that obtained from a tonometer. The sensitivity of the model to changes in the eye due to glaucoma is tested.

In Chapter 4, the mathematical model is used to investigate the requirements of conducting an internal C_f based IOP measurement. The energy and size requirements of a miniature device and the sensitivity and resolution of a pressure sensor that is capable of monitoring glaucoma internally are determined.

In Chapter 5, a MEMS based piezoresistive sensor is characterised for measurement of IOP as a surface load. The deflection of the sensor and the pattern of stress variation when subjected to IOP loads are analysed. These analyses assist in determining the optimal location of piezoresistors on the surface of the sensor and are used to calculate the electrical output that would be obtained from the sensor. The structural dimensions of the sensor, its resolution and the output voltages that are obtained from it are calculated and summarised at the end of this chapter.

Chapter 6 provides an overview of the integrated MEMS system and options for enabling signal conditioning, powering and data transmission. The response that is obtained if a miniature device were implanted in the eye is tested under worst case operating conditions. The sensitivity of the electrical output that is obtained when a MEMS pressure sensor is combined with the device to difference in C_f levels is then determined using the mathematical model.

In the seventh chapter a brief description of the type of actuator that can be used for the development of a MEMS device is provided along with possible fabrication and packaging details for the device and pressure sensor. Issues with reference to biocompatibility and implanting the MEMS system are discussed.

1.5 Results Achieved

The use of a mathematical model describing the working of a device inside the eye of time based IOP and volume changes for providing continuous C_f based IOP measurements were investigated. The requirements of a miniature device that could be used to make internal C_f based IOP measurements were derived from the investigations. The requirements of a MEMS pressure sensor to measure IOP was determined. The working of the device and sensor were tested using the mathematical model and the sensitivity of the measurement to differences in C_f values is presented. The powering, fabrication and packaging details of the MEMS system are discussed.

1.6 Contributions

A paper entitled “A MEMS Glaucoma Monitoring Device” has been published in the International Society for Optical Engineering Journal (SPIE) and a poster presentation was given during the International Symposium for Micro and Nano materials at University of Technology in Sydney held 11-15 December.

2 Literature Review

2.1 Introduction

The previous chapter demonstrated that glaucoma is a threatening condition that results in irreversible vision loss in humans and animals. The literature review will highlight the importance of C_f based IOP monitoring and the steps involved in undertaking it. Current glaucoma monitoring techniques are introduced in this chapter along with information about recently developed alternate methods of measuring IOP and existing miniature glaucoma implants. Information about the use of MEMS technology for the development of sensors to monitor IOP is included in the review to make a comparison between existing technologies and determine the kind of advancements that will be required to make C_f based IOP monitoring continuous and implantable.

2.2 The importance of C_f based IOP monitoring

It was shown in the previous chapter that the blockage of fluid flow in eyes leads to rise in IOP that can be detected by monitoring a decrease in the level of outflow facility or C_f, a parameter that is reflective of an increase in flow blockage. Currently the disease is controlled by managing the IOP levels of a patient by administering the appropriate medication or by laser or incisional surgery.

2.2.1 C_f measurement

The level of outflow facility in the eye is defined as the rate of outflow of aqueous per mmHg of raised IOP per minute with the units, µl/min/mmHg [31]. It is taken to be the reciprocal of resistance to outflow, represented by the symbol R ($R=1/C_f$). A decrease in the level of outflow facility accompanies an increase in the level of resistance indicating an increase in the obstruction to fluid outflow from the eye.

The values closer to 0.3 µl/min/mmHg indicate normal outflow facility and the values closer to 0.15 µl/min/mmHg are regarded as being indicative of severe fluid blockage [32].

Detecting an increase in C_f levels requires continuous measurement of outflow facility along with flow and IOP levels in the anterior chamber of the eye [32]. These measurements then offer the possibility of administering timely corrective action by picking up the development of near critical conditions in the eye which inturn facilitate the treatment and management of glaucoma. Thus, eliminating the risk of blindness [33].

Clinical C_f based glaucoma monitoring involves raising IOP temporarily and measuring its time based fall. A change in eye volume is used to cause a temporary change in IOP and C_f measurements are made from the time based pressure volume relationship of the eye represented in Equation 2.1 given in [13].

$$C_f = \Delta V / T \left(P_{av} - [P - P_v]\right) \quad (2.1)$$

Where

C_f = the coefficient of outflow facility (µl/min/mmHg)
ΔV = change in eye volume (µl)
P_{av} = average of initial and final IOP during measurement (mmHg)
P = IOP in the eye (mmHg)
P_v = exit pressure (mmHg)

T = measurement time (minutes)

Research has shown that the presence of either raised IOP or low C_f alone could falsely indicate glaucoma [34], but a measurement that allows the clinical interpretation of both the parameters simultaneously will be able to provide a true indication of the extent of glaucoma in the eye. Although the monitoring of C_f values helps to determine any change or increase in glaucoma, the process in itself is not direct and depends on a host of other variables in the eye [35]. The transient nature of those variables is heightened by the onset of glaucoma and adds to the complexity of C_f based glaucoma monitoring [35].

2.2.2 Tonography

The name given to the clinical method of measuring C_f is tonography. It is defined as the continuous measurement of IOP to determine the facility of outflow to determine the presence of glaucoma [24]. The changes in IOP produced by the constant application of a known external weight over the globe of the eye are recorded over time in tonography. The weight causes an instant elevation of IOP along with simultaneous changes to fluid inflow and outflow rates. The rate of fall of IOP is then measured after the removal of the weight. The phenomenon is illustrated in Figure 2.1 [36].

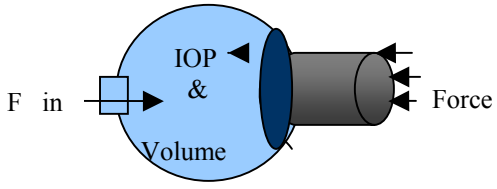

Figure 2.1 Principle of Tonography

A change in the net volume of the eye is brought about during the measurement when fluid inflow is increased by the weight of the instrument. Additional fluid reduces the eye volume and leads to an instant rise in IOP. The eye then naturally

regulates flow and reduces the raised IOP. Outflow facility is calculated in tonography by the loss in volume expressed in terms of a difference in time between the fall of raised IOP to the original level (refer Equation 2.1). When affected with glaucoma the eye loses much of its flow regulating and IOP stabilising mechanism [32].

Figure 2.2 depicts Friedenwald's nomograms that were traditionally used to calculate C_f values [37]. The logarithmic values of initial and raised IOP values were included along with variations in the rigidity of the eye and the C_f values were manually interpreted by numerical fitting of the data from a standard nomogram.

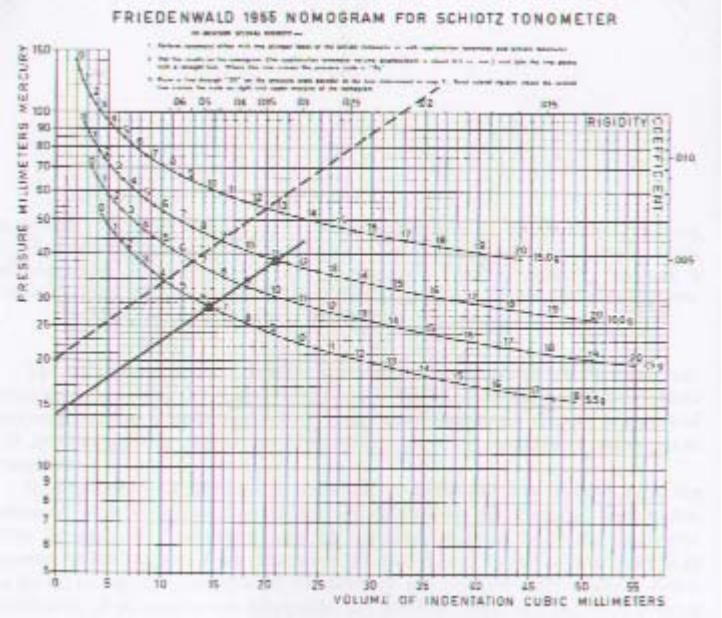

Figure 2.2 Friedenwald 's nomogram used to calculate C_f values[13]

Towards the eighties computerised methods of interpreting and calculating C_f were introduced but they have not been standardised yet [38]. A detailed discussion relating to the exact method of calculating C_f has not been included in this literature review as it warrants intricate clinical knowledge and discernment which is outside the scope of this thesis.

A tonograph is the name given to the electronic reading obtained while recording the rate of fall of pressure in an eye during tonography. An illustration of a sample tonograph is provided in Figure 2.3. A tonograph resembles a pressure decay curve where a rate of fall of lesser than 25% a minute indicated a pronounced blockage and rate of fall of 5% per min indicated minimal blockage [23].

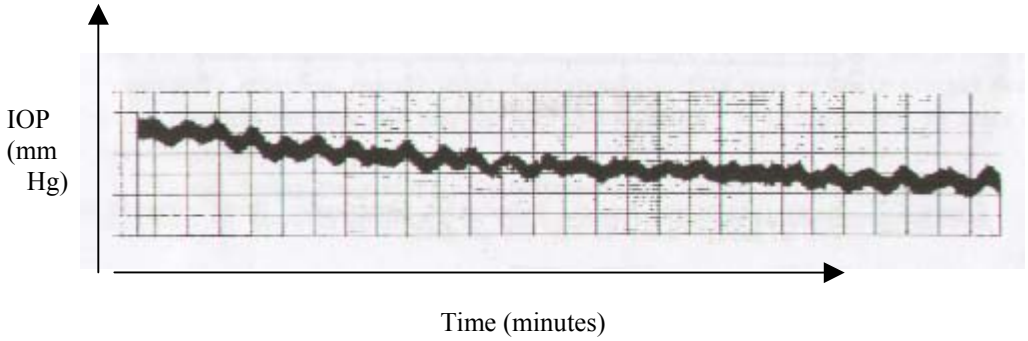

Figure 2.3 Illustration of a sample tonograph [35]

2.2.3 Different methods of measurement

The Different kinds of instruments used in tonography are listed below in Table 2.5. All the methods rely on the principle of initiating a rise in IOP by changing the effective volume of the eye externally and the difference lies in achieving the change.

TYPE	SENSOR	RANGE	METHOD	ACTION	FUNCTION	REFERENCE
Indentation Tonography	Pressure Sensor	0-50 mm Hg	Schiotz Tonometer.	Constant depth indented on cornea over 4 mins	Measure IOP and C_f from tonogram	39
Manometry	-	0-50 mm Hg	Needle to inject fluid into eye	Fluid reservoir connected to u-tube manometer to read pressure for 4 mins	Measure IOP and C_f from tonogram	23
Suction cup Tonography	-	0-50 mm Hg	Vacuum cup placed over eye	Suction cup connected to manometer - read pressure for 4 ins.	Measure IOP and C_f from tonogram	39

Table 2.1 Different methods used in tonography .

The main methods used to change the volume of the eye during tonography measurements are described in the following paragraphs.

Manometry

Manometry involves direct cannulation of the anterior chamber with a needle to increase IOP in the eye. The effective internal volume of the eye is reduced in manometry by adding water through a needle that is connected via a tube to a (saline) fluid filled reservoir [23]. The change in volume causes an instant rise in IOP required for the measurement. The use of the manometer has been restricted to animal research in literature as the process requires anaesthetisation and is painful to administer.

Indentation Tonography

A Schiotz tonometer is used to indent the eye and alter the flow and IOP equilibrium due to the effective reduction of the net volume of the eye. A tonograph produces a recording of the rate of fall of IOP dropping with time and the extent of the blockage was interpreted from the rate of fall. A nomogram was to calculate the C_f values. Weights ranging from 1 gram to 5 grams are used to indent the eye for measuring IOP using a Schiotz tonometer [23].

The use of the Schiotz tonometer was the most popular method of measuring C_f in human eyes [36]. However it is not in use these days and is restricted to research purposes. Figures 2.4 and 2.5 below illustrate the method by which the measurement is administered.

Figure 2.4

Figure 2.5

Measurement of IOP using a Schiotz tonometer [13]

Suction Cup tonography

In suction cup tonography, a circular cup was placed over the eye and sealed into place with vacuum. The cup occluded the outlets and prevented the outflow of fluid. The effect of the weight of the cup was similar to the weight of a Schiotz tonometer and produced the same effect of reduction in eye volume. The rate of fall of IOP was noted as a measure of the eye's response to the alteration in flow-

pressure equilibrium and the level of (C_f) was calculated from the IOP response [23].

The tonography type measurement methods of have been described to be painful in the literature as they require the use of anaesthetics for the measurements [40]. Consecutive readings did not yield similar results [41]. However it can be summarised that the measurement of C_f levels had the potential to indicate the presence of glaucoma.

2.3 Current glaucoma monitoring methods

Currently Glaucoma is monitored by instantaneously measuring IOP using tonometers in a laboratory set-up.

2.3.1 Tonometry

The principle of tonometry is based on the Imbert-Fick law [42], which assumes the eye to be a fluid filled spherical system. The Imbert-Fick law states that if a plane surface is applied with a force F on to a thin spherical membrane within which a pressure P exists then for an equilibrium condition the expression is given by Equation 2.2.

$$P = \frac{F}{A} \qquad (2.2)$$

where,

P = IOP

A = area of the applied force (3.06mm diameter or 1.732 mm^2)

F = weight applied on the eye (1-10 grams)

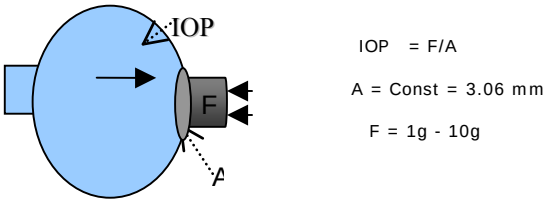

Figure 2.6 Illustration of the Imbert-Fick law in Tonometry

As pressure is equal to the force applied per unit area, placing the instrument over the eye gives an immediate indication of the IOP. Most of the IOP measurement methods are based on the applanation technique which is based on the Imbert-Fick law which is illustrated in Figure 2.6.

2.3.2 Different Kinds of Tonometers

Different kinds of tonometers are listed in Table 2.2 below.

Type	Sensor	Range	Method	Action	Function	Reference
Applanation Tonometer	Pressure Sensor	0-40mm Hg	Goldmann tonometer	Variable force applied on constant area of cornea	Measure IOP instantly	[43]
Indentation Tonometer	Pressure Sensor	0-50 mm Hg	Schiotz Tonometer.	Depth indented into cornea using constant force	Measure IOP instantly	[44]
Non contact Tonometer	Photoelectric sensor	0-50 mm Hg	Air-Puff applanation	Area on cornea flattened by pressurised air jet	Measure IOP instantly	[44]
MacKay Marg Tonometer	Time record of force	0-50 mm Hg	Spring plunger footplate arrangement		Estimate IOP from time record of force	[44]
Automated Handheld Tonometers	Pressure sensor	0-50 mm Hg	Tonopen tonometers	Miniature tonometers based on Goldmann applanation	Measure IOP instantly	[44]

Table 2.2 Different types of tonometers

Applanation Tonometry

Applanation tonometry has been adopted as the universal standard measurement principle for external IOP measurement [44]. The measurement method is based on the Goldmann applanation principle. In this method the instrument is mounted on a clinical slit lamp bio-microscope and a probe like structure is impressed upon the cornea to flatten a circular area of diameter 3.06 mm using a knob. A force is imparted on the eye through the probe, which is varied between 1 and 10 grams to measure IOP between 5 to 50 mmHg within the eye. Patients require the assistance of either a skilled operator or an Ophthalmologist, who has access to these facilities as illustrated in the Figures 2.7 and 2.8.

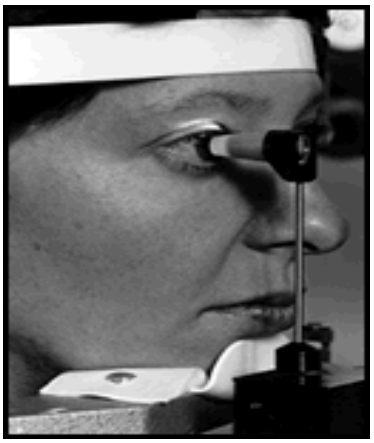

Figure 2.7 Measurement of IOP [13]

Figure 2.8 Goldmann tonometer [13]

Indentation Tonometry

In Indentation tonometry a Schiotz tonometer is used to apply a known weight on the eye and the extent of indentation on the cornea is measured. This method is also based on the Imbert-Fick law. But unlike in the applanation principle in this case the depth to which the instrument sinks in the eye is measured. It has been recorded that indentation tonometry causes IOP to be raised due to the weight of the instrument and produces a falsified reading of IOP [44].

A variation of the indentation type of tonometry is non-contact or air-puff tonometry where a stream of pressurized air is impressed on the cornea from the instrument. The amount of flattening caused on the cornea is then sensed using a photoelectric sensor. IOP is then calculated from the known force of the air stream and the photo electrically sensed diameter of applanation at the exact instant [44].

Mackay-Marg and Tonopen Tonometers

The Mackay-Marg tonometer is another variation of indentation tonometers where IOP is obtained as an estimate of the time record of the force used to counteract corneal bending pressure and the IOP within. The calibration and interpretation of this particular pressure measurement has been described to be complicated [45]. The tonopen or pneuma tonometer is a compact and mobile tonometer based on the Goldmann applanation principle that was designed for use without the need for a laboratory set up as in the case of the other tonometers [44]. Figure 2.9 below shows an illustration of the tonopen tonometer.

Figure 2.9 Tonopen Tonometer [105]

Despite its availability it has not been able to replace the Goldmann applanation tonometer which remains the standard tonometer for clinical purposes today. Tonometers play an indispensable part in the treatment of glaucoma. Figure 2.10 illustrates the different kinds of tonometers. Operating these instruments requires the time and efforts of skilled operators. IOP measurements are performed once every three months, over a 12 hour period to assess the efficiency of treatment [36]. The readings obtained from a tonometer are collected over the period of a

day to study the trend in fluctuation of IOP. Changes to the treatment routine are made with inference from the results to maintain a target IOP level in a patient

Figure 2.10 Different types of tonometers [13]

.

Though tonometers can be used for taking instantaneous IOP measurements and are used by physicians to assess the efficiency of treatment being provided, this measurement does not help to indicate any change or rise in the condition of the disease occurring at times outside of the measurements.

2.4 Alternate IOP measurement methods

The following section of the review will focus on recent attempts undertaken to replace tonometry by continuous IOP measurements.

2.4.1 Miniature methods to monitor IOP

C.C. [46] Collins developed the first miniature pressure sensor to record IOP information continuously in 1967 and since then an extensive amount of research has been devoted to the development of candidate technologies that could be used to replace tonometer measurements. Various transduction methods that could be utilised to sense and monitor IOP have been reported in literature. The different methods are described in Table 2.3.

METHOD	DATA TRANSMISSION	RANGE	TYPE OF IMPLANT &SIZE	FUNCTION	REFERENCE
Magnetic Permeability	Not specified	50-150 kPa	Implantable in the Lens. 6.76mm^2	Measurement of IOP	47
Doppler effect	Not specified	50-150 kPa	Detect IOP based shift in frequency of eye	Measurement of IOP	48
Strain gauge	RF transmission with antenna on contact lens	Not specified	Relate change in radius of eye to IOP	Measurement of IOP	49
Capacitive pressure sensor	RF transmission with on chip antenna	14-220 kPa	Implantable in Lens-with a silicone coating 6.25mm^2.	Measurement of IOP	50
Micro mechanical Tonometer	Not specified	50-150 kPa	6mm by 6mm	Measurement of IOP	51

Table 2.3 Transduction methods to measure IOP.

Researchers have pursued the feasibility of utilising physical phenomenon such as magnetic permeability and ultrasound Doppler effect as alternate approaches to IOP measurement. It has been suggested that a pressure sensor be coupled to an element whose change in magnetic permeability could be related to a change in IOP [48]. The detection of a shift in resonance of the eye shell when subjected to an audio signal by the ultrasonic Doppler effect has been reported to have the potential to monitor IOP [49]. The development of micromechanical tonometers has been reported [51]. However these methods require extensive experimental evidence and validation to be clinically accepted as standard forms of IOP measurement.

2.4.2 Discussion

From this section it can be inferred that the miniaturisation of tonometry has been attempted and several alternative methods of IOP measurement have been reported in the literature. However, it can be seen none of them have succeeded in replacing external tonometry measurements and have not included any aspect of C_f based glaucoma monitoring.

2.5 Miniature glaucoma implants

This section provides information about a class of clinically significant glaucoma implants that are being used successfully. The technology and methods employed for the development and use of these implants will be discussed here.

2.5.1 Surgical implants

Miniature implants developed for the treatment and surgery of glaucoma have been successful and are currently in use. The implants are mainly micro-surgical devices that are used mainly for pressure regulation purposes and are implanted in regions close to the anterior chamber of eye, where most of the drainage occurs (Refer Section 1.2.2).

The implants reduce IOP in the eye by promoting fluid flow when there is a severe blockage that cannot be treated by surgery or medication. They are designed to allow fluid to flow either through in-built tubes or across their flat surface to bypass blockages and successfully drain out through the drainage channels [52]. They are also used to keep a surgically created outlet in the person's eye for fluid drainage from closing [53]. These micromechanical implants are compact enough to be surgically positioned under the white (sclera) of the eye or in close proximity to the anterior chamber.

The microsurgical implants can be divided into two broad categories

1. Drainage devices &
2. Glaucoma valve implants

The drainage devices are designed to dissolve a few months after implanting under the white of the eye. The devices dissolve leaving behind the space occupied by them, which allows fluid to drain out of the eye keeping IOP low. They are often up to 19 mm in length and 1 mm wide.

The valve implants are larger drainage devices [27] which have been used in the treatment of glaucoma patients since 1969.The valves help to increase outflow of fluid from eyes to keep pressure low. The valve consists of a long tube which is inserted into the anterior chamber in front of the iris allowing the fluid to pass across it to the back of the eye, where the rest of the implant is located. Illustrations of valve implants and drainage devices are presented in Figures 2.11, 2.12 and 2.13.

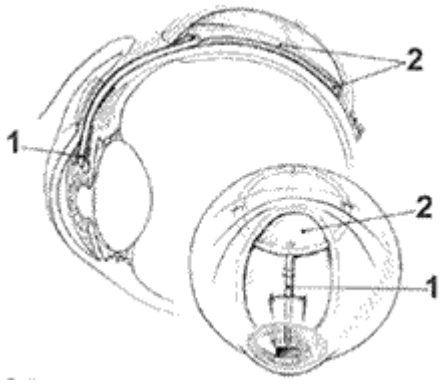

Figure 2.11 Location of valve implants [54]

1. Tube in anterior chamber
2. Flat plate of implant under sclera, behind anterior chamber

Micro pressure valves have been developed to help with filtering of excess fluid in the eye when surgery or treatment fails to reduce and regulate IOP levels. The miniature valves developed for this purpose are not more than $5\times5\times2$ mm^3 in volume and are known as Molteno and Ahmed valve implants. They are

manufactured to assist with artificial IOP regulation and assist with glaucoma treatment after surgery [54].

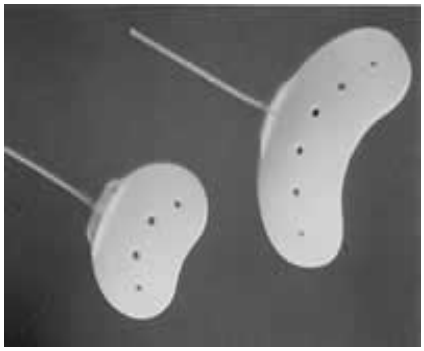

Figure 2.12 Valve implants [54]

Figure 2.13 Drainage devices [54]

There have been reports of electrochemically powered self-actuating, automatic pressure regulators capable of maintaining IOP under the required target level [55]. The purpose of these implants was to maintain IOP at a certain level by controlling fluid-flow in the eye by using a micro-valve integrated with a pressure regulating device. Implants of this type are still under development at the MESA, Research institute, in the University of Netherlands.

The problems associated with such micromechanical implants are that they may not function effectively over time due to the possible clogging of the tube with tissue. Scarring may occur around the implant and prevent re-absorption of fluid into the eye from the drainage areas. As implanted valves are foreign bodies, inflammation and bleb formation could occur in the eye after surgical implantation. Surgically created holes for drainage of fluid inside and in regions around the eye heal with time which then renders the flow and pressure regulation valves ineffective.

2.5.2 Discussion

Literature shows evidence of miniature devices designed to regulate and control IOP inside the eye. Although they provide invaluable assistance in glaucoma treatment there are considerable problems associated with the use of surgically implantable micro-mechanical devices and surgical glaucoma implants.

Despite their advantages these implants will not be able to provide an early indication to a patient of the onset of critical conditions inside the eye as they are not linked to C_f based glaucoma monitoring. Though the miniature surgical drainage and pressure regulation devices are not equipped to monitor any changes in the C_f levels of the eye the technology used for the development of these implants and the surgical procedures associated with their use suggest that it will be possible to undertake the development of a miniature implantable glaucoma monitoring device based on the support of similar relevant medical and technological knowledge.

2.6 MEMS based miniature IOP sensors

It was introduced in Section 1.3 that MEMS technology has the potential to combine sensing and actuating mechanisms alongside with signal processing and transmission electronics on a single implantable chip. The technology presents the possibility of integrating powering and transmission components onto a single chip which will make the availability of MEMS devices capable of continuously monitoring and transmitting data possible. Ocular implants, blood-glucose monitors, drug-delivery systems and implantable pressure sensors are some of the interesting outcomes from the advancements in MEMS technology [30].

Recently this technology has been favoured for the production and development of miniature IOP sensors [28]. The objective behind the development of implantable MEMS pressure sensors was to replace one-off laboratory based IOP

measurements for glaucoma patients and make continuous IOP monitoring readily available.

2.6.1 MEMS IOP sensors

As MEMS sensors allow for the sensing and transmission electronics to be made available on a single microchip the IOP readings recorded from an implanted sensor are transmitted through the integrated signal conditioning units to external read out units or hand held devices [56].

The methods adopted by the MEMS sensors to measure IOP are similar to the pressure sensing methods used for industrial and automotive applications. Therefore the measurements are reliable and trusted methods are used to fabricate and package the devices. Table 2.4 lists the different types of implantable MEMS sensors proposed in the literature that have the capacity to monitor IOP.

SENSOR-MECHANISM	DATA TRANSMISSION	REFERENCE PRESSURE	RANGE	SIZE OF SENSOR CHIP	FUNCTION	REFERENCE
Diaphragm movement Capacitive element	RF transmission with on chip antenna	Absolute (measured against vacuum as reference pressure).	80-130 kPa	Implantable in eye lens. 2.6mm×2.6mm & 10.5mm antenna	Continuous measurement of IOP	[56]
Diaphragm movement Capacitive and Piezo resistive elements.	Not specified	Absolute	N/ A	Not specified	Continuous measurement of IOP	[57]
Diaphragm movement-Capacitive Sensing	On Chip-Frequency transmission	Absolute reference	0- 26kPa	Implantable 0.8mm×3.8mm and telemetry chip	Continuous measurement of IOP	[58]
Strain Gauge based sensing	RF transmission with on chip antenna	None	N/A	Strain gauge sensors built onto a contact lens	Continuous measurement of IOP	[59]

Table 2.4 Different MEMS IOP Sensors Proposed in literature.

It can be seen from the table that absolute capacitive pressure sensing technology has remained the most popular method for developing MEMS IOP sensors. The MEMS capacitive pressure sensing is based on the parallel plate capacitor theory [60], where the sensor consists of a movable sensing element and a fixed reference element (which could both be several arrays of miniature capacitive elements). When an external pressure load is applied on the movable plate (sensing element) of a parallel plate capacitor, the plate deflects in proportion to the applied pressure. The deflection changes the distance between (vacuum gap) the fixed and movable plates of the capacitor, which results in a pressure dependent change of capacitance that is detected as a voltage change. The relation between capacitance, charge, voltage and movable plate dimensions are given in Equations 2.3 and 2.4 below [60].

$$C = \frac{Q}{V} \tag{2.3}$$

Where

$$C = \frac{A \times \varepsilon \times \varepsilon_0}{x} \tag{2.4}$$

C= Capacitance

A= Area of the electrodes (depends on height (h), length (l) and thickness (t))

ε = Relative permittivity of the medium between the electrodes usually taken as 1 for air

$\varepsilon_0 = 8.854 \times 10^{-12}$ F/m (permittivity of vacuum)

x = distance between the two plates

The dimensions of the movable plate (h, l, t) are adjusted to suit the sensitivity of the sensor. The parallel plate capacitor is connected to either to a LC circuit [61] or to a integrator and amplifier [62] for detecting the change in voltage.

The use of MEMS strain gauges embedded onto contact lenses that can relate fractional changes in IOP to a change in the radius of the eye have been reported recently [59]. The sensor arrangement could be connected to external telemetry equipment that will allow for transmission of the pressure recordings to an external source. The differential changes in radius of the external eye (cornea) due to change in IOP causes a corresponding change in the output of strain gauge embedded into a contact lens. The method promises to be a good alternative to the capacitive sensing method that requires surgery for implantation. The output of the strain gauge is monitored to observe changes in IOP. Miniature antennas have to be integrated along with the sensors to allow for the transmission of IOP data to an external recording device.

2.6.2 Sensor based monitoring system

The main components of a MEMS based pressure sensor system can be divided into the sensing element, signal conditioning unit, power supply and transmission system. All these components integrated into a single device constitutes an implantable MEMS sensor system.

Several groups have worked successfully to develop implants that can monitor pressure continuously using MEMS capacitive pressure sensors and have presented results with animal testing [56]. The reported implants are integrated within artificial eye lens implants or located at the back of the eye. Miniature signal conditioning units also accompany the microelectromechanical sensors. ASIC chips using CMOS electronics are used for processing and storing the IOP information. The sensor systems are accompanied by either temperature sensing and control or feedback systems to administer corrective action within the implanted system [58].

The pressure sensor is coupled with an on chip or external antenna for transmission of data. Inductive coupling between an external primary coil and a secondary coil house in the implant provides energy to the sensor system. Radio frequency (RF) transmission based on inductive coupling has been reported to be

used for telemetry. IOP monitoring can be performed within a distance of up to 3 meters by the use of such inductive coupling systems [56].

The presence of telemetry components increases the size of the sensor implant. The transmission antenna [31] is often the largest component in this type of single chip miniature implants. All three systems integrated together on a single chip constitute a MEMS implantable sensor system.

The implantable sensors can be used to record IOP data continuously and allow for frequent IOP measurements.

2.6.3 Discussion

It can be noted that implantable MEMS based sensor systems allow for continuous IOP measurements. Though these sensors have the potential to replace tonometry and make IOP measurement continuous they do not possess the capability of monitoring the C_f levels of a patient. Whether or not the MEMS technology can be utilised for C_f monitoring remains to be investigated.

2.7 Conclusions

The literature review has highlighted the following key points. C_f based IOP monitoring has the potential to detect the onset of glaucoma, but the actual measurement procedure is complex and hence the measurement is now restricted to research purposes. Existing monitoring methods and recent developments fall short of addressing the clinical monitoring aspect of glaucoma and there is no method to detect the onset of critical conditions in a patient.

MEMS technology has the potential to provide an integrated monitoring system for glaucoma capable of fore warning threatening conditions to a patient and micro machined MEMS implants have been developed to surgically assist and

treat glaucoma. However, no attention has been devoted to the development of a C_f based IOP monitoring system.

The miniature pressure sensor outputs that have been quoted in the literature have not been characterised to monitor C_f based IOP measurements. The requirements of a system that can provide in-situ monitoring of glaucoma have to be established. Making the measurement internal and continuous would allow for real time monitoring of flow and IOP levels and pick up the changes in parameters as they occur and providing on-demand glaucoma monitoring to the patient.

The method of conducting the measurement, its size and energy requirements will have to be determined. The characterisation of an IOP sensor that will capable of monitoring C_f and IOP will have to be undertaken, the range and type of output voltages that will be obtained from the measurement will have to be determined. Hence the requirements of a prototype MEMS device are investigated and its requirements are determined in this thesis

3 Method of Analysis

3.1 Introduction

In this chapter a mathematical model of the eye will be used to analyse how normal eye function is affected by glaucoma. The model will help to examine the principle behind IOP measurement and serve as the basis for undertaking further investigations relating to internal IOP measurement.

3.2 Functioning of the eye

Researchers have observed that the working of the eye can be compared to a fluid-pressure system within a deformable volume where the amount of fluid entering is in equilibrium with the amount leaving. Adler's text [13] provides a graphical description of the fluid-pressure system which forms the basis for undertaking glaucoma monitoring measurements. An illustration of the system is provided in figure 3.1 below.

In Figure 3.1 the presence of a blockage at the outlets is indicated by R_0 values. The R_0 values represent the resistance to fluid flow at the eye outlets, their reciprocal is given by $R_0 = 1/C_f$, where C_f represents the outflow facility level in the eye. As depicted in Figure 3.1, as a blockage intensifies the values of R_0 increase and the value of C_f

decreases correspondingly. Thus eyes with a low value of outflow facility are taken to represent a severe fluid blockage that triggers a host of pathological conditions that are collectively described as glaucoma [23].

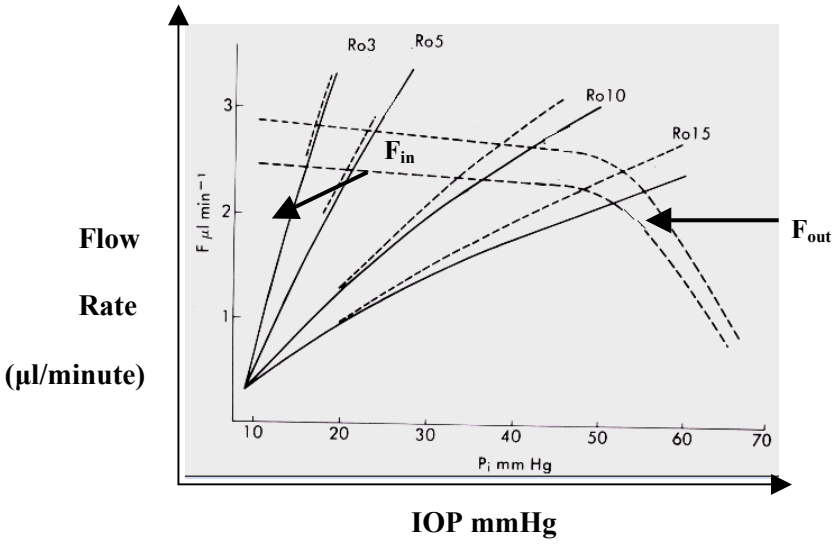

Figure 3.1Relation between flow rate, IOP and resistance to outflow in the eye. [13]

The presence of a blockage to fluid flow triggers the eye's natural regulatory mechanism, which increases fluid production rates (depicted by the lines rising upwards in the Figure above). The increase in fluid production is not matched by the outflow rates (shown by dashed lines falling down) due to the presence of a blockage. This leads to a change in the flow equilibrium of the system.

The eye's working balance is maintained by a balance of a steady state IOP at balanced flow equilibrium. As the flow equilibrium is altered on account of the blockage, IOP rises and stabilises at a higher level than before. The altered flow rates stabilise with time at the higher IOP as illustrated by the Figure 3.1 points where the inflow and outflow lines intersect). The cycle continues as long as the blockage intensifies and the system continues to stabilise after every change in equilibrium at higher values of IOP. Thus the working of the eye can be compared to that of a closed loop system with positive feedback as illustrated in Figure 3.2 below.

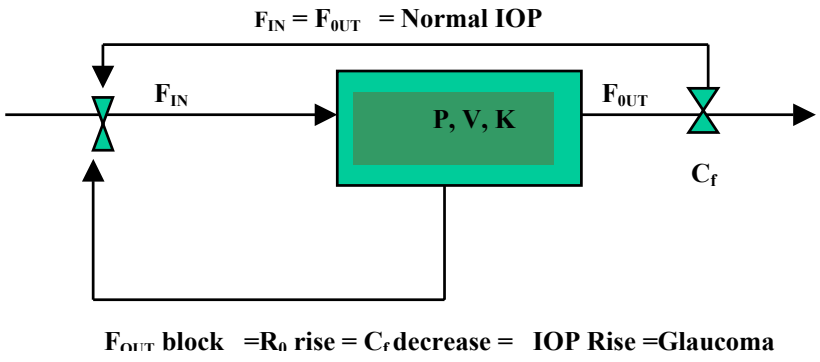

Figure 3.2 Eye depicted as a closed loop system with positive feed-back.

The Figure 3.2 illustrates the phenomenon described by Figure 3.1 which can be explained as the higher the flow blockage the greater is the resistance at the outlets. The lowering of Cf values and rising of IOP accompany this. Glaucoma research [23] has indicated that tonography type (refer section 2.3) glaucoma measurements that involve measuring both outflow facility (C_f) and IOP levels in a patient can provide a warning of an imminent rise in IOP [24]. The major variables linked with this measurement are

1. IOP
2. Volume of the eye (V)
3. Rigidity of the eye (K)
4. Out flow facility of the eye (C_f)

where IOP is intraocular pressure in the eye, the volume of the eye (V) describes the extent of fluid that can be contained within the eye. The rigidity of the eye (K) refers to the elastic nature of sclera (transparent outer covering) of the eye and outflow facility (C_f) is described as the ease with which fluid can leave from the outlet channels of the eye. The influence diagram in Figure 3.3 below illustrates the link between the variables and IOP.

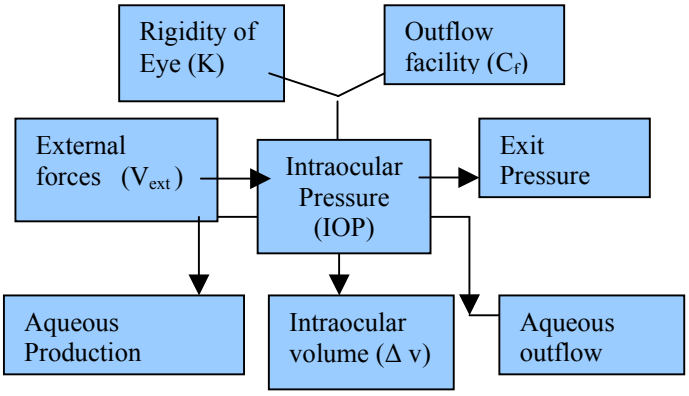

Figure 3.3 Influence diagram indicating the major variables involved in c_f based glaucoma monitoring [35]

Evidence in the literature suggests all the variables depicted in the influence diagram impact on C_f based IOP measurement. Some of the variables vary within a given range while others remain constant during the measurement [44], [63]. The range of the variables to be monitored are

1. IOP - 10-mmHg -35 mmHg
2. Flow Rate - 2 µl/min -3 µl/min
3. Volume - 250 µl
4. C_f - 1.5 µl/min/mmHg -3.0 µl/min/mmHg

The values require that the accuracy and precision of the measurements be within the micro-range. During external C_f based IOP measurements eye volume is reduced using a force [24], IOP rises to a higher value instantly upon changing eye volume and then decays with time. The change in eye volume is held till the eye responds by reducing IOP back to original level. Although a C_f based IOP measurement is dependent on the pressure, volume and flow relationship of the eye and involves the impact of a host of other related variables, it has been known to possess the potential to indicate any impending rise in IOP. Therefore an equivalent model of the eye will be required to study the principle behind the working of the eye and C_f based IOP measurement for glaucoma monitoring.

3.3 Time dependent model of the human eye

Several mathematical models and formulations have been proposed for the study of the behaviour eye mechanics [64], [65], and fluid flow within the anterior chamber [66]. These models have been used as the basis for conducting surgery and taking measurements of the eye [67], [68]. However, a time dependent mathematical model of the eye developed and investigated by Collins and Van Der Werff [35] has been adopted in this thesis to study the principle behind the C_f based IOP measurement method. The model is based on previous models of the flow and pressure of the eye [69], [70], [71]. It has been modified to study the time-based response of the eye to glaucoma measurements. It has been noted that the results from Collins and Van der Werff's model agree well with clinical measurement results on human eyes.

Due to the lack of clinical test data, the model was tested in this thesis by inputting values used during typical clinical measurements into the mathematical model and studying the results obtained.

A differential equation that describes the effect of volume changes on the fluid-pressure equilibrium of the eye forms the basis of the mathematical model. The differential equation governs the rate of change of IOP by taking into account the time-based effect of change in pressure of the eye due to changes in volume, flow rates, C_f levels and rigidity. The derivation of the differential equation is presented below.

3.3.1 Pressure dependence of flow and volume

The derivation in [35] starts with Equation 3.1 which shows that a change in intraocular volume (dV/dt) includes a term which represents the change in the amount of aqueous fluid entering or leaving (dv_{aq}/dt) along with a term to represent the changes imposed on the eye volume ($\frac{dv}{dt}$)

$$\frac{dV}{dt} = \frac{dVaq}{dt} + \frac{dv}{dt} \tag{3.1}$$

The change in the amount of aqueous fluid entering and leaving (dv_{aq}/dt) can be taken to be the rate of change of aqueous volume. This is represented in Equation 3.2 as the difference between aqueous production and outflow rates, both of which are pressure dependent.

$$\frac{dVaq}{dt} = C_p\left(P_c - IOP\right) - C_f\left(IOP - P_{out}\right) \tag{3.2}$$

The terms $C_p\,(P_c - IOP)$ and $C_f\,(IOP - P_{out})$ represent the pressure dependent fluid inflow and exit rates of the eye. The term C_f represents the resistance at the outlets of the eye. P_c, and P_{out} stand for critical pressure at the outlet, outlet pressure respectively. The equation for rate of change of aqueous volume is rewritten substituting Equation 3.3 for C_f and Equation 3.4 for P_{out}, where the constants a_1 and a_2 are taken to be 0.05 and 1.125, constants $a_3 = 0.48$, $a_4 = 4.26$ and the exit pressure, $P_{out} = 9$ mmHg respectively. These values are kept constant for all human eyes.

$$C_f = \left(\frac{1}{a_1 \cdot IOP + a_2}\right) \tag{3.3}$$

$$P_{out} = a_3 \cdot IOP + a_4 \tag{3.4}$$

Thus a new equation for the rate of change of aqueous volume in terms of flow rate and pressure is given by Equation 3.5 below.

$$\frac{dVaq}{dt} = C_p\left(P_c - IOP\right) - \frac{(1 - a_3)IOP - a_4}{a_1 P + a_2} \tag{3.5}$$

This equation represents the pressure dependence of the fluid flow rates which indicates that both the rate of change of eye volume and flow rates are linked closely to IOP. (The numerical values used for substitution into equation 3.5 are $C_p = 0.046$ µl/min/mmHg,

$a_1 = 0.0306$ µl /min^{-1}, $a_2 = 1.428$ mmHg / µl/ min, $a_3 = 0.5$ (dimensionless), $a_4 = 4.26$ mmHg, and $P_c = 50$ mmHg as taken in the mathematical model in [35].

3.3.2 Pressure and volume dependence of rigidity

A mathematical formulation, Equation 3.6, is used to describe the effect of including the viscoelasticity of the corneal shell of the eye along with the time dependence of rigidity and volume of the eye.

$$\Delta P = \Delta V . K_t (K_{eq} + K_f e^{-mft} + K_s e^{-mst}) \quad (3.6)$$

Any change to intraocular volume will result in a change in IOP which will consist of an equilibrium pressure difference (ΔP_{eq}), a fast relaxation curve (ΔP_{fast}), and a slow relaxation curve (ΔP_{slow}) as described in Equation 3.7

$$\Delta P = \Delta P_{eq} + P_{fast} + \Delta P_{slow} \quad (3.7)$$

Equation 3.6 can be rewritten to arrive at a formula that describes the volume based change in IOP in terms of rigidity.

$$\Delta P / \Delta V = K_t (K_{eq} + K_f e^{-mft} + K_s e^{-mst})$$

Or

$$dp/dv = K_t (K_{eq} + K_f e^{-mft} + K_s e^{-mst}) \quad (3 .8)$$

In Equation 3.8, $K_t = (K_{eq}+K_f +K_s)$ which demonstrates that if a known volume is added into the eye it will alter the flow-pressure equilibrium. Alteration of the flow-pressure equilibrium will result in a pressure rise that will be re-established after a

pressure decay. As described earlier, the resulting pressure decay will have an equilibrium pressure difference a fast relaxation component and a slow relaxation component (refer Equation 3.6). The elements of the pressure decay are represented by the terms on the right hand side of Equation 3.8. The term K_{eq} represents the rigidity of the eye and the terms K_f and K_s represent decaying exponentials that control the stress relaxation and the viscoelastic response of the eye.

Thus the model includes the effect of stiffness of the eye along with the relaxation exponentials to capture and study the rate of fall of pressure required for C_f monitoring. The ocular and blood vessel rigidities in the equation have the values, $K_f^* = -0.38$, $K_s^* = -0.47$, $m_f = -1.803\ min^{-1}$ and $m_s = -0.072\ min^{-1}$ respectively as taken in the mathematical model in [35]. Hence the Equation 3.8 can be used to calculate the pressure decay that would result in the eye after a change in volume.

If in the Equation for times $t << 1$, the terms in the brackets on the right hand side simplify to 1, then the value of the equation reduces to K_t. K_t can also be substituted by $(a \times P + b)$, the unifying formula for ocular rigidity, where $a = 0.0123\ \mu l^{-1}$ and $b = 0.0$ mmHg/ µl and Equation 3.8 can be rewritten in a new form as shown below.

$$dp/dv = \left((a \times P)K_{eq} + K_f e^{-mft} + K_s e^{-mst}\right) \qquad (3.9)$$

The equation indicates that the rigidity of the eye is linked with time based variation of eye volume and IOP.

3.3.3 Time dependence of IOP

Having illustrated the dependence of change in volume on IOP, flow rates, and rigidity of the eye, the rate of change of eye volume can be rewritten as shown in Equations 3.10 and 3.11 below.

$$\frac{dV}{dt} = \frac{dV}{dp} \times \frac{dp}{dt} \quad \text{or} \quad \frac{dp}{dt} = \left(\frac{\frac{dv}{dt}}{\frac{dv}{dp}} \right) \tag{3.10}$$

$$\frac{dp}{dt} = \left(\frac{\frac{dv}{dt}}{1 \Big/ \frac{dp}{dv}} \right) \tag{3.11}$$

Equation 3.11 can then be rearranged by substituting the value of dv/dt by Equations 3.1 and 3.2 and the value of dp/dv by equation 3.9. The new Equation 3.12 represents the governing equation for the rate of change of IOP.

$$\frac{dp}{dt} = \frac{C_p (P_c - IOP) - C_f (P - P_{out}) + dV / dt}{1/(aP + b)(K_{eq} + K_f e^{-mft} + K_s e^{-mst})} \tag{3.12}$$

Equation 3.12 is taken as the universal equation that describes the time-based variation of IOP as it includes the terms that represent changes in production and outflow of aqueous humor, rigidities of the human eye and changes in eye volume. The effect of arterial pulsations that were included in the original model has been excluded here as this was outside the scope of this research. It was ensured that the removal of that parameter did not affect final output produced by the model.

All pressure, volume, flow and rigidity values along with the constants and variables that have been used with the model lie within the original ranges used.

3.4 Simulation and modelling results

As the mathematical model (Equation 3.12) is based on the time dependent pressure–volume relationship of the eye it was modelled using Matlab software. A number of simulations were conducted using the model to analyse the principle behind IOP

measurement by studying eye responses under the influence of glaucoma. For the simulations IOP was varied between 10 mmHg and 50 mmHg, the volume of anterior chamber was taken to be 250 µl, outflow facility (C_f) was varied between 0.15 µl/min/mmHg and 0.3 µl/min/mmHg and the rigidity was varied by increasing K_{eq} between 0.15 - 0.45 (dimensionless).

3.4.1 Eye response to external measurements

The mathematical model was used to study the eye response to external IOP measurements. When an instrument like a tonometer was used to measure IOP the output that would be obtained would be recorded in the form of a pressure against time graph as illustrated in Figure 3.4 below. In tonometry, applanating $1.02 \times 10^{-5} m^2$ on the surface of the eye using a 5.5 gram weight causes IOP to rise instantly and decay with time thereafter.

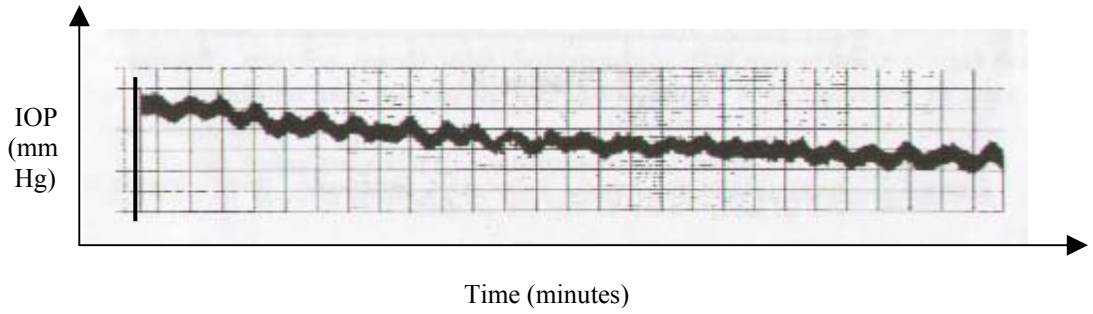

Figure 3.4 Illustration of a sample tonogram [35]

The model was used to calculate the change in IOP that will be obtained if a 5.5 gram weight similar to the one that was used in the tonogram was used to applanate $1.02 \times 10^{-5} m^2$ or take up 12.21 mm^3 of eye volume. The outflow facility level was taken to be 0.33 µl /min/mmHg, the value of rigidity was set at 0.15 and IOP was set at 15 mmHg in the model so that these values corresponded to the typical values for a normal eye. It was assumed that eye volume was changed in the first minute of the simulation. The results are presented in Figure 3.5 below.

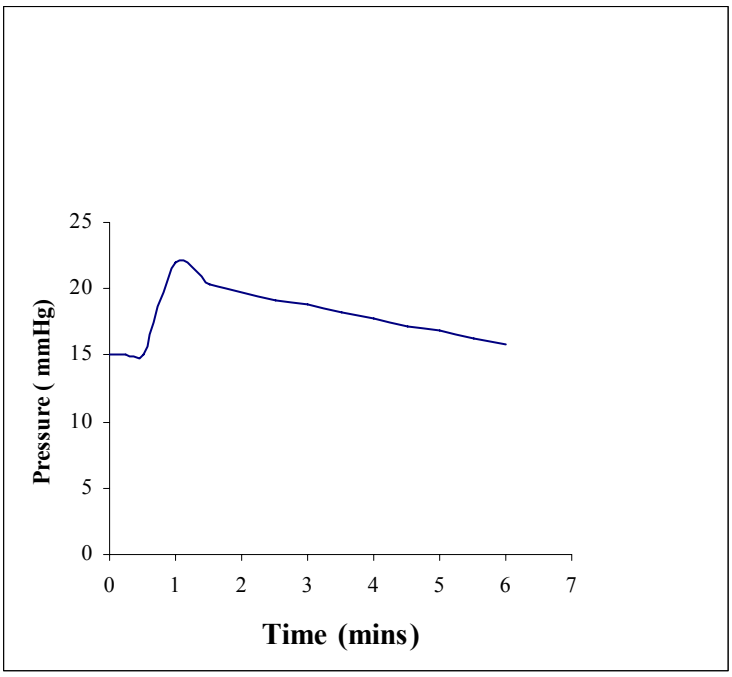

Figure 3.5 Output from model

It can be seen from Figure 3.5 that when values equal to those used in an external test are input into the mathematical model, it produces an output where IOP rises instantly after a change in eye volume. It has been quoted in the literature that a tonometer causes a 100% rise in IOP. However it can be observed from Figure 3.5 that the model shows that the initial rise in IOP is not as sharp as that in the tonogram and the rise in IOP less than 100%. As the effects of arterial pulsations have not been included in the model, the pulsations that are clearly visible in the sample tonogram (Figure 3.4) have not been reproduced in the model's output. Thus it can be noted that the model is able to reproduce the pressure trend produced by a tonometer. The model output will be further tested to see whether it is sensitive to changes in C_f and K.

3.4.2 Eye behaviour with glaucoma

The information presented in Figures 3.6 and 3.7 represent the sensitivity of IOP to changes in outflow facility (C_f) and rigidity (K).

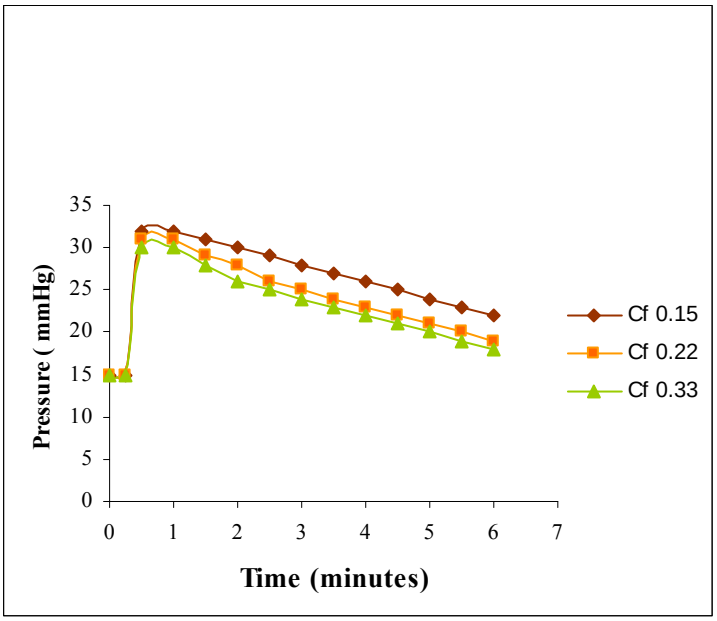

Figure 3.6 Effect of variation in C_f on IOP

Figure 3.6 shows that the output obtained from the model changes with C_f values. It can be seen that as C_f decreases and IOP rises to higher levels. The rate of fall of IOP is also noted to change along with the C_f values.

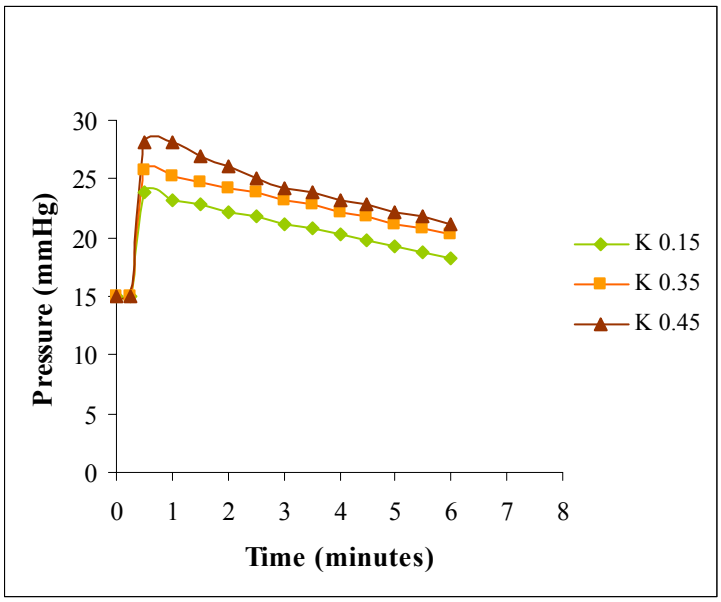

Figure 3.7 Effect of variation of rigidity values on IOP.

From Figure 3.7 it can be noted that as the rigidity of the eye shell increases, there is an increase in the level to which IOP rises for a given volume based change over time. Thus it can be seen that the mathematical model is capable of producing a response that illustrates the sensitivity of IOP rise and fall to changes in C_f and K values. This aspect of the model indicates that it can be used to analyse the behaviour of an eye when it is affected with glaucoma.

Hence it can be taken that the results from the model are comparable to those expected from external test measurements. The model can be used for further study and investigation of the requirements of MEMS based glaucoma monitoring system in this thesis.

3.5 Conclusion

The use of an experimental mathematical model of the eye is proposed and investigated for the analysis of an internal method of C_f based IOP monitoring by decreasing the volume of the eye. The capability of the mathematical model is illustrated by demonstrating its sensitivity to the key variables involved with the measurement. Comparing its output to that expected from external tests validates the use of the experimental mathematical model. The simulations have proven that the model will be useful for further study and investigation of glaucoma monitoring methods.

4 Investigating System Requirements

4.1 Introduction

It was determined previously that in order to continuously monitor glaucoma by tracking C_f levels, the IOP had to be temporarily raised inside the eye and the time taken for it to fall back to original level recorded. The investigations into the requirements of a MEMS system that will be capable of raising and measuring IOP inside the eye are outlined in this chapter. The mathematical model of the eye presented in the previous chapter was used for the investigations. The investigations were used to collect information to help determine the requirements of a micro system that was able to create the changes in the eye to enable C_f based IOP measurements.

4.2 Investigations

The first part of the investigations focused on deriving the requirements for raising IOP inside the eye and deriving the functional requirements of a suitable MEMS device from that method. The second part of the investigations determined the needs of a sensor that would be capable of capturing the required IOP measurements.

4.2.1. Requirement to raise IOP inside the eye

The objective of this section is to use the mathematical model of the eye to analyse how IOP can be raised inside the eye by 100% above the starting level.

4.2.1.1 Effect of varying eye volume

It is assumed in the mathematical model that the starting IOP in the eye is 15 mmHg. The value of outflow facility is taken as 0.30 mmHg/µl,/min and rigidity (K) taken at 0.15 (no units). These values represent normal conditions in the eye. In the simulation internal eye volume is taken to be 250 mm^3 based on the anterior chamber dimensions provided in [35] to be 250 µl, which represents the approximate volume of the anterior chamber. Eye volume is decreased by 45 mm^3, 55 mm^3, 65 mm^3 and 75 mm^3 using the model and the changes obtained in IOP for the different reductions in volume are presented in Figure 4.1 below.

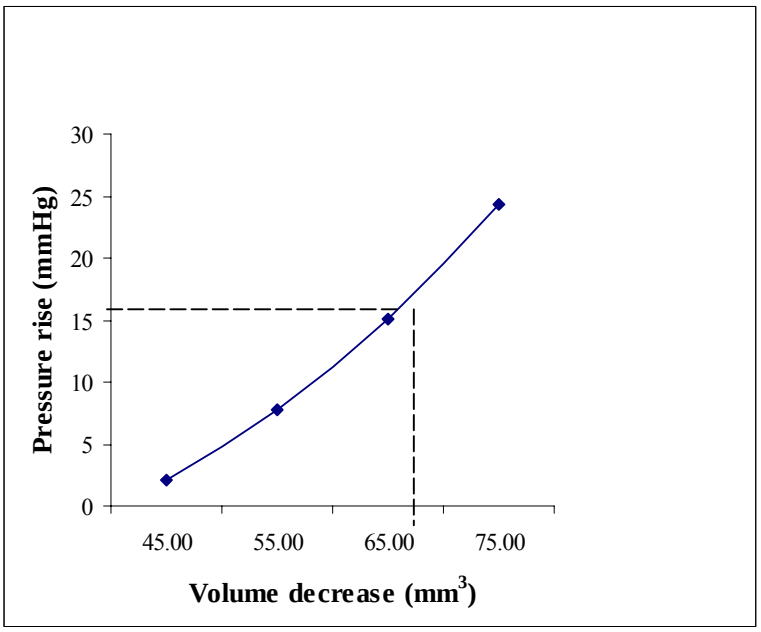

Figure 4.1 Pressure rise obtained vs decrease in eye volume

Given that the mathematical model was developed on the basis of the pressure volume relationship of the eye, it can be seen from Figure 4.1 that reducing the effective internal eye volume causes a rise in IOP. It is observed that an approximate decrease of 65 mm^3 in eye volume would cause IOP to rise by 15 mmHg which would equal a 100% rise from the starting pressure level. As the anterior chamber volume was taken to be 250 µl or 250 mm^3, decreasing its volume by 65mm^3 would be equal to taking up approximately 26% of internal eye volume.

4.2.1.2 Effect of varying duration of volume reduction.

It has been determined that IOP can be raised by reducing eye volume. The following sections will investigate the requirements of a MEMS device that will be able to raise IOP in the eye by reducing eye volume.

The following simulations were conducted to study the impact of duration of volume change on IOP rise. The values considered for the simulation were as follows: IOP = 15 mmHg, outflow facility (C_f) = 0.30 mmHg/µl/min, Rigidity (K) = 0.15 (no units), decrease in eye volume = 65 mm^3. The effect of providing volume reduction was studied over a period of several minutes and the results are presented in Figure 4.2. The symbol T_v in the figure represents the time at which volume reduction is commenced in the simulation.

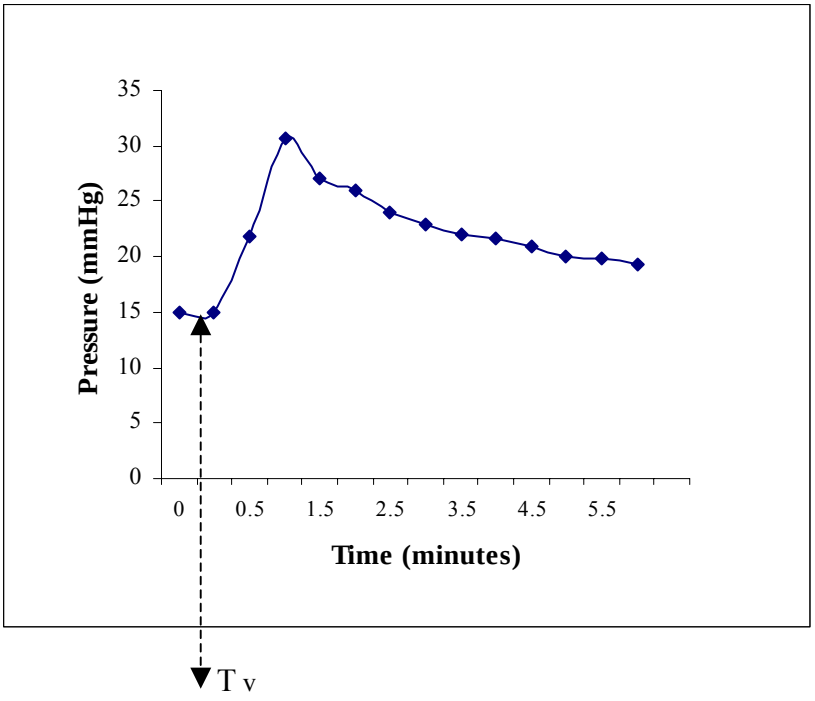

Figure 4.2 Effect of IOP rise with time due to volume reduction.

From Figure 4.2 it can be seen that providing a volume reduction causes IOP to rise from 15 to 30 mmHg (100% increase) under one minute. Under the effect of the volume change, IOP begins to fall rapidly after reaching a maximum and later stabilizes at 4 mmHg above the starting level.

Figure 4.2 illustrates that a pressure curve similar to the one produced by a tonometer (refer Figure 3.4) could be achieved inside the eye by creating a volume change within one minute and maintaining that change until the eye responds by reducing IOP.

4.2.1.3 Effect of varying magnitude of volume reduction

The following simulations were conducted to study the effect of magnitude and time-based differences of volume change on IOP rise. The values considered for the simulation were as follows, IOP = 15 mmHg, outflow facility (C_f) = 0.30 mmHg/µl/min, Rigidity (K) = 0.15, decrease in eye volume = 5-65 mm^3. The effect of variation in the magnitude of volume reduction on IOP was noted for two minutes and results are presented in Figure 4.3.

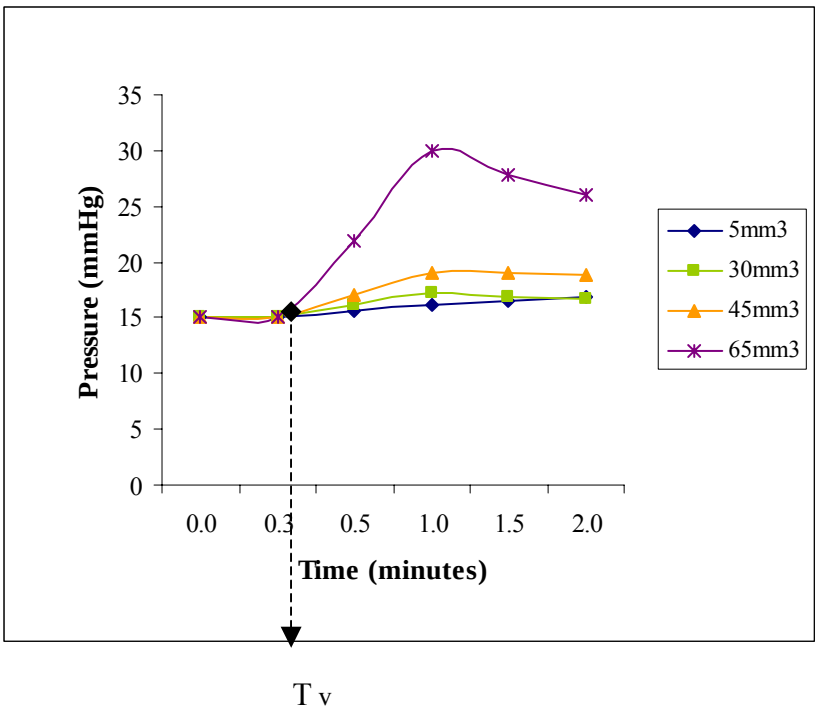

Figure 4.3 Pressure rise vs time for different volume magnitudes

It can be observed from the figure that the rise in IOP obtained by reducing 65 mm^3 of eye volume would be 100%. The figure also shows that reducing volume by 5mm^3 or less would cause little or no rise in IOP.

It can be noted that the volume change is assumed to be provided instantly in the above simulations. The effect of delaying the time in which the volume reduction comes into full effect is studied by increasing the time taken to reduce eye volume by from one to four minutes approximately. The values considered for the simulation are as follows starting IOP = 15 mmHg, outflow facility (C_f) = 0.30 mmHg/µl/min, Rigidity (K) = 0.15, decrease in eye volume = 65 mm^3 .The results are presented in Figure 4.4.

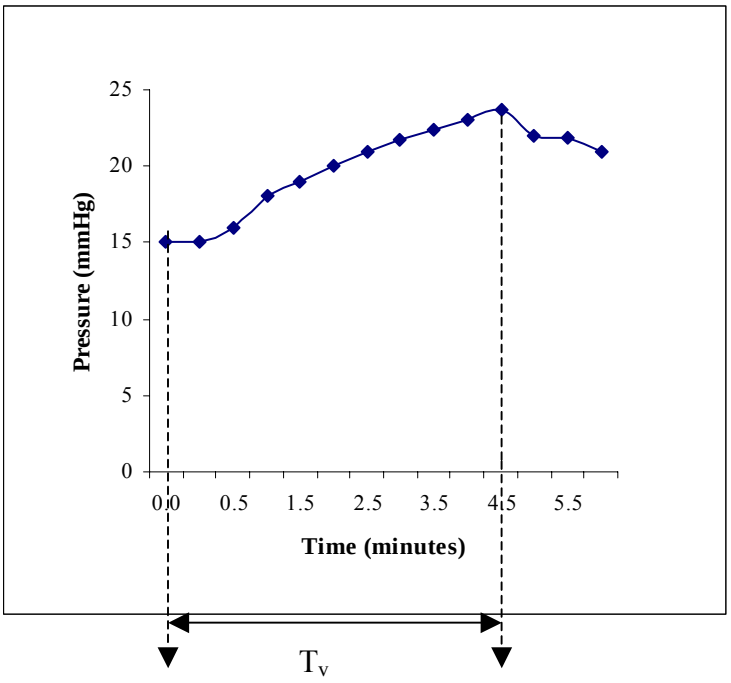

Figure 4.4 Effect of IOP rise with delayed T_v

It can be seen that from the results plotted in Figure 4.4 that if the volume change is not provided instantly then IOP does not rise sharply. IOP does not climb to 100% even after the reduction in volume comes into full effect as it did previously when the volume reduction was provided instantly (refer Figure 4.3).

If the reduction in eye volume could be translated to an increase in the size of a potential device that could expand to take up 26% of eye volume, then such a device

could be used for raising IOP internally. It has been demonstrated earlier that a volume reduction of less than 5mm^3 does not affect IOP. Therefore, the effect on IOP if a device of initial size less than 5mm^3 were to be implanted in the anterior chamber whose size could be increased to approximately 65 mm^3 within a minute, is simulated using the mathematical model. The results obtained are presented in Figure 4.5 below.

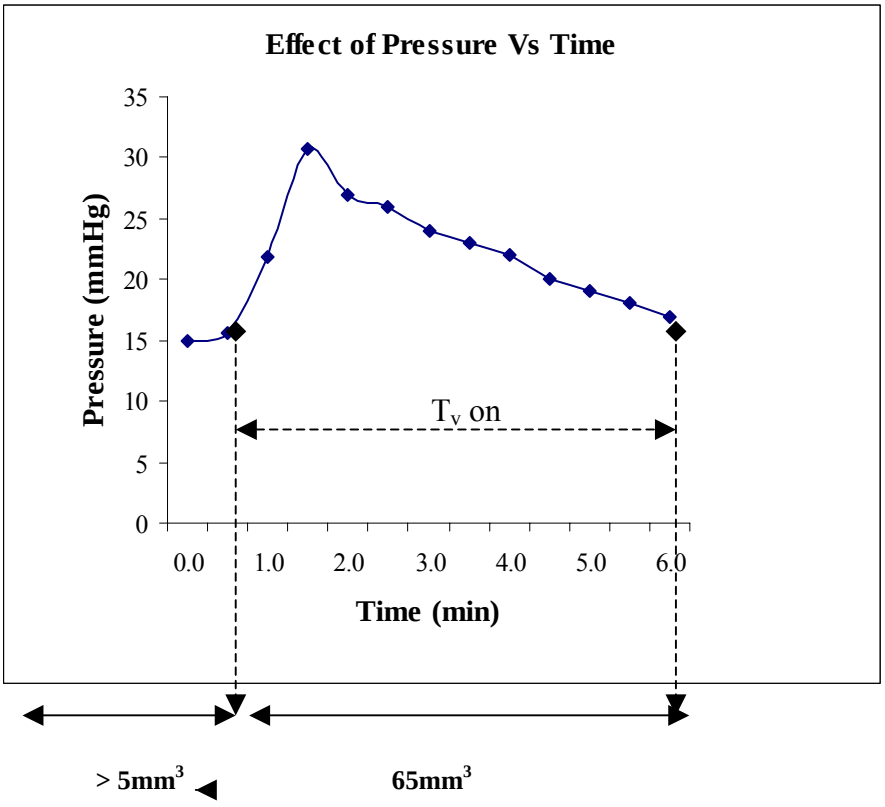

Figure 4.5 Pressure rise Vs Time based on change in magnitude of volume reduction.

The results show that the effect of reducing eye volume from 5mm^3 to 65mm^3 instantly would be similar to the IOP curve obtained from a tonometer. The Figure 4.5 shows that if a device of initial size less than 5mm^3 were to be implanted in the eye, then IOP could be raised by making the device expand to 65mm^3 instantly. The symbol T_v on represents the time for which the change in volume is maintained in the simulation.

Thus, it has been demonstrated that the first requirement of monitoring C_f levels, that is, to raise IOP by 100% within the eye, could be achieved by reducing the internal eye volume by approximately 26%. The change in eye volume would have to be maintained

until the eye responded by reducing IOP to a starting level for the measurement to be completed.

4.2.1. 4 Energy required

An estimation of the energy that will be required for instantly taking up 26% of internal eye volume is calculated in this section.

The calculations are based on the pressure-volume work relation for an isothermal system as the volume reduction in the eye is assumed to be initiated at constant pressure where there is no exchange of thermal energy involved. The work that will be done to create the volume change is calculated using Equation 4.1 below.

$$W = - P\Delta V \qquad (4.1)$$

As it is assumed that an internal structural would expand in volume and spend energy to reduce the effective internal volume of the eye, the value for the work done is given a negative sign. The energy that will be calculated is for the time taken to initiate a volume change until IOP rises and stabilises.

The values used in the simulation were as follows:

$P = IOP = 15$ mmHg

ΔV = eye volume reduction /volume change end time - volume change start time = one minute.

Eye volume was reduced by 45 mm^3, 55 mm^3 and 65 mm^3 respectively over one minute, with C_f = 0.30 mmHg/µl/min and Rigidity (K) = 0.15. The change in eye volume was carried out instantaneously and the energy consumed for every step reduction in volume observations was recorded in Figure 4.7.

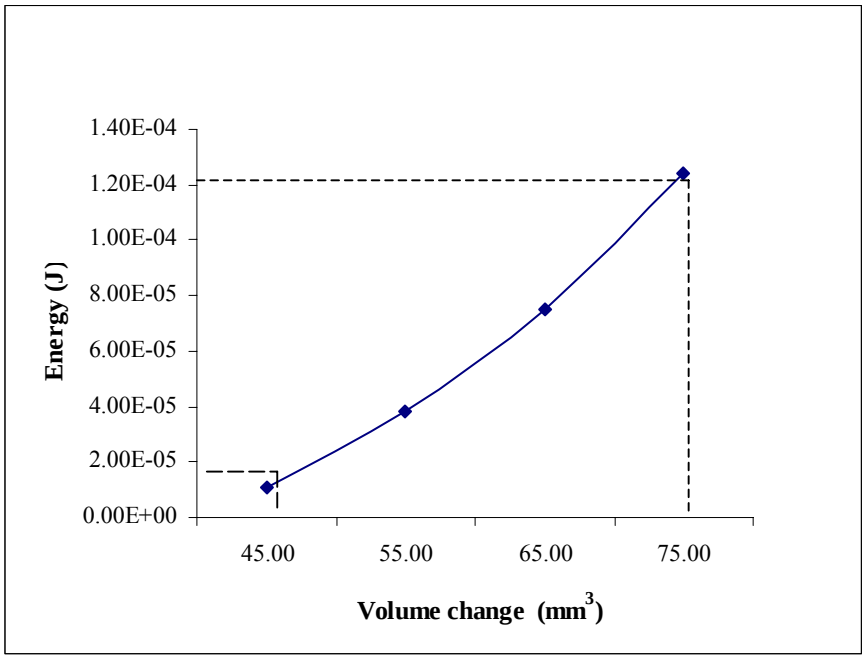

Figure 4.6 Energy consumed Vs eye volume change

It was noted from Figure 4.6 that the energy consumed during a volume change in the eye increased along with the magnitude of the volume change. The energy that would be consumed by a 45 mm^3 volume change was calculated to be $1.09e^{-5}J$, which increased to $7.5e^{-5}J$ for 65 mm^3 and to 0.00012J for a 75 mm^3 reduction in eye volume respectively.

It was shown in Section 4.2.1a that in order to raise IOP by 100% inside the eye, the volume reduction would have to be equal to approximately $65mm^3$. The energy required to reduce internal eye volume by 65 mm^3 would be 7.5 $e^{-5}J$. This value only provides an indication of the energy that will be required to create the change in volume inside the eye.

The total energy required to conduct the measurement will depend on forces that will be required to keep the volume change in place until the measurement is completed which depend upon the type of actuator that would be employed for the purpose and its physical characteristics. As the characterization of an actuator is outside of the scope of this thesis, the total energy required for the measurement is not calculated here.

However, a brief introduction to the type of miniature actuator that could be used for the volume change is provided in Chapter 7 (refer to Section 7.2).

4.2.2 Requirement to measure IOP

The following simulations were conducted to analyse the effects of measuring IOP inside the eye after raising it by 100%. The requirements of a miniature sensor that will be capable of measuring IOP internally will be brought forward by the investigations presented in this section.

4.2.2.1 Sensitivity of Pressure sensor

It was found in Section 3.3 that during external measurements, a difference in the level of C_f in the eye served to indicate an increase in the severity of glaucoma. The following simulation was conducted to determine the kind of pressure information that will need to be recorded by an internal sensor. The values used in the simulation are as follows:

IOP = 15 mmHg,
Rigidity (K) = 0.15
Decrease in eye volume = 65 mm^3

The IOP fall was recorded immediately after starting the volume reduction. The value of outflow facility was decreased from 0.30mmHg/µl/min to 0.15mmHg/µl/min to study its impact on sensor activity. The results are recorded in Figure 4.7 below.

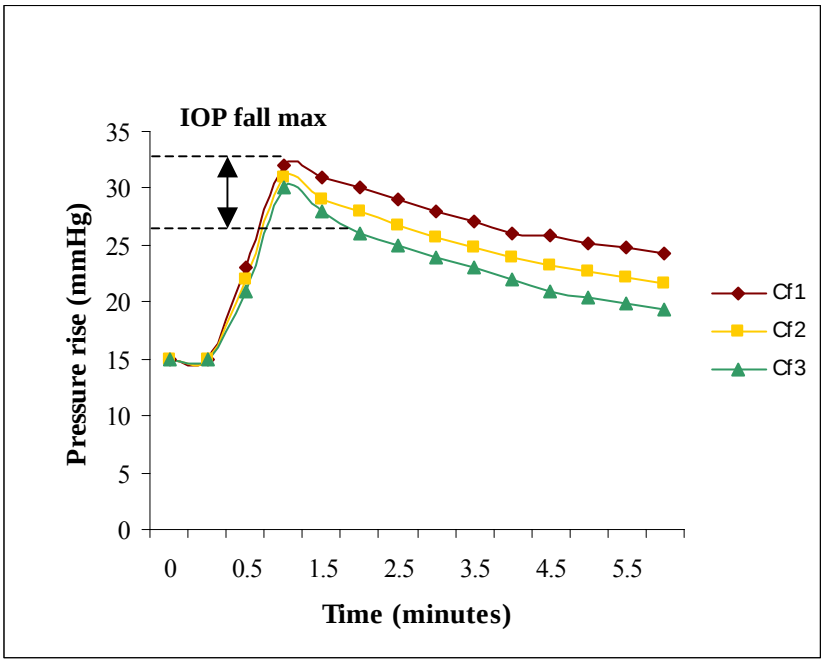

Figure 4.7 Indication of time for recording IOP fall

The legends C_f1 = 0.15mmHg/µl/min (poor), C_f2 = 0.22mmHg/µl/min (mildly low) and C_f3 = 0.33mmHg/µl/min (normal), represent typical levels of outflow facility in the eye. The symbol IOP fall max indicates the time during which there is maximum fall in IOP.

It can be seen from Figure 4.9 that eyes with smaller C_f values show a slower rate of fall of IOP. The fall per minute of IOP for an eye with normal outflow facility, C_f = 0.33mmHg/µl/min denoted in the figure by the green curve is quicker than the fall per minute observed in an eye with poor outflow facility, A = 0.15mmHg/µl/min, that is denoted by the red curve in the same figure.

Thus, it can be observed from the simulation that the fall of IOP for an eye with very poor outflow facility was less than 1 mmHg per minute (from 31 mmHg to 30 mmHg) and was up to 5 mmHg per minute for an eye with normal outflow facility (30 mmHg to 26 mmHg). It is noted that the IOP fall in the first minute of the simulation was comparable to the clinical values recorded by other glaucoma researchers [24]. Thus, for a pressure sensor to be sensitive to changes in C_f values, it should be capable of recording the fall of 1mmHg of IOP over one minute.

The symbol Pressure fall max in Figure 4.7 represents the time of the maximum rate of fall of IOP. If a sensor could produce an output such that the difference in the rate of fall of IOP can be detected, then it could provide an indication of the level of glaucoma in the individual's eye. The simulation demonstrates that the sensitivity of the sensor would have to extend between approximately 1mmHg/min to 4mmHg/min.

4.2.2.2 Alarm levels

From the results presented in Figure 4.8, it can be inferred that if the pressure information from the sensor were to be processed electronically to calculate the rate of fall of IOP, then an alarm indicating the level of C_f can be issued to alert a patient to the change. Figure 4.10 below shows the potential alarm conditions for a glaucoma patient based on the simulation results.

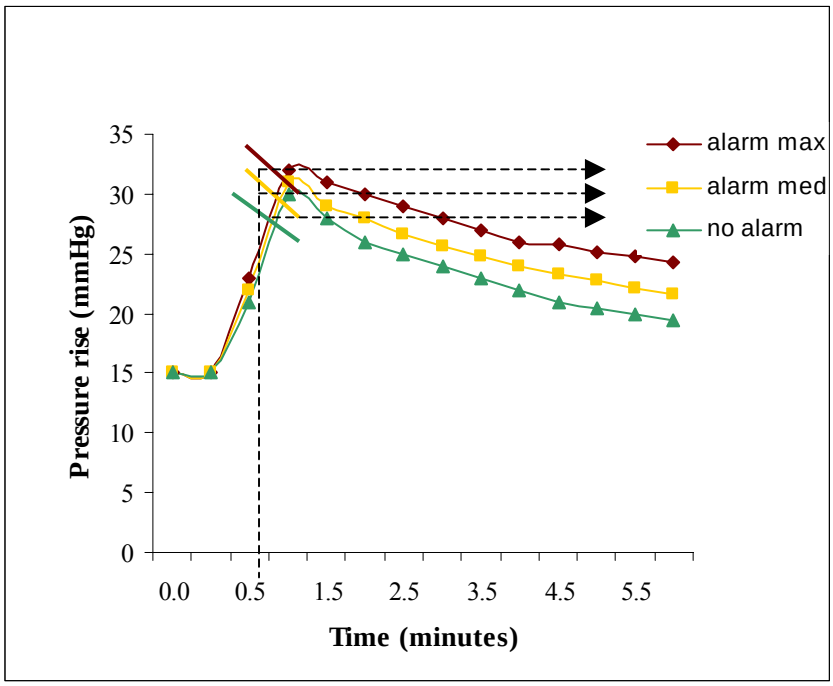

Figure 4.8 Alarm Indication

If the rate of fall was calculated to be less than 1mmHg/min, it would indicate a severely low level of C_f (alarm max). Rates closer to 2mmHg/min would indicate a mild decrease in C_f (alarm med) and fall rates of 4mmHg/min or more would indicate a normal C_f level (no alarm). The alarm levels could provide an instant indication of the condition to the patient after processing the IOP information.

Thus, it has been demonstrated that in order to monitor C_f levels by measuring the rate of fall of IOP, a pressure sensor with a resolution of 1mmHg would be required.

4.3 Schematic of a MEMS glaucoma monitoring device

A schematic representation of a MEMS device that can monitor glaucoma from inside the eye can be drawn from the results of the investigations undertaken in Section 4.2. Figure 4.9 below illustrates the location of the inside the anterior chamber of the eye.

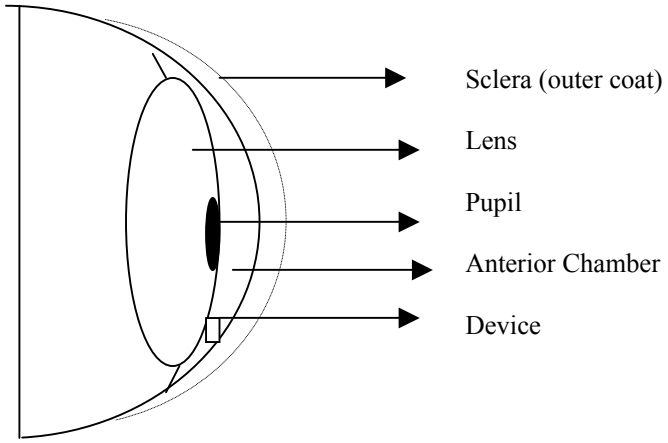

Figure 4.9 Location of Device inside eye.

It was determined that if a device were to be employed for internally raising IOP by 100%, its dimensions should be equal to 4×4×4mm or approximately 65mm^3. The device could increase from a minimum size (less than 5mm^3) to 65mm^3 so that it could remain implanted without affecting IOP levels outside of measurement times. It has been calculated that the space taken up by the 65mm^3 reduction in eye volume will be equivalent to taking up 26% of internal eye volume.

An illustration of the proposed structure of the device during measurement is provided in Figure 4.10. It is assumed in the illustration that the fully expanded size of the device will not cover the pupil and not interfere with visual activity. Therefore, the size of the device before and during measurement will be suitable for implanting within the anterior chamber of the eye.

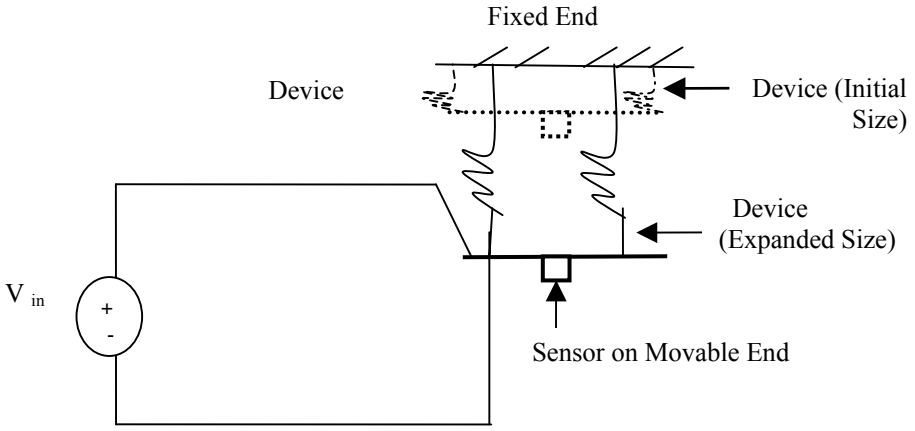

Figure 4.10 Schematic of Structure of Device and Sensor

4.3.1. Discussion

Figure 4.10 shows that the device could possibly have fixed and movable ends both attached to a material with elastic capability, which will allow for the increase in size required for measurement. The increase in the size of the device would have to be maintained until a sensor recorded the rate of fall of IOP (shown in Figure 4.9) and the measurement completed.

The energy that will be required to create the volume change inside the eye was calculated to be $7.5e^{-5}$J. There has been the mention of thin batteries of 20mAh ratings (400μm thick) and micro-batteries with ratings of 100μAh/cm^2 (< 10μm thick) that could be suitable for powering implants [72].

The thin batteries (400μm thick) that are currently available are large in size (2.5×2.9cm^2). The micro-batteries (< 10μm thick) that may be suitable for implanting within the anterior chamber of the eye are still under development [72].

If it were assumed that a 100μAh/cm^2 micro-battery were assumed to be used for powering the device, then the energy required for one measurement (7.5 e^{-5}J) will be equal to draining 1.25μA of current per second from the battery. If it were assumed that

the time taken to conduct a test is approximately one minute, then it would be possible to extract 4,320 tests continuously from such a battery. This translates as being able to conduct one test daily for 11 years. Thus a portion of the powering requirements for the measurement could be met by available technology.

4.4 Conclusion

The feasibility of internally monitoring C_f by artificially reducing the eye volume and measuring the response of the eye in terms of rate of fall of pressure has been explored through the investigations conducted using a mathematical model of the eye. The details specific to the measurement method are thoroughly investigated in this chapter. The investigations have revealed that it will be possible to measure C_f based on IOP from within the eye.

It has been determined analytically that IOP can be raised instantly by reducing the inner eye volume using a miniature device that can increase in size from 2×2×1.5 mm to 4×4×4 mm. In order for the eye's response to be captured effectively, the rate of fall of IOP in the eye will have to be recorded soon after the increase in device volume and the change will need to be maintained until a pressure sensor records the rate of fall of IOP.

Based on the requirements of the device, it can be inferred that the mechanism suited to increase its volume and reduce the effective eye volume could be modelled as an elastic body with potential energy to which a pressure sensor could be attached to make the required measurements. The energy consumed by the measurement method can be met by currently available micro-batteries.

The requirements specific to sensitivity and resolution of the sensor have been established through the investigations. The development of a suitable miniature pressure sensor required to accompany the glaucoma monitoring device will be explained in the next chapter.

5 Development of MEMS Pressure Sensor

5.1 Introduction

The need for a miniature pressure sensor was established in the previous chapter and its requirements were investigated. Based on those requirements investigations relating to the size, dimensions and the range of output voltages that will be obtained from such a sensor capable of sensing the rate of fall of IOP in an eye will be discussed in this chapter.

5.2 Piezoresistive Pressure Sensing

Piezoresistive pressure sensing technology facilitates the development of miniature pressure sensors that can be easily combined with simple signal conditioning electronics and are suitable for use along with implantable devices [73]. They have been reported to have the advantage of combining simple circuitry and small size of the sensing element with good sensitivity over capacitive pressure sensors which require reference pressure elements, complex signal conditioning circuitry and suffer from high electromagnetic interference [60]. The response time of these sensors has been measured to lie within a few milliseconds and their fabrication and packaging methods are very popular with industry. Therefore piezoresistive pressure sensing technology will be used in this

chapter to develop a MEMS pressure sensor that can be made small enough to be combined with a miniature device and monitor IOP.

5.2.1 Theory

Dr. Charles S Smith discovered the Piezoresistive effect in 1954 [74], the effect was defined as the change in resistivity of certain materials due to applied mechanical stress/strain. When a material experiences a strain due to an applied mechanical load, the strain varies the inherent resistivity of the material by altering the position and motion of the constituent atoms in the material. Silicon was discovered to possess excellent piezoresistive characteristics, twenty times larger than those of other metals, and has been used since 1974 to produce pressure sensors [75]. For a three dimensional silicon crystal, the electric field vector (ε) is related to the current vector (J) given by Equation 5.1 below where it can be seen that the electrical resistivity of a piezoresistive material is dependant on stress.

$$\varepsilon = [\rho_e + \pi + \sigma] \cdot J \qquad (5.1)$$

where

ε = Electric Field vector

J = Current Density

ρ_e = Resistivity Tensor

π = Piezoresistive tensor

σ = Stress tensor

Electrical connections made into the material enable conversion of the change in resistivity of the piezoresistive material into a measurable electrical signal. The mechanical and electronic properties of silicon enable the excellent conversion of a mechanical deformation into an electrical signal.

5.2.2 Use of Piezoresistive Pressure sensors

The first monolithic integrated piezoresistive pressure sensors were developed in the 1970s and since then have found widespread commercial applications. C.C Collins proposed the feasibility of using a miniature transcutaneous pressure transponder [46] based on the piezoresistive theory, to be suited for biomedical applications. Though there have not been many reports of the use of piezoresistive pressure sensing for the development of IOP implants they are still very popular for industrial applications such as environmental monitoring, tyre gauge monitoring, barometric sensing, use in medical instrumentation and monitoring, pneumatic gauges, engine control and in home appliances.

Very low range piezoresistive pressure sensors (0-0.75006 mmHg) are sold by a number of companies around the world. Figures 5.1 and 5.2 illustrate the front view and side view of the dimensions of a typical miniature pressure sensor.

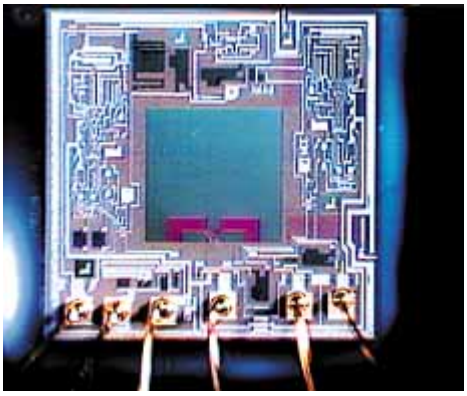

Figure 5.1 Front view of a miniature pressure sensor [76]

The silicon membrane used for sensing pressure is usually a square as shown in the figure above and lies on the top face of the die. It is smaller in size than the die itself. Piezoresistors whose resistance changes with accordance to pressure applied on the silicon membrane are embedded onto it. The sensing elements and electronics are built

on the top side of the sensor, which is supported on either side by pedestals and sidewalls that form a part of the packaging. Figure 5.2 shows the typical dimensions of a low pressure piezoresistive sensor.

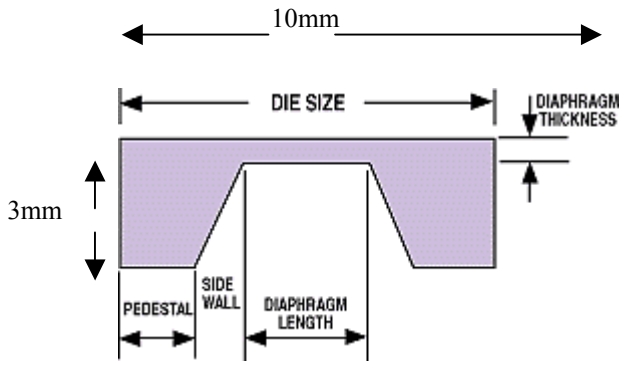

Figure 5.2 Side view of a miniature pressure sensor [76]

From the above figures it can be seen that the dimensions of a typical low pressure sensor are of the order of several millimetres and not suitable for implanting. Table 5.1 lists some of the sizes and applications of a few commercial low pressure range piezoresisitive pressure sensors, available today.

From Table 5.1 typical values for the size of a silicon die are found to range between 650 µm and 25 µm. Few of these sensors are capable of measuring pressures in the range of 0 to few thousand mmHg [79], [76]. One of the smallest single chip absolute pressure dies available in the market, the SM5108 manufactured by SI Microsystems [79], measures 650×650×650 µm and has a range of 0-772 mmHg with a span of 30mV.However, for the very low pressure range (0-375 mmHg) the size of the sensor die in the [76] and [77] sensors starts at 2.5 mm reaching up to 21mm with a span of 30 mV.

PRODUCT	RANGE (mmHg)	SPAN	TYPE	VIN	APPLICATIONS	SENSOR AREA (A) & THICKNESS (T)	RESPONSE TIME	REFERENCE
Mouser 1263	0-15	20 mV	Differential/ absolute	16V	HVAC, Medical instrumentation, Environmental control	A-27 mm by 12.2 mm T – N/A	-	[77]
MPXM2053	0-375	40 mV	Gauge	16 V	Robotics, Pressure-Switching Controllers, Non-Invasive pressure monitoring	-	1 m Sec	[78]
SM-5108	0-772.56	35mV	Absolute	5V	Tyre pressure monitoring Engine control, Pneumatic gauges	A - 0.65mm ×0.65mm T- 0.65mm	-	[79]
Motorola X - ducer	750	40mV	Absolute	5V	Load, Level monitoring, Engine management, Personal blood and bedside pressure meters.	A- 2.5×2.76mm T- 25 μm thick	-	[76]
SM-5103	15-150	75mV	Gauge	5 V	Gas analysis, HVAC, level detection	A-3.4mm×3.2 mm. T -0.5mm	-	[80]

Table 5.1- Commercially available low pressure piezoresistive sensors

Thus it can be observed that when the pressure range is decreased then the size of the pressure sensor increases. The miniature low- pressure sensors documented in the literature have not been characterised to measure IOP [77], [80]. Information that will be required for the use of a very small membrane inside the eye like the size of the sensing membrane and the range of output voltages that can be obtained from it will be determined in the following sections of this chapter.

5.3 Investigating reduction in size of sensor membrane

In order to capture the physics of the problem, the calculations were based on finite element (FEM) analysis. FEM software, ANSYS (version 7) [81]was used to compare the theoretical predictions for load-deflection behaviour of thin membrane structures. A thin elastic structural element denominated as shell-63 in the ANSYS element reference library, having 8 nodes and three degrees of freedom was used to simulate the MEMS pressure sensor membrane.

5.3.1 Sensor Deflection

An analysis will be performed in this section to see how reducing the typical dimensions of a sensor membrane will affect its response. The response of a sensor membrane is measurable only if the deflections under applied pressure loads are well under the breaking limit of the membrane and are repeatable [82]. Silicon has been documented to produce repeatable deflection under an applied load, but when considering very small membrane dimensions, it needs to be investigated whether the deflections will be under the breaking range of the membrane. Figure 5.3 below shows how pressure will be applied uniformly across the surface of the membrane in the z direction.

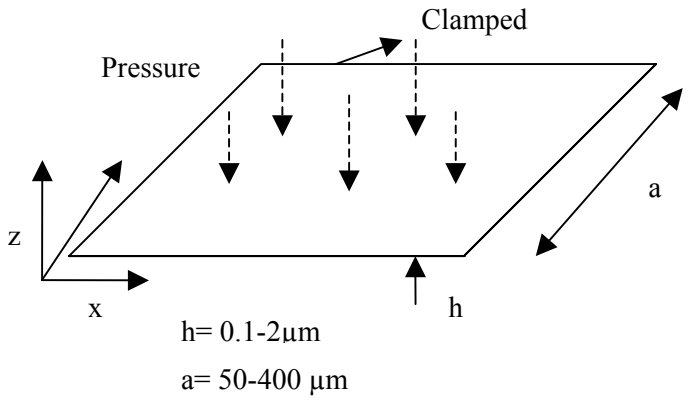

Figure 5.3 Top surface of square sensor membrane with side (a) and thickness (h)

The size (a) of the sensor will be varied between 50µm and 400 µm and the thickness of the membrane will be varied at 0.1µm, 0.2µm, 1µm and 2µm respectively. The membrane will be subjected to IOP as surface loads each time. The range of pressures applied will fall between 15 mmHg and 48.754 mmHg that correspond to the range of 15mmHg-50 mmHg. Investigations will be carried out using the linear- small deflection theory for elastic materials proposed in [83]. When it is considered that all the edges of a membrane will be clamped to ensure maximum response under load application, Timoshenko predicted that the maximum deflection for a fully clamped square structure could be calculated by Equation 5.1[84].

$$W_{max} = 0.00126 \times \left(\frac{P \times a^4}{D} \right) \qquad (5.1)$$

where,

P = Pressure applied

h = Thickness of the diaphragm

a = Width of plate

D = Flexural rigidity of the plate.

For a square diaphragm, fully clamped on all four sides as shown in Figure 5.2 the flexural rigidity is given in [84] according to Equation 5.1.

$$D = \frac{Eh^3}{11} \qquad \text{(no units)} \qquad (5.2)$$

where, the parameters used were, E (Young's Modulus of Silicon) = 16.825×10^9 kg/m^2.

The deflections that would be obtained from the membranes were calculated theoretically using Equation 5.1 and verified using Finite Element Method Software (FEM) [85]. The results obtained from the software were within 1% of those predicted theoretically and are plotted in Figures 5.3 and 5.4.

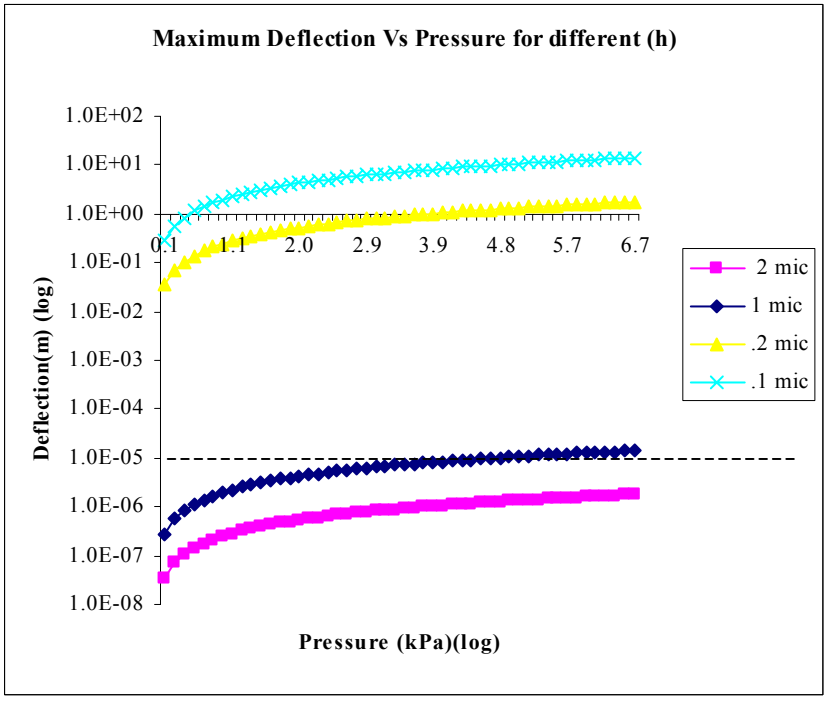

Figure 5.3 Range of deflections obtained for different values of thickness (h).

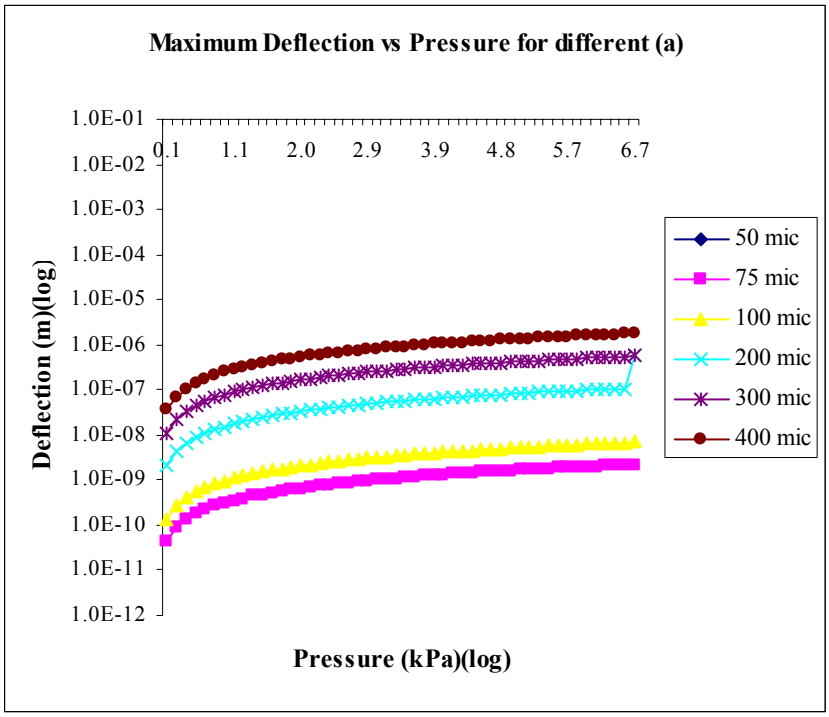

Figure 5.4 Range of deflections obtained for different values of side (a).

5.3.2 Discussion

From the analysis it was found that for a thickness h < 2 µm, the maximum deflections exceeded the thickness of the membrane. The horizontal dotted line in Figure 5.3 indicates the points beyond which the deflections exceed the thickness of the membrane. Therefore only a diaphragm thickness of 2 µm produced deflections that were well under their thickness when subjected to surface loads in the IOP range. Reducing the size of the diaphragm below 400 µm produced deflections in the range of 10^{-12} m upon application of IOP loads as seen in figure 5.4. As deflections in the range of 0.1×10^{-9} m can be more easily detected than deflections of the order of 10^{-12} m, a combination of a 400 µm wide membrane with a thickness of 2 µm is considered for further analysis.

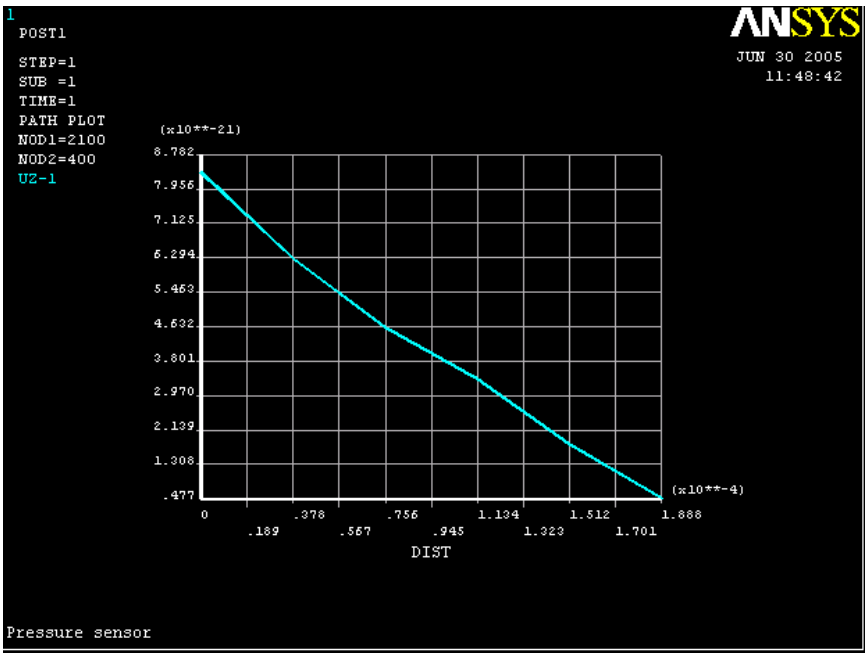

Figure 5.5 range and pattern of deflections obtained on the surface of the membrane

The figure 5.5 above plots the deflections from the centre of a membrane to its edge. From the FEM analysis it was determined that the deflections obtained was maximum at the centre (0, 0) of the membrane and was minimum at the edges. The results obtained were symmetrical along both the x and y axes.

Table 5.2 below lists the maximum deflection that will be obtained from the 400×400×2 µm sensor under typical IOP loads. As IOP in human eyes does not exceed 50.5mmHg even under worst circumstances, it can be seen from table 5.6 that the maximum deflection from the sensor corresponding to that pressure can be seen to be less than 50% of the membrane thickness.

IOP (mmHg)	Maximum Deflection (m)
15	5.7×10^{-7}
18.75	7.1×10^{-7}
24.75	8.9×10^{-7}
30	1.1×10^{-6}
34.50	1.2×10^{-6}
37.50	1.3×10^{-6}
41.25	1.8×10^{-6}
45	1.7×10^{-6}
50.25	1.8×10^{-6}

Table 5.2 IOP and corresponding values of maximum deflection

The overall size and thickness of the sensor are reduced by 250 μm and 600 μm respectively. The range of deflections obtained for a membrane of these dimensions when subjected to IOP loads were between 0.07 μm and 1.8 μm. Therefore we can conclude that a smaller square sensor membrane of dimensions 400×400×2 μm will ensure a stable response under the IOP range that needs to be monitored in glaucoma.

5.4 Determining the Electrical Output from the Pressure Sensor

As a first step towards determining an electrical output from the sensor, an analysis of the stresses that will be created on the sensor due to IOP loads will be studied using FEM software. The stress analysis will help to provide an understanding of the factors that will affect the placement and location of piezoresistors, which will play a major role in determining the electrical output from the sensor.

5.4.1 Stress Analysis

IOP is assumed to be applied uniformly over the x-y plane that deforms in the z plane as given in Figure 5.6 below.

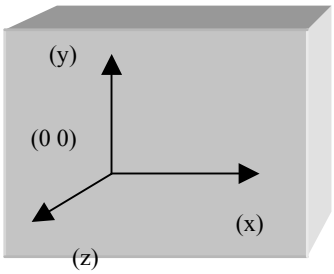

Figure 5.6 Silicon membrane with centre (0, 0), and direction (z) of pressure application

The surface stresses are calculated by the software according to Equations 5.3 and 5.4 below where T_x denotes in plane forces along the x axis, T_y denotes in plane forces along the y axis, t is the thickness at the midpoint of the element along the z axis, σ_x denotes surface stresses that will be output in the x direction and σ_y denotes the surface stresses that will be output in the y direction.

$$T_x = \frac{t(\sigma_x \text{top} + 4\sigma_x \text{mid} + \sigma_x \text{bot})}{6} \tag{5.3}$$

$$T_y = \frac{t(\sigma_y \text{top} + 4\sigma_y \text{mid} + \sigma_y \text{bot})}{6} \tag{5.4}$$

The pattern of stresses obtained from the FEM analyses of the silicon micro-membrane were consistent with the Timoshenko's predictions in [84] and are illustrated in Figure 5.7 below. The regions of maximum stress along the transverse direction are depicted in

the figure. It can be seen that the stresses were maximum at the clamped edge centres and minimal at the unbound centre of the membrane.

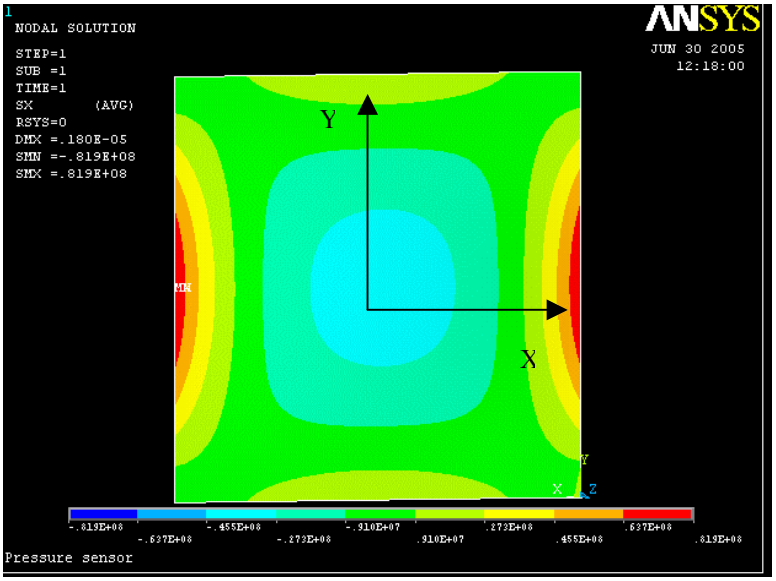

Figure5.7 Pattern of Stresses obtained on the sensor membrane (along transverse axis).

The stress pattern was found to vary similarly for longitudinal stress along the y axis due to the symmetry of the membrane. This is illustrated in Figures 5.8 and 5.9, which depict the stress variation from the edge centre to the ends of the membranes along x (transverse stress) and y (longitudinal stress) axes individually.

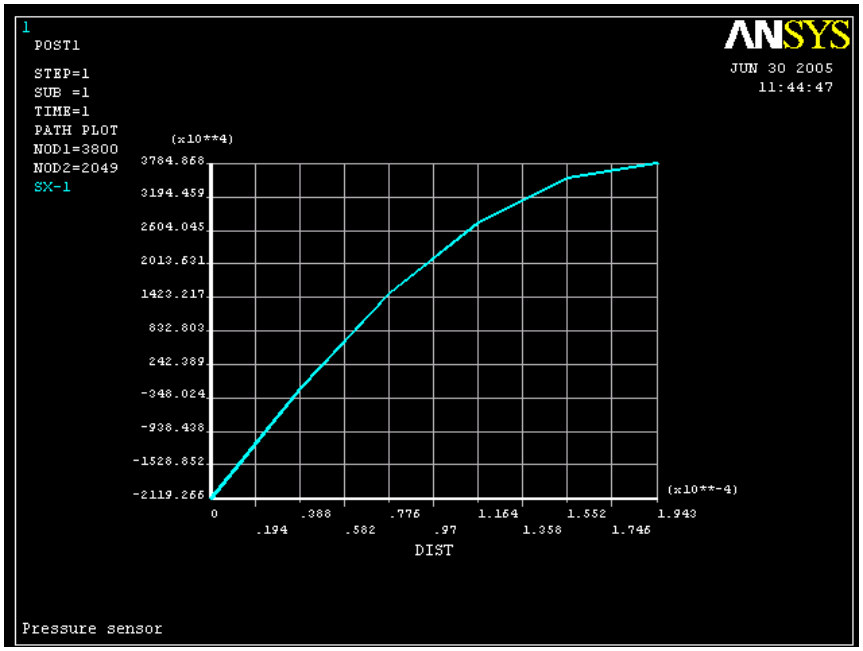

Figure 5.8 Pattern of stresses along x axis of the membrane

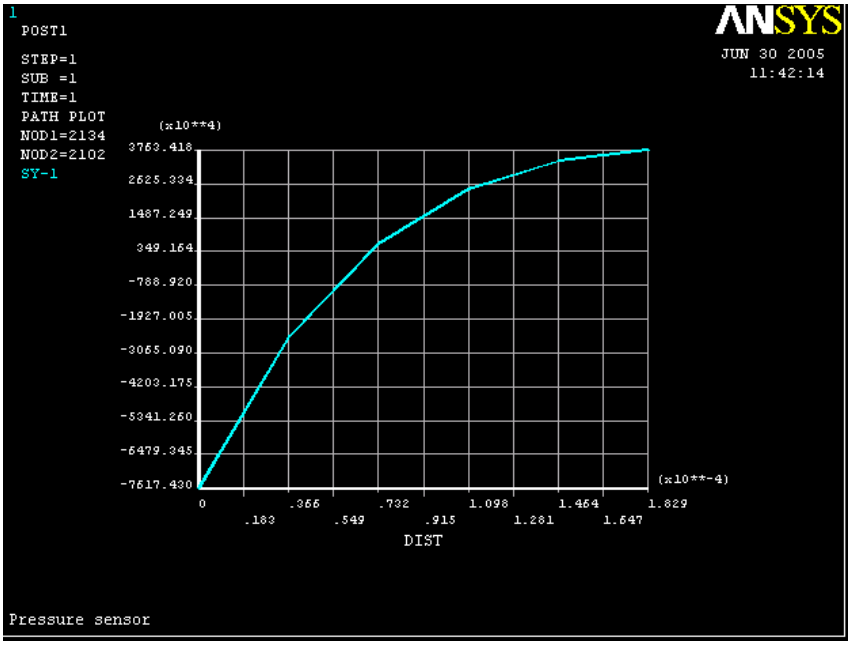

Figure 5.9 Pattern of stresses along the y axis of the membrane

The pattern of stress variation remained similar when the simulations were repeated for different IOP loads, with a noticeable increase only in the magnitude of the stress. The maximum stresses obtained along the longitudinal and transverse directions for the different IOP loads applied on the membrane are listed in table 5.2 below. The stresses were determined from the FEM analysis to lie between 18.4×10^{4}mmHg to and 61.4×10^{4}mmHg

IOP (mmHg)	**$\sigma_{xx\ max}$ (Pa) or (7×10^{-3} mmHg)**	**$\sigma_{yy\ max}$ (Pa) or (7×10^{-3} mmHg)**
7.5	1.4×10^{10}	1.37×10^{10}
15	2.5×10^{10}	2.46×10^{10}
22.5	3.3×10^{10}	3.28×10^{10}
30	4.1×10^{10}	4.09×10^{10}
37.5	5.73×10^{10}	5.73×10^{10}
45	6.55×10^{10}	6.55×10^{10}
52.5	8.19×10^{10}	8.19×10^{10}

Table 5.3 Stresses obtained on sensor as a result of IOP loads.

where,

$\sigma_{xx\ max}$ = Maximum edge centre stresses along x axis

$\sigma_{yy\ max}$ = Maximum edge centre stresses along y axis

From Table 5.2 it can be observed that the stresses along the transverse and longitudinal axes are similar in magnitude. As the stress created under the maximum IOP load of 50.25 mmHg was found to be 61.4×10^{4}mmHg, it led to the interpretation that the stress magnitude would be under the 22.5×10^{6} mmHg - 60×10^{6}mmHg, breaking limit of silicon [77]. Thus the pattern and magnitude of stresses that will be created as a result of IOP loads have been determined from analysis. It can be stated that a silicon membrane having dimensions $400\times400\times2$ μm can withstand IOP loads.

5.4.2 Wheatstone Bridge and Piezoresistors

A Wheatstone bridge circuit configuration is traditionally used to derive an electrical output from a piezoresistive pressure sensor [60]. A typical Wheatstone bridge circuit is illustrated in Figure 5.10 below.

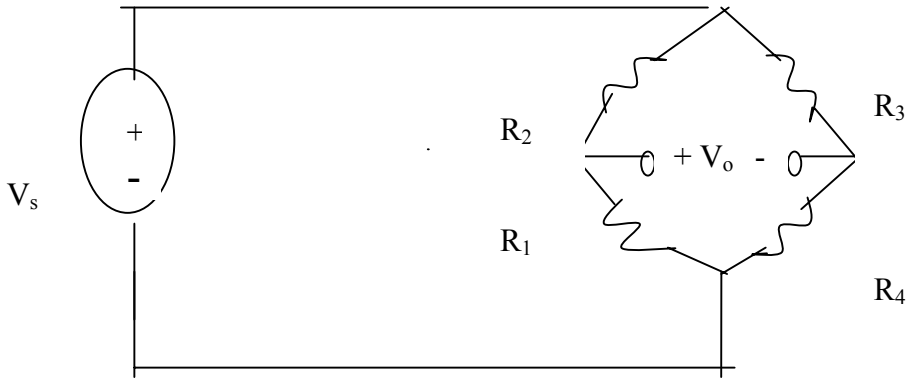

Figure 5.10 Wheatstone -bridge network

In the circuit four piezoresistors are connected to each other as shown in the figure above. A input voltage V_s is applied and an output voltage V_o is measured where output voltage is related to the input voltage by Equation 5.5

$$V_o = V_s\left[\frac{R_1 \times R_3 - R_2 \times R_4}{(R_1 + R_3)\times(R_2 + R_4)}\right] \tag{5.5}$$

The values of the piezoresistors are taken such that $R_1 = R_3$ and $R_2 = R_4$, this condition will ensure that that the offset output voltage in the unstressed state of the resistors be zero. Equation 5.5 then simplifies to Equation 5.6,

$$V_o = V_s\left[\frac{R_1^{\,2} - R^2{}_2}{(4 \times R_1 R_2)}\right] \tag{5.6}$$

The stress dependence of the resistivity of a piezoresistor is expressed in Equation 5.7

$$dR/R = \sigma_l\pi_l + \sigma_t\pi_t \quad (5.7)$$

When the piezoresistor is subjected to a longitudinal stress σ_l and transverse stress σ_t, then there is a fractional change in resistance due to the piezoresistive effect. Here, π_l= Longitudinal piezoresistive coefficient and π_t = Transversal piezoresistive coefficient. The piezoresistors are taken to be oriented along the [110] direction of a (100) silicon wafer .The values for p-type silicon piezoresistive coefficients are considered in this thesis as they have been noted to have a larger sensitivity when compared to n-type silicon piezoresistors. The values for p-type piezoresistors are tabulated in Table 5.3 [77].

	$\pi_{11}\ 10^{-11}Pa^{-1}$	$\pi_{22}\ 10^{-11}Pa^{-1}$	$\pi_{44}\ 10^{-11}Pa^{-1}$
p-type	6.6	-1.1	138.1

Table 5.4 Piezoresistive Coefficients for p- type silicon[77].

The piezoresistive coefficients of the resistors are calculated by Equations 5.8 and 5.9

$$\pi_l = \tfrac{1}{2}(\pi_{11} + \pi_{22} + \pi_{44}) \quad (5.8)$$

$$\pi_t = \tfrac{1}{2}(\pi_{11} + \pi_{22} - \pi_{44}) \quad (5.9)$$

The output voltage is obtained by differentiating Equation 5.7 with respect to R_1 and R_2 given by

$$\Delta V_o = V_s \times 2\left[\frac{dR_1}{(R_1)} + \left|\frac{dR_2}{R_2}\right|\right] \cdot (1-\eta) \cdot \frac{r}{(1+r)^2} \qquad (5.10)$$

$$\text{where, } r = \frac{R_1}{R_2} \quad \text{and} \quad \eta = \frac{1}{1+\left\{\frac{1}{\frac{dR_1}{R_1} + \frac{dR_2}{R_2}}\right\}}$$

The term η in equation 5.10 causes the output to become non-linear, therefore in order to maximise V_{out} the effect of η must be made neglibile. Maximising the magnitudes of dR1/R1 and dR2/R 2 in equation 5.7 can do this. Maximum fractional change in resistance in response to applied loads can be achieved by placing the piezoresistors in the regions of maximum stress on the membrane. The stress analysis conducted in section 5.3 (refer Figure 5.7) indicates that the maximum stress zones on a piezoresistor surface due to IOP loads are concentrated along the edge centres of every side of the membrane. The choice of locations is shown in Figure 5.11 below.

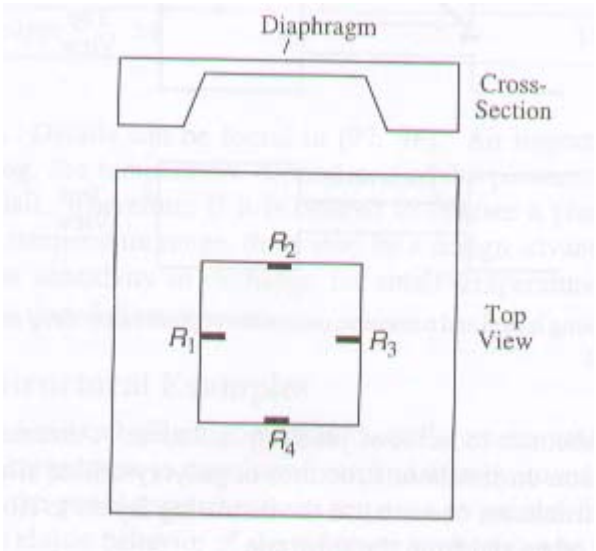

Figure 5.11 Illustration of resistor placement in a bridge network [77].

If the piezoresistors could be located at positions along where the variation in stresses along both their longitudinal and transverse axes is minimum then maximum output voltage can be obtained from the sensor.

The stress profile of the regions under maximum stress is studied to analyse the impact of the effect of longitudinal, transverse on those areas to determine any disruption that can be caused to the response of a resistor.

The variations in stress along the transverse and longitudinal directions are plotted in Figures 5.12 and 5.13 below. It can be seen from the trends plotted that the maximum longitudinal stress is concentrated along a distance measuring less than 0.1μm and the maximum transverse stress is concentrated across a distance measuring less than 1 μm.

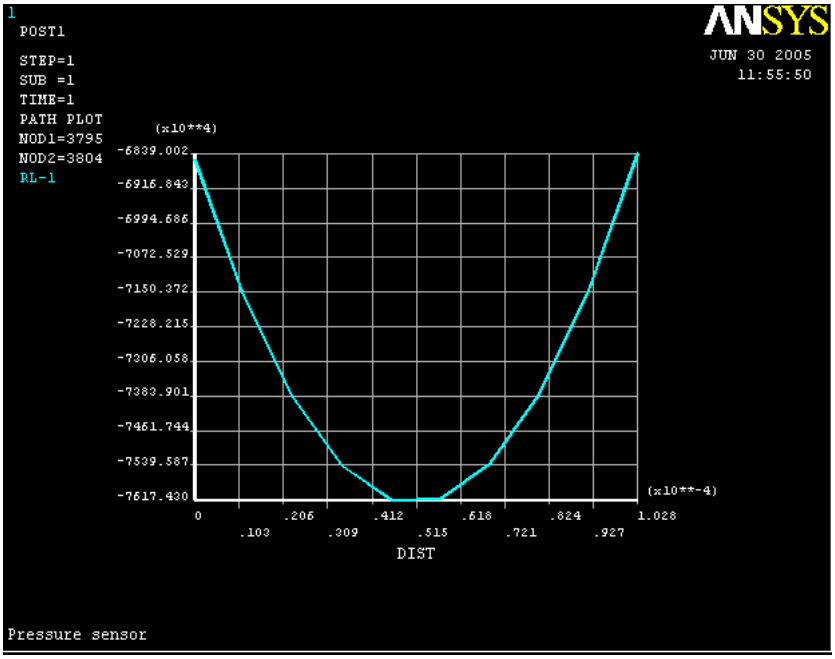

Figure 5.12 Longitudinal stress variation along x axis at max IOP

The figures show that there is sharp variation in stress values in both the areas. Although the maximum stresses are spread across very small distances it can be noted from Figure 5.7 that stresses of lower intensity extend around the edge centers.

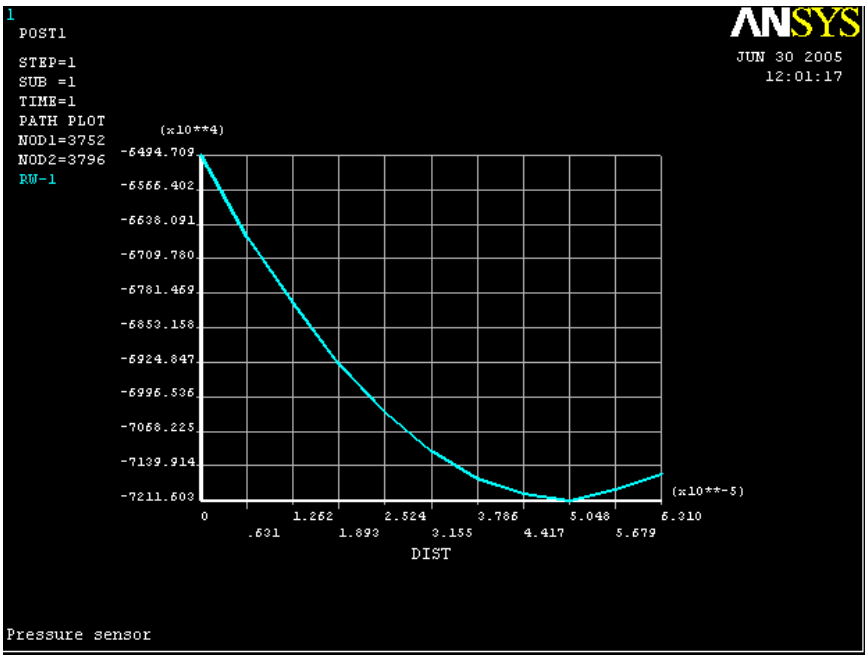

Figure 5.13 Transverse stress variation along x axis at max IOP

Thus from the results it can be conclude that if the stresses along the length and width of a piezoresistor will vary greatly when placed along regions of maximum stress on the membrane. The difference in average stresses along R_1 and across R_2 will cause the fractional change in resistance (dR_1/R_1 and dR_2/R_2) to be unequal. This non uniformity in stress will cause a reduction in output voltage.

In order to nullify the effect of difference in fractional change in resistance the average of stresses at 5 points along the expected length and width of both the resistors are calculated. The length of the resistor is assumed to be 10 μm and the width is assumed to be 5 μm. The distribution of the points across the area of the resistor is shown in Figure 5.14.

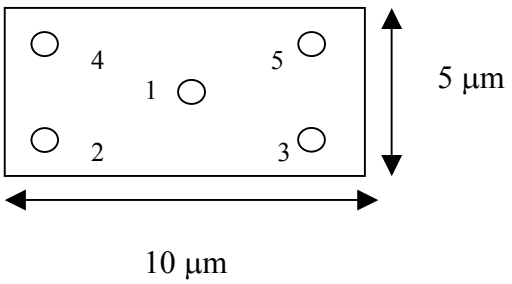

Figure 5.14 Stress averaging locations on a resistor.

The stress analysis was repeated for different IOP loads. The average fractional change in resistance $(dR/R)_{avg}$ was determined by averaging the values obtained for fractional change in resistance along the dimensions of each resistor (refer Equations 5.6, 5.7 and 5.8).

5.4.3 Discussion

The values obtained for the average fractional change in resistance $(dR/R)_{avg}$ for different uniformly applied IOP loads are presented in Table 5.4 .

IOP (mmHg)	$\mathbf{dR_1/R_{1\ avg}}$	$\mathbf{dR_2/R_{2\ avg}}$
7.5	8.5	-5.8
15	12.8	-9
22.5	16.8	-12.8
30	22.3	-15.9
37.5	25	-18.4
45	32	-35.4

Table 5.5 (dR/R) avg values for different IOP loads.

The change in resistance alters the balance of the Wheatstone bridge and produces an output voltage given by equation 5.10. The value for η is calculated using $(dR/R)_{avg}$ values. Typical values for input voltage are taken at 3V and the values of R_1 and R_2 are taken at 5 kΩ and 1.5 kΩ respectively [79]. The values for $(\Delta V_{out}/V_{in})$ are plotted for different IOP loads in Figure 5.16 below.

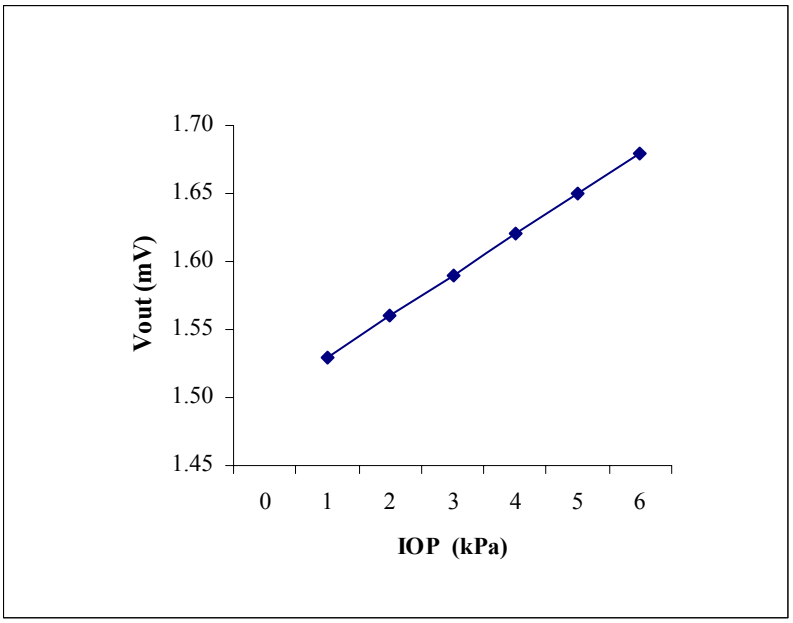

Figure 5.16 Output voltages that will be obtained for IOP loads

From Figure 5.16 it can be seen that the electrical output from the MEMS sensor will varies linearly with the change in IOP and will be capable of detecting IOP loads (15-40mmHg) where 1mmHg = 0.133 kPa. The sensitivity of the piezoresistive pressure sensor (mV/V/kPa) is calculated by dividing the change in output voltage over input voltage ($\Delta V_{out}/V_{in}$) by the applied uniform IOP and the results are plotted in Figure 5.17 below.

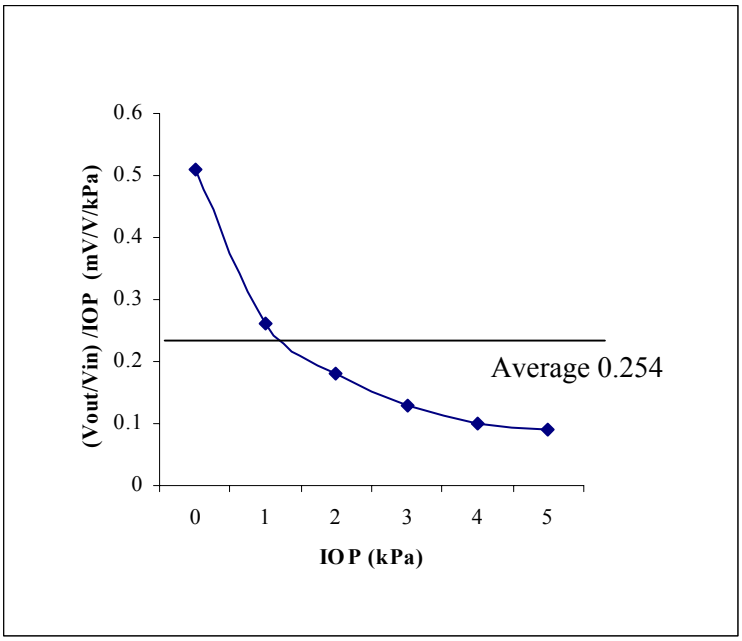

Figure 5.17 Sensitivity of the Piezoresistive Pressure Sensor.

The calculations demonstrate that voltages between 1.50 mV and 1.70 mV will be indicative of IOP changes inside the eye. The average sensitivity of the MEMS pressure sensor has been calculated to be 0.254 (mV/V/kPa) which is comparable to the output obtained for miniature pressure sensors in literature [86]. However the dimensions of the sensor developed to measure IOP are smaller and the pressure range considered much lower than of those considered in literature. The theoretically optimal MEMS sensor dimensions to monitor IOP are listed in Table 5.18.

Range	15mmHg –50.25mmHg
Membrane – width & length	400 μm,400 μm
Membrane thickness	2 μm
Maximum stress	18.4×10^4mmHg to and 61.4×10^4mmHg
Maximum Deflection	0.53 μm -1.76 μm
Resistor length and width	20 μm, 5 μm
Resistor values	5kΩ and 1.5kΩ
Out put Voltage	0- 0.56 mV
Input Voltage	3V

Table 5.6 MEMS Piezoresistive Pressure sensor data

It has been theoretically determined that the linearity of the sensor will not vary as the deflections remain small and linear for the given pressure range. The maximum stresses lie between 18.4×10^4mmHg to and 61.4×10^4mmHg. The maximum tensile stress that silicon can be subjected has been documented in literature [5] to be between 22.5×10^6 mmHg - 60×10^6mmHg. As the maximum stresses at P max are only in the 10^4mmHg a range, the sensor will not fracture under the applied pressure loads. Due consideration should be given for any reduction in magnitude of the output of the sensor which may arise due to packaging and fabrication constraints.

It was determined from previous investigations that the resolution of the sensor should be 1 mmHg. As it has been demonstrated that the sensor will be able to produce a detectable output for IOP loads less than 1 mmHg, it will be well suited to detect a decrease the C_f levels of the eye. The performance of the sensor will be tested and the results will be presented in a following chapter.

5.5 Conclusion

The size, deflection and output voltages of the MEMS piezoresistive pressure sensor that can monitor IOP have been calculated after investigation. The location of piezoresistors on the surface of the sensor that will provide the extraction of maximum sensitivity of the sensor were determined by analysing the patterns of the surface stresses of the sensor in response to IOP as a load.

It was found that reducing the width and thickness of the diaphragm affected the pressure-based deflection obtained from the miniature sensor. The maximum range of stresses obtained under the operating pressure fell under the breaking limit of Silicon, thereby eliminating the issue of fracture. A Wheatstone bridge combination could be used to detect an output produced from embedding piezoresistors on the locations determined on the surface of the membrane. The output voltages that could be obtained from the miniature sensor would be between 0-0.56mV.

Thus it will be possible to conclude that a miniature sensor of adequate size, sensitivity and resolution can be used to measure IOP in the eye. The feasibility of developing a MEMS piezoresistive pressure sensor that is capable of sensing IOP loads in the eye to monitor glaucoma has been presented in this chapter.

6 Testing of MEMS system

6.1 Introduction

In this chapter, a description of the working of the MEMS glaucoma monitoring system will be provided with the layout of the device and sensor, along with the powering and signal conditioning units. The system response will be tested under conditions of extreme outflow facility, rigidity and for cases where energy consumption can be minimised. The electrical outputs that will be obtained from the pressure sensor in response to different glaucoma conditions will be presented at the end of the chapter.

6.2 Schematic of the MEMS glaucoma monitoring system

Based on the investigations undertaken in this thesis, a schematic representation of the MEMS implantable glaucoma monitoring system is provided in Figure 6.1 below. The requirements of a device and pressure sensor were determined from Chapter 4 and a structural representation was presented (refer Figure 4.12). The development of a suitable miniature pressure sensor was undertaken in Chapter 5. The schematic representation of the entire system includes the powering, transmission and signal conditioning units along with the device and sensor.

6.2.1 Description of layout

The functional requirements of the monitoring system have been established through the investigations undertaken and presented in the earlier chapters of this thesis. It was determined that in order to measure an increase in the level of glaucoma in an eye, the system should be able to detect a decrease in C_f values. From the work done in chapter 4, it can be seen that this could be realised by using an expandable micro device which can increase in size from 2×2×1.5 mm to 4×4×4 mm, to temporarily raise IOP by 100% and employing a pressure sensor to measure the fall of IOP over several minutes.

Figure 6.1 provides an illustration of the main components of the MEMS monitoring system. The device and the pressure sensor combined with the power source would form the major components of the implantable unit.

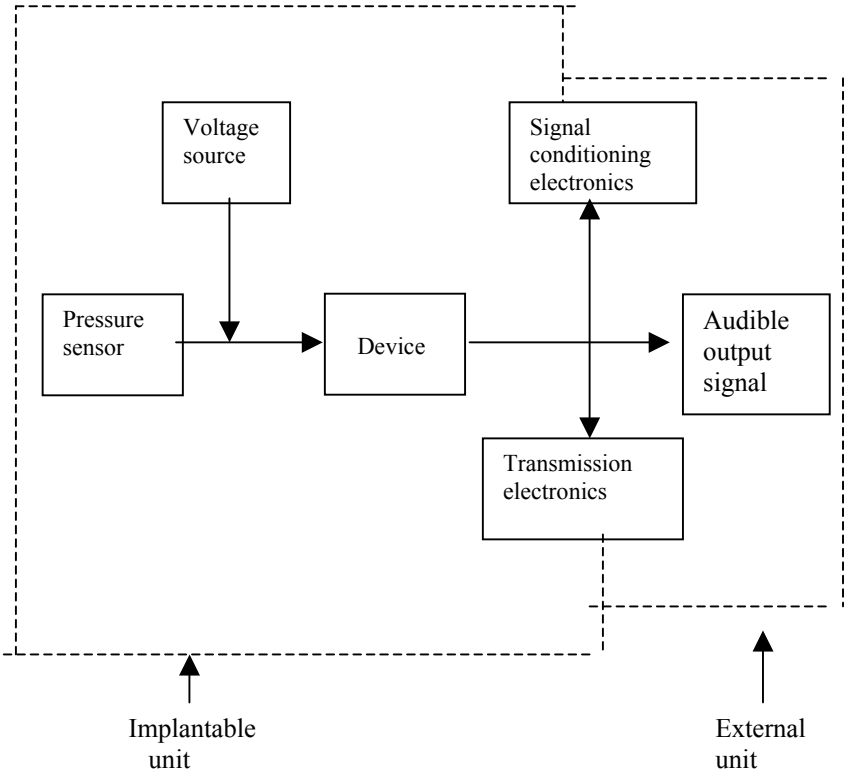

Figure 6.1 Components of the MEMS glaucoma monitoring system

The device would have to be able to expand and reduce eye volume by approximately 26% and hold the change over a period of several minutes for the measurement to be completed. The pressure sensor should begin to measure IOP soon after the change in eye volume. The signal conditioning unit should process the rate of fall of pressure and relay an alarm signal to an external readout or visual display unit through the transmission chip. The transmission and signal processing electronics could be included on the implantable chip with the device and sensor or left as external elements as indicated in the figure to suit any size constraints.

6.2.2 Signal conditioning

An illustration of an existing signal conditioning unit designed for use with a MEMS pressure sensor is shown in Figure 6.2 [56]. Such a signal conditioning unit would help to process, decode and digitise the required pressure information. Micro-processor based pressure to frequency converter modules are incorporated along with amplifiers and filters into the sensor chips for converting the pressure information obtained from the sensor into a transmissible form [87]. The converter modules are equipped with CMOS electronics based signal conditioning units as shown in the illustration.

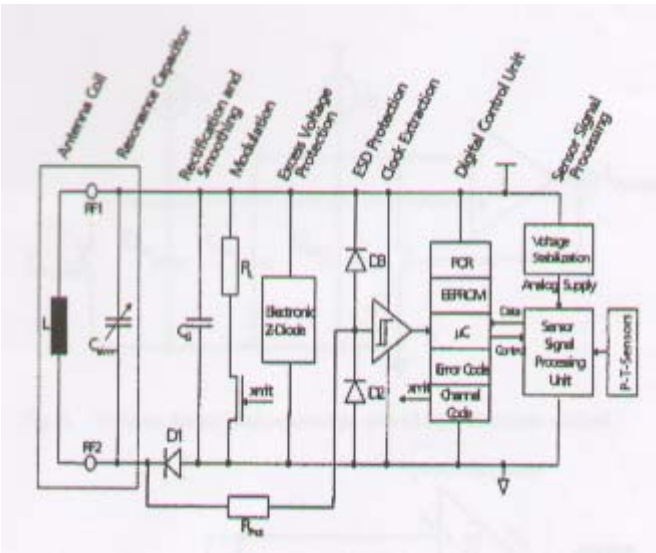

Figure 6.2 Existing signal conditioning circuit for a MEMS pressure sensor [56].

Similar systems with timers and clocks could be developed for integration along with the sensor to determine the rate of fall of IOP and trigger alarms when required.

Amplifier circuits are used along with piezoresistive pressure sensors to amplify the voltage output that is usually in the range of 10^{-3} to 10^{-6} Volts [88].

6.2.3 Powering and data transmission

Powering could be undertaken using commercially available micro batteries or using RF based wireless transmission units [62], [73]. Battery-less powering is preferred for use in biomedical implants as it would remove the need to recharge and reduce the risk of contamination presented by the presence of a battery but will need a separate transmission system to accompany it [58].

However, if a wireless powering unit were to be used it could be coupled with a data transmission system and implemented either as a transcutaneous or an embedded system. In RF wireless powering systems, an external primary coil driven by a DC current source is used to transfer power to an implanted receiver coil via magnetic field coupling, where the receiver coil and transmitting antenna are attached to the sensor system on the implant [61]. The pressure sensor used along with such systems is usually a capacitive pressure sensor and the configuration is illustrated in Figure 6.3 below.

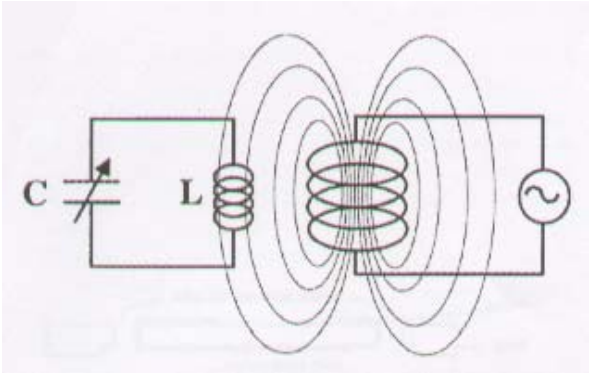

Figure 6.3 RF based inductive coupling for wireless transmission [89]

Wireless transmission of pressure data from piezoresistive pressure sensors used in implants have been recorded to transmit data up to a distance of a few metres with the use of RF inductive coupling [90]. The power supply used to power these implantable

units has been quoted in the literature to have a rating of 135 mV and power consumption of 65 μW [91]. Therefore, they pose only a minimal threat to the biological system in which they are housed. Alternatively, sufficiently rated micro-batteries could also be used to power and transmit IOP data from the implant to an external device.

6.3 Testing system response

A mathematical model is used in this section to study the response that will be obtained if a miniature device capable of expanding were implanted (refer Figure 4.12) to reduce eye volume. It was determined from investigations (refer Section 4.2), that the initial size of an implantable device should be kept less than 5 mm^3 so that it does not interfere with IOP levels at times other than the measurement. The IOP curve that will be obtained when eye volume is reduced by expanding a device instantly from 5 mm^3 to 65 mm^3 is tested using the model under the potentially worst operating conditions inside the eye.

6.3.1 Worst case conditions

For a device with initial size less than 5 mm^3 increasing in size to 65 mm^3, the rise in IOP for eyes with severely low outflow facility (C_f = 0.15mmHg/μl/min) and normal rigidity (K = 0.15) appears to be as outlined in Figure 6.4. The total test time is assumed be 10 minutes and the volume of the device is assumed to increase within one minute of starting the test. The simulations were repeated with the initial IOP set at 15 mmHg and at 25 mmHg to study the responses that would be obtained under normal and high starting points respectively. The symbol d_{on} in the Figure represents the time for which the device was turned on inside the eye during the simulation.

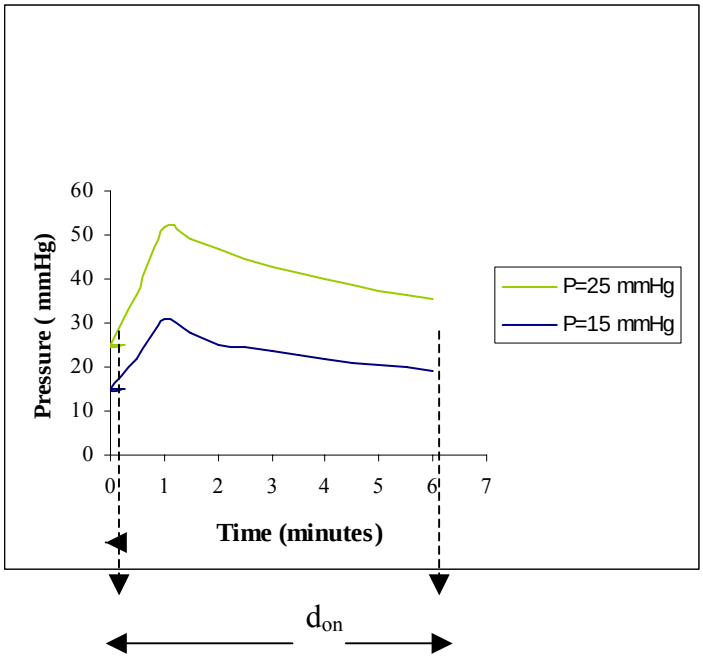

Figure 6.4 Comparing IOP measurements for severely low C_f value

It can be observed from Figure 6.4 that upon increasing the device size in eyes with very low C_f values causes the IOP to rise by nearly 100% and then falls off almost instantly, stabilizing at a few mmHg above starting level irrespective of the difference in starting IOP. The output obtained from the model when a device is used to reduce eye volume in eyes with severely low C_f is similar to that obtained for eyes with normal C_f levels (refer to Section 4.2).

The results obtained when a device with initial size less than 5 mm^3 increases in size to 65 mm^3 implanted inside an eye with abnormally high rigidity (K = 0.45) and very low outflow facility (C_f =0.15mmHg/µl/min) is recorded in Figure 6.5 below. The total test time is assumed be 10 minutes and the volume of the device is assumed to increase within one minute of starting the test. The simulations were repeated with the initial IOP set at 15 mmHg and at 25 mmHg to study the responses that would be obtained under normal and high starting points respectively.

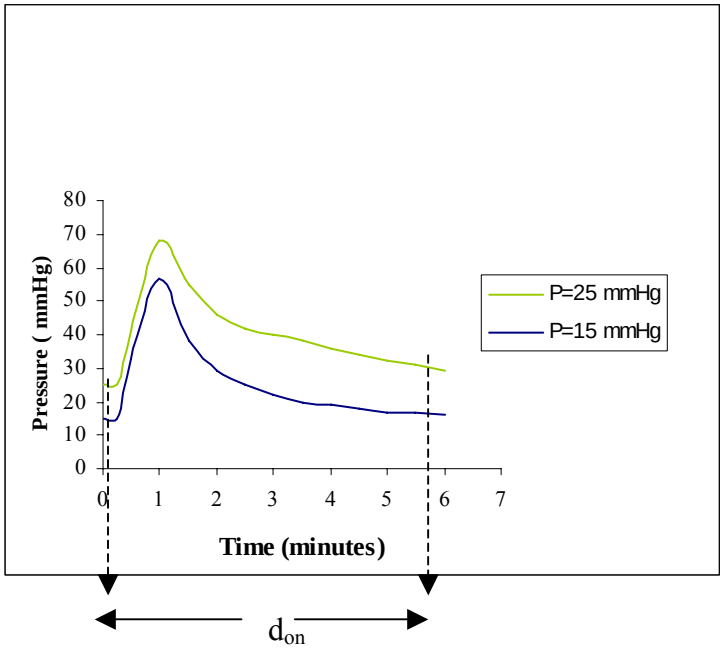

Figure 6.5 Comparing IOP measurements for very high K value

It can be seen in the Figure above that the expansion of a device inside an eye with very high rigidity causes IOP to rise by approximately 200% for both cases of IOP starting levels.

6.3.2 Discussion

The responses obtained from the simulation demonstrate that the rise in IOP obtained when the test will be conducted in eyes with very low outflow facility and very high rigidities is much larger than the typical values (refer to Section 4.2). Most glaucoma patients could suffer from either low outflow facility or high rigidity. This could lead to a high rise in IOP during measurements which could expose patients to the risk of permanent blindness [63].

6.4 Effect of reducing device size

6.4.1 Smaller device size

An attempt was made to limit the extent to which IOP would rise, to reduce the risk to patients with high rigidity and low outflow facility during measurements. It was found in the previous section that a smaller device size could lead to a lower rise in IOP. Therefore, increasing device size from 5mm^3 to 45 mm^3 based on a mathematical model, was tested for an eye with very low outflow facility (C_f = 0.15mmHg/µl/min) and very high rigidity (K = 0.45). Initial IOP was set at 15 mmHg in the model. The results from the simulation are shown in Figure 6.6 below.

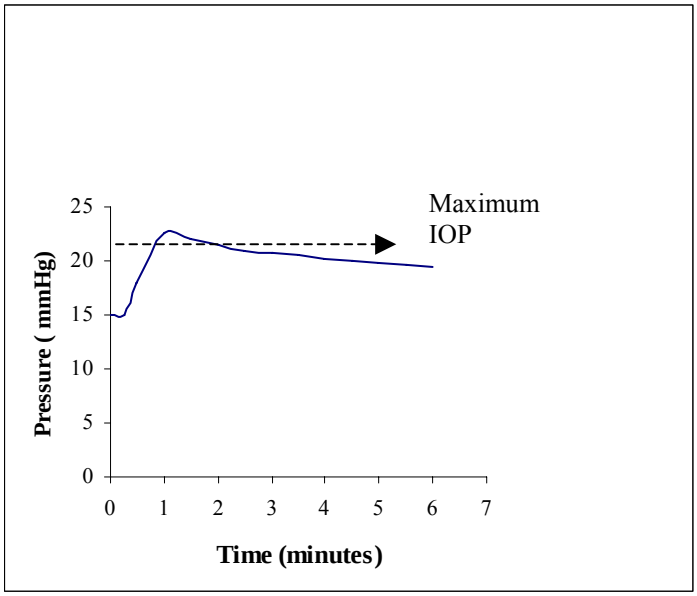

Figure 6.6 IOP rise with smaller device size (45mm^3)

It can be seen from the figure above that when size of the device size was increased to 45mm^3 when compared to 65 mm^3, IOP rose by approximately 50% as opposed to 100% in previous cases (refer to Section 6.3)

6.4.1.1 Detecting difference in C_f values

The impact of having a smaller rise in IOP on detecting a difference in C_f levels was studied by running the above test in eyes with different C_f values, where:

C_f1 = 0.15 mmHg/µl/min (poor),
C_f2 = 0.22 mmHg/µl/min (mildly low) and
C_f3 = 0.33 mmHg/µl/min (normal)

represent the typical levels of outflow facility in a human eye. The simulation was repeated for normal (K = 0.15) and very high (K= 0.45) values. The results from the simulation are presented in Figures 6.7 and 6.8. The symbol Press diff in the figures denotes the times during which there is a difference in the rate of fall of IOP.

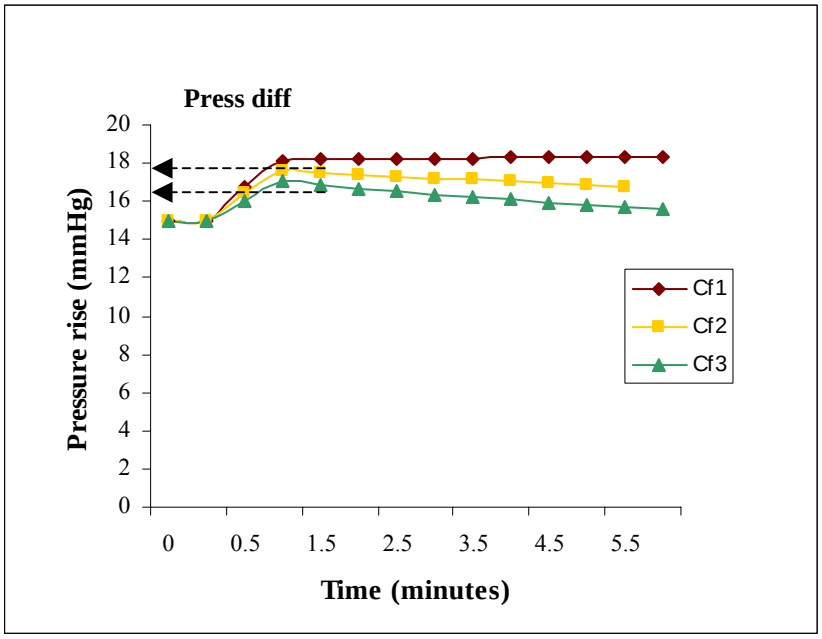

Figure 6.7 Sensitivity to C_f with smaller device size with k= 0.15

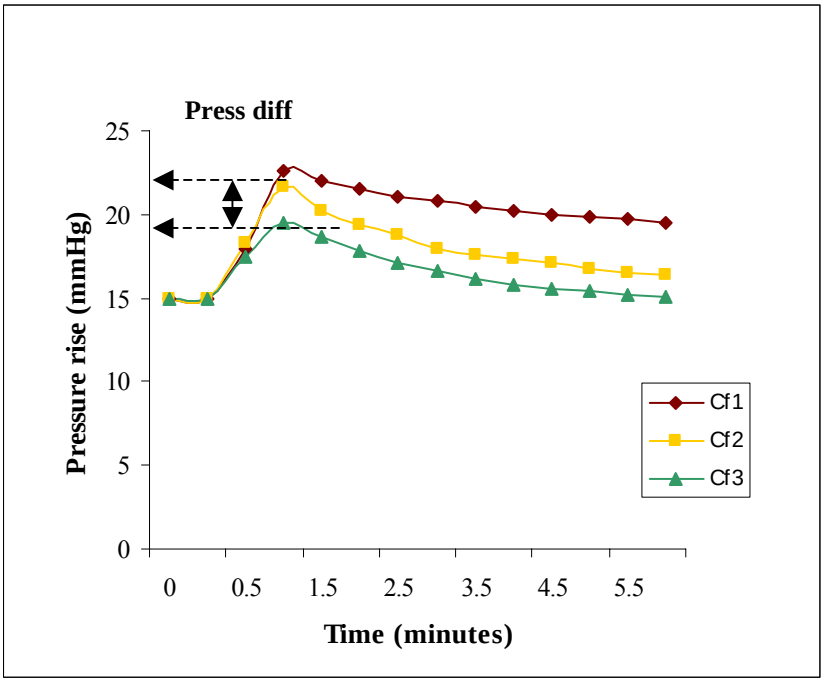

Figure 6.8 Sensitivity to C_f with smaller device size with k= 0.45

6.4.1.2 Discussion

It can be seen from Figure 6.7 that when a smaller device size is used in an eye with normal rigidity (K = 0.15), there is hardly any difference in the rate of fall of IOP. However, it is observed from Figure 6.8 that if a smaller device size were used for measurement in an eye with high rigidity (K = 0.45) there is a difference of approximately 2 mmHg in the rate of fall of IOP during the first minute of the test.

6.4.2 Optimal Device size

As using a device size of 45 mm^3does not show a difference in the rate of fall of IOP in a normal eye (refer Figure 6.7) this size may not be suitable for measurement purposes. Therefore, a slightly larger device size (55 mm^3) is used in the next simulation. The

value of rigidity is set as normal in the simulation (K = 0.15) and initial IOP is set at 15 mmHg. The simulation was repeated for different C_f values and the results are presented in Figure 6.9.

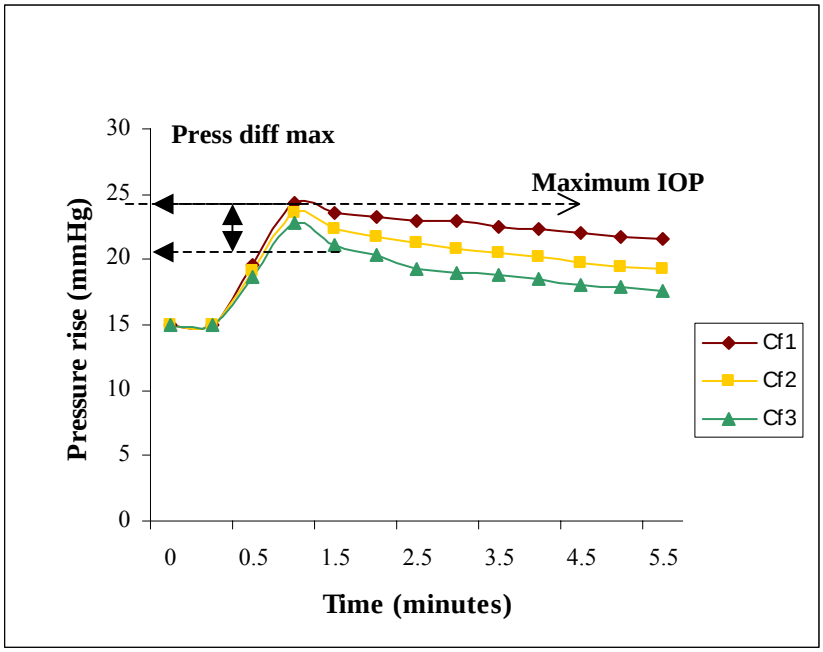

Figure 6.9 Sensitivity to C_f with smaller device size (55mm^3) device size with K= 0.15

It can be seen from the figure above that the rise in IOP is approximately 67% when a device of size 55mm^3 is used in the simulation. It can also be observed that there is detectable difference in the rate of fall of IOP in the first minute of the test. The fall per minute of IOP is 1mmHg per minute for poor C_f levels (C_f 1 = 0. 15 mmHg/µl/min) and is 3mmHg per minute for normal C_f levels (C_f 3 = 0.30 mmHg/µl/min). These values are similar to the ones obtained when 65mm^3 was used to create the volume change (refer Section 4.2.2).

As previously demonstrated in Section 6.4.1, repeating the test in an eye with normal rigidity will show a greater difference in the rate of fall of IOP.

6.4.3 Discussion

The measurement has been simulated for the worst case situations inside the eye. The results demonstrated that using a device of 55mm^3 approximately, would result in a safe

rise in IOP in eyes with low outflow facility and very high rigidity. Using a device of a smaller size would not allow detection of a difference in the rate of fall of IOP and using a device of a larger size could be potentially harmful to patients.

It was calculated that using a 55mm^{3}device size for the measurement will consume 3.82e^{-5}J of energy (refer Section 4.2.1). The percentage of eye volume that is taken up by the device during measurement was calculated to be approximately 22%. However, the energy consumed and the space taken up inside the eye is less than that calculated for 65mm^3 (7.49 e^{-5}J and 26% respectively) in Chapter 4.

6.5 System output with optimal device size

It was determined in Chapter 4 that the sensor would be required to have a resolution of 1mmHg to detect a difference in C_f levels (refer Section 4.2.2). It was subsequently determined in Chapter 5 that a MEMS piezoresistive pressure sensor could produce a voltage output corresponding to every mmHg fall in IOP (refer to Section 5.4, Figure 5.16).

The electrical output that will be obtained from the miniature piezoresistive pressure sensor, when it is included with the device, is calculated using the mathematical model. The legends represent typical levels of outflow facility in the eye:

C_f1 = 0.15 mmHg/µl/min (poor),
C_f2 = 0.22 mmHg/µl/min (mildly low) and
C_f3 = 0.33 mmHg/µl/min (normal)

Starting IOP is set at 15mmHg and rigidity is set at (K= 0.15) in the simulation to represent the typical values for a normal eye. The sensitivity of the sensor to differences in C_f levels is recorded from the model output and illustrated in Figure 6.10 below.

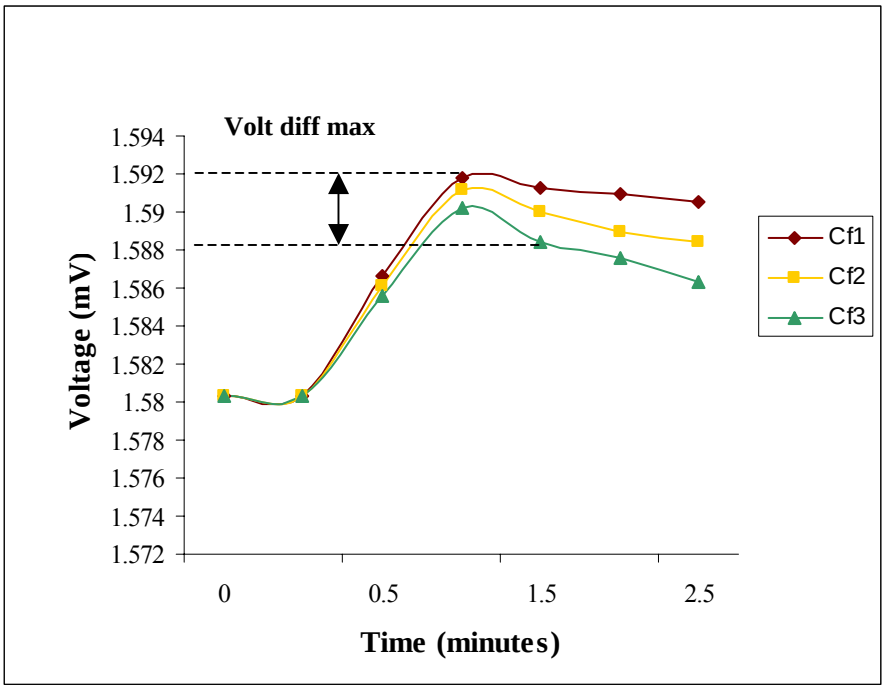

Figure 6.10 Voltage vs time for different C_f levels.

It can be seen from Figure 6.10 that there is fall in voltage output with time that corresponds to the difference in C_f levels. The symbol Volt diff max in the above figure indicates the time during which there will be maximum change in voltage in the sensor's output.

It was determined previously that for eyes with very poor outflow facility level (C_f1 = 0.15mmHg/µl/min) the rate of fall of IOP is less than 1 mmHg/min. This corresponds to less than 1mV fall in voltage over time from the sensor for an eye with C_f1 in Figure 6.10. Similarly, there is nearly a 2mV fall and 3 mV fall in voltage over two minutes for C_f2 and C_f3 respectively.

From the range of the output voltages obtained, it can be inferred that approximately 5µV/mmHg will have to be measured to detect a difference in the C_f levels of a person. An amplifier could be integrated with the pressure senor unit to amplify the voltage

output for processing and transmission purposes [60]. As the response time of piezoresistive pressure sensors has been reported to be in the 1 millisecond range, it will be capable of responding to IOP monitoring [77].

If a timer were to be integrated with a signal conditioning unit and sensor that could time the fall in voltage over a minute after the volume change, then an alarm could be triggered to indicate the level of severity of glaucoma in the eye (refer Figure 6.1).

Thus, from the results of the simulation, it can be inferred that a detectable electrical output can be obtained from the MEMS monitoring system and be used be to indicate the presence of glaucoma in an individual's eye.

6.6 Conclusion

An overview of the implantable glaucoma monitoring system along with the powering and signal conditioning units has been presented in this chapter. It has been demonstrated that a device of initial size less than 5 mm^3 or (1×1×5mm) that can expand to approximately 55 mm^3 or (3×3×6mm) could be used to monitor C_f levels from within the eye. The results demonstrated that such a device would raise IOP by 67% above starting level during measurement.

It would be possible to detect a difference in the rate of fall of IOP based on severity of glaucoma using a MEMS piezoresistive pressure sensor. The device has been successfully tested using the mathematical model for the worst case conditions in the eye.

It was observed that the MEMS pressure sensor could be integrated with the device to detect the fall of less than 1mmHg/minute of IOP by a corresponding output voltage in millivolts.

Using a smaller size device allows for a safe C_f based IOP measurement in eyes with severe glaucoma. The results have shown that a smaller device size allows for a

discernible detection of the difference in the rate of fall of IOP even though IOP is not raised by 100%. The results have shown that the output from the model would be similar to the pressure data that would be obtained when a tonometer is used to measure a difference in the C_f levels of a patient. It was observed that the sensitivity and resolution of the sensor were not affected by reduction in size of the device. This implies that the overall device size and powering requirements of the monitoring system could be minimised from the values determined initially in Chapter 4.

7 Review of Technology for Fabrication and Packaging

7.1 Introduction

The likely methods that can be used for the fabrication and packaging of the expandable device and pressure sensor of the glaucoma monitoring system will be discussed in this chapter. Bio-compatibility and implanting issues will also be discussed.

7.2 Device fabrication

7.2.1 IPMC Theory

It was previously determined previously in chapter 6 that a miniature device that will be capable of expanding from an initial minimum size (1×1×5 mm) to a size large enough (3×3×6 mm) to raise IOP temporarily in the eye will play the most important role in internal glaucoma monitoring. The device will reduce effective internal eye volume by expanding and maintain the change in size for the duration of the measurement which indicates that the device will have to have movable parts (refer Figure 4.12).

Ionic polymer metal composite (IPMC) materials have been found to be suitable for the development of miniature, low powered, biocompatible implants [92]. Due to their fluid based activation characteristics they could be considered as potential candidate materials for the development of the implantable glaucoma monitoring device.

IPMC materials are a class of electrically active polymers that have the capacity to provide an actuation displacement of >3% with 10-30 MPa tip force under a driving voltage of 0.1-7 Volts [93]. This class of electrically active polymers requires a fluid medium to operate and has been cited to have the potential to be used in biomedical and glaucoma implants due to their superior electro-mechanical properties of low actuation voltage, low density and repeatability when compared to other micro actuators [94].

Studies so far have considered sample sizes 25×3×0.19 mm [94]. Almost all of the characterisations have been based on cantilever type arrangements of the sample with the governing Equation 7.1 given below [95].

$$\delta = PL^3 / 3EI \qquad (7.1)$$

Where

δ = Deflection obtained

P = Applied point load

L = Length of the strip

E = Young's modulus of the material

I = Moment of Inertia of the material

The material properties of these polymers are dictated by the presence of Li^+, Na^+ , K^+ and tetra-butyl ammonium (TBA^+) ions. When placed in a fluid medium, on the application of a supply voltage the positive ions in the polymer film move towards the negative electrode causing a change in the volume of the polymer film as illustrated in Figure 7.1.

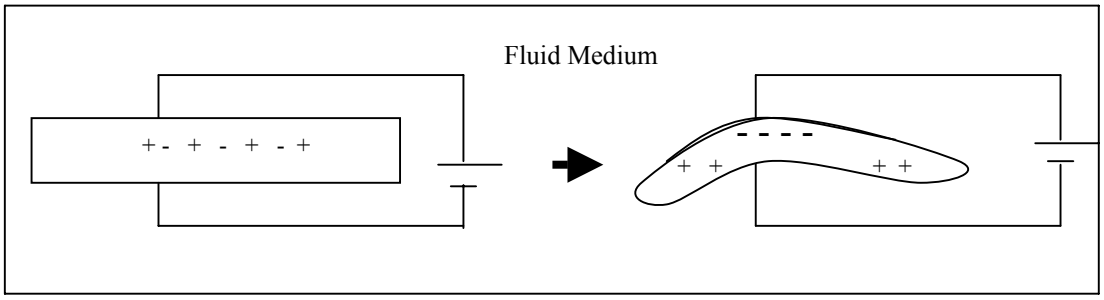

Figure 7.1 Deformation of an IPMC strip under applied electric field.

The electro-mechanical response of these polymers is followed by relaxation owing to their ionic content. Analytical and electric macro models have been developed to characterise their response to applied electric potentials under a range of operating conditions [96].

It has been reported that IPMC strips can be developed with contractile, flexing, undulating and serpentine configurations [93]. Therefore the feasibility of reduction in size and related displacement characteristics of this class of materials needs to be investigated if intended for use in glaucoma monitoring systems.

The fabrication of polymer based microstructures with movable parts has been undertaken using LIGA [97]. LIGA is a micro fabrication process that combines x- ray lithography, electro-forming and moulding techniques for the fabrication of micro-structures with structural heights reaching several micrometers with varied shapes.

The advent of this technology has enabled the development of micro-pumps with a flexible polyimide micro-membrane for applications in micro-fluidics. Several types of movable, stepped, slanted micro structures for use in micro-pumps, valves, nozzles and other micro-fluidic applications have been extruded and built using the LIGA technique [98].

Thus this particular fabrication process could be utilised for the fabrication of a glaucoma implant with an expandable volume while still being attached to the sensor and other digital electronics.

7.2.2 Fabrication

A LIGA micro-mould is combined with injection or reaction moulding techniques to create a microstructure specific to the application required. LIGA allows for electro-less plating and deposition of metal inserts into the polymers, whether they are of the shape hardening variety or are rubber/silicone like elastic polymers. The process sequence for preparing IPMC strips has been provided in [99]. A solution of the commercially available polymer film is prepared without any discontinuities or air-bubbles. The solution is poured into a casting frame much like the procedure used to create rubber like elastic micro-structures using a high aspect ratio electro-deposited metal mould. The liquid solution is dried and thermally treated to increase the mechanical stiffness of the film. The film is boiled in hydrogen peroxide (H_2O_2) and water at very high temperatures of 75-100° C for an hour and prepared by boiling in de-ionized water. The process is illustrated in Figure 7.2 below.

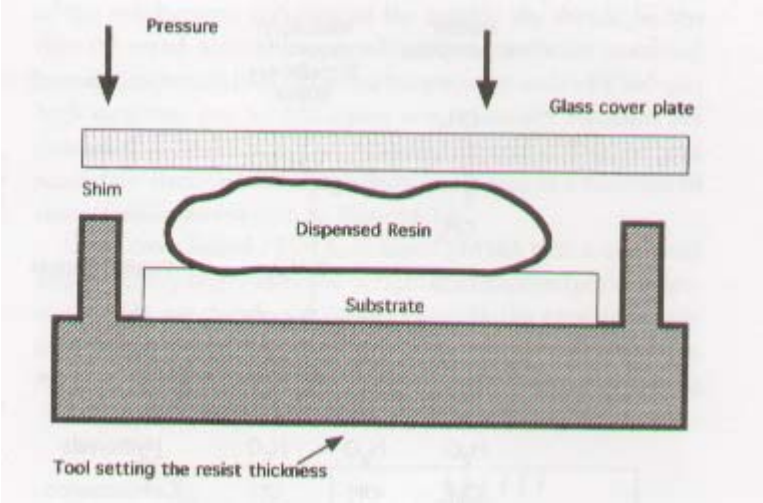

Figure 7.2 LIGA fabrication process for polymer based microstructures [99]

The film is plated with electrodes on both sides by an electro-less plating method. The electro-less plating method used in LIGA allows for shaping and manipulation of metals with the polymers during and after deposition.

Thus combining IPMC fabrication methods with a LIGA type set-up could lead to the production of the shape and size of the device required by the glaucoma implant. Finite element method (FEM) tools like ANSYS can be used to study the electromechanical response of this type of material as demonstrated in [100]

7.3 Pressure Sensor Fabrication

Bulk micromachining and surface micromachining are two of the methods widely used to fabricate micro pressure sensors [60]. During the process several steps are undertaken to fabricate the mechanical structures on a silicon wafer and deposit the electronic components that need to be combined with the sensor. Combining electronics with the sensor imposes limitations on the type of fabrication method being used.

Polysilicon surface micromachining combined with a CMOS process has been recommended by various texts [75] for the fabrication of micromechanical piezoresistive pressure sensors. This combination enables the use of higher operating temperatures when compared to bulk-micromachining. An illustration is provided in Figure 7.3.

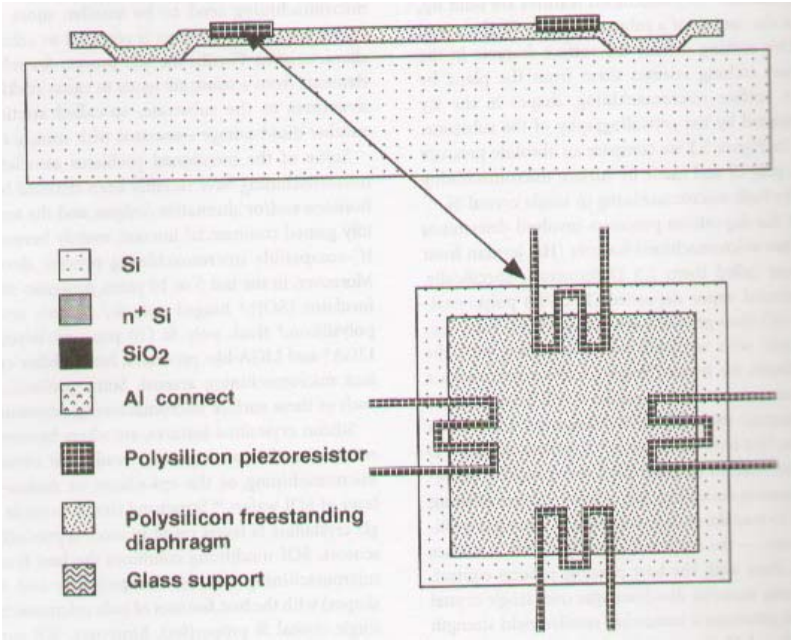

Figure 7.3 Surface micro machined pressure sensor [99]

Using specially fabricated wafers such as SIMOX for fabrication reduces the number of process steps and allows for easy packaging of piezoresistive pressure sensors [99].

7.4 Packaging and Biocompatibility

7.4.1 Packaging and Biocompatibility

Micro-machine packaging protects the device from any harmful interactions with the surrounding environment. However it is also responsible for allowing the device to create changes to environment and for the sensor to measure the impact of physical parameters. In the case of the glaucoma monitoring device, the packaging should allow for change in size of the device as well as protect the device and sensor electronics from the fluid in the eye.

Packaging could introduce extra strain and cause the final sensor performance to vary [101]. The issues of biocompatibility and waterproofing are of major concern in biomedical and ocular implants. The material used for biocompatible encapsulation of the implants has been reported to be a medical-grade polymer, Nu Sil MED-2000 and MED-1511 [58]. Silane, silicone-elastomer materials are also used to package biomedical implants, due to their non-corrosive and inert nature. The elastomer packaging also serves to isolate the sensor and its associated structures from the surrounding environment by providing adequate water-proofing and offers protection against any electrical or chemical leakage from the implant. These commercially available polymers are used to seal the implants externally. A thickness of up to 20μm has been reported to be used for coating micro sensor structures, without compromising device output [58].

The bio-compatible encapsulation intended for the glaucoma implant will have to take into consideration the presence of movable parts within the implant. The encapsulation will have to accommodate structural activity owing to the increase in volume of the device and still be able to provide sound waterproofing without interfering with the device output and sensitivity in a major way.

ANSYS simulations could be used to study the effects of packaging [101]. Hermetic sealing of bio-medical implants prevents contamination by body fluids. Studies have shown that hermetic sealing does not affect the performance of the implant [102].

7.4.2 Implanting

Great progress has been achieved with the technology that allows for successful implantation of medical implants. Minimally invasive surgical methods and microsurgery are often used to implant bio-medical ocular implants. Laser technology is used for surgical cutting and precise positioning of miniature implants in the eye [103]. The devices might require adjustment to suit individual patient requirements as the level of IOP has been documented to differ in individuals. Whether the device and sensor might need adjustment to suit an individual eye's physical characteristics and IOP range could be a cause of concern with reference to large scale production of the device [104]. This requires further attention.

One of the several problems that is often encountered after implanting the device is bleb-formation [54]. Additional tissue similar to scar tissue sometimes grows on ocular implants which could pose a serious issue by compromising device performance. Research needs to be undertaken to be able to overcome the effects of bleb-formation and scar tissue growth on the ocular implants to preserve maximum device output over a prolonged period of time.

7.5 Conclusion

A feasible method of developing and fabricating a MEMS device that will allow for a change in size within low activation energy limits to suit a biological system is presented. MEMS pressure sensor fabrication and packaging methods are discussed and the issues surrounding bio-compatibility and successful implanting of the device are included. Thus the feasibility of fabricating and packaging the device and pressure sensor of the MEMS glaucoma monitoring system have been presented in his chapter.

8 Conclusions and Further Work

The aim of this thesis was to investigate the development of a MEMS glaucoma monitoring system. The literature review demonstrated the importance of a C_f based glaucoma monitoring system and it's potential to forewarn the patient of a rise in IOP due to flow blockage in glaucoma. A mathematical model of the eye was used to study the effects of eye volume, rigidity and outflow facility on internal IOP measuremnet and the results were compared with tonometer measurements. The model was then used to conduct simulations to arrive at the requirements of an implantable glaucoma monitoring system.

Based on the investigations performed, it was determined that an expandable device could be used to raise IOP temporarily in the eye and an indication of C_f levels could then be obtained by determining a difference in the rate of fall of IOP using a MEMS pressure sensor.

The device size, measurement method and energy requirements were determined from investigations. The energy requirements have indicated that a major portion of the powering can be undertaken using either miniature batteries or other available technology and allow for daily tests to be conducted over a number of years. A suitable pressure sensor was developed to record the fall of IOP after introducing the volume change. The response of the system was tested for worst case conditions and the expected electrical output of the sensor was determined.

Possible methods of powering the implant, providing data transmission and signal conditioning were also presented. An overview of the fabrication and packaging details of the device and sensor were discussed in the thesis along with implanting and biocompatibility issues.

The theoretical basis for undertaking the development of a MEMS glaucoma monitoring system was established based on a survey of the existing literature and further investigation undertaken in this thesis. These investigations clearly demonstrate that it is possible to measure IOP continuously within the eye to indicate the onset or increase in the severity of glaucoma.

The requirements of a MEMS device have been determined and a potential class of actuators has been nominated for undertaking its development. However, the mechanism, stiffness, shape of the device, the electrical activation required to support change in device size and the energy requirements of the entire measurement need further investigation. A standardised method of extracting C_f data from the measured rate of fall of IOP would need to be established.

A prototype of the device would need to be built and tested in an environment similar to the eye to compare the output that will be obtained from it to the theoretical results. The packaging and fabrication of the prototype are required to be addressed and implemented.

References

1. The Merck Manuals online medical library,2006, Eye Disorder, Glaucoma, viewed 1 February 2003, <http://www.merck.com/mmhe/sec20/ch233/ch233a.html>

2. Glaucoma Research Foundation,2006, Glaucoma facts and stats, viewed 15 December 2005,< http://www.glaucoma.org/learn/glaucoma_facts.html>

3. R. Wilson, T. M. R., W.M. Grant "Race as a risk factor for progressive glaucoma." Ann Opthalmol **17**(10): 653-659. (1985).

4. J.Evans and R.Wormald "Is the incidence of registrable age-related macular degeneration increasing?" Br J Opthalmol **80**: 9-14.(1996).

5. S.N.Martin, J.Sutherland, et al. "Molecular characterization of congenital glaucoma in a consanguineous Canadian community: a step towards preventing glaucoma related blindness." J Med Genet **37**(6): 422-427.(2000).

6. R.Vogel and R.P.Crick "Association between intraocular pressure and loss of visual field in chronic simple glaucoma." Br J Opthalmol **74**(1): 3-6.(1990).

7. Investigators., T. A. "The Advanced Glaucoma Intervention Study (AGIS): The relationship between control of intraocular pressure and visual field deterioration." Am J Ophthalmol **13**(4): 429-440.(2000).

8. G.Georgopoulos, D.Andreanos, et al. "Risk factors in ocular hypertension." Eur J Ophthalmol **7**(4): 357-363.(1997).

9. Group, C. N.-T. G. S. "Comparison of glaucomatous progression between untreated patients with normal-tension glaucoma and patients with therapeutically reduced intraocular pressures." Am J Ophthalmol **126**: 487-497.(1998).

10. R.Sampaolesi, N. Calixto, et al. "Diurnal variation of intraocular pressure in healthy, suspected and glaucomatous eyes." Mod Probl Ophthalmol **6**(1-23).(1968).

11. S.Asrani, R. Zeimer, et al. "Large diurnal fluctuations in intraocular pressure are an independent risk factor in patients with glaucoma." J Glaucoma **9**(2): 134-142.(2000).

12. W.M.Grant and J. F. B. Jr "Why do some people go blind from glaucoma?" Ophthalmology **89**(9): 991-998.(1982).

13. Adler and F.Heed, Eds. (1895). Adler's Physiology of the Eye- Clinical Application, 9 th edn, St.Louis:Mosby-Year Book, c1992.

14. H.Davson (1984). The intraocular pressure. The eye, vol 1-a,Vegetative physiology and biochemistry,ed 3. H.Davson. London, Academic Press.

15. Glaucoma Foundation Australia,2006,What is Glaucoma ,viewed 10 July 2004 < http://www.glaucoma.org.au/whatis.htm>

16. L.I.Larsson, E.S.Rettig, et al. "Aqueous flow in open-angle glaucoma." Arch Ophthalmol **113**(283-286).(1995).

17. L.I.Larsson, E. S. Rettig, et al. "Aqueous humor dynamics in low-tension glaucoma." Am J Ophthalmol **116**: 590-593.(1993).

18. R. Rand Alingham, Karim F. Damji, Sharon Freedman (2004),Shield's Textbook of Glaucoma, 5th edn, Lipincott Williams &Wilkins Philadelphia USA, c 2005

19. I.Gonzalez, P.E.Pablo, et al. "Assessment of diurnal tensional curve in early glaucoma damage. ;20(1-3):113-115." Int Ophthalmol **20**((1-3)): 113-115.(1996-97).

20. J.S.Freidenwald "Contribution to the theory and practice of tonometry." Am J Opthalmol **20**: 985-1024.(1937).

21. M.A.Kass "Timolol treatment prevents or delays glaucomatous visual field loss in individuals with ocular hypertension: a five-year, randomized, double-masked, clinical trial." Trans Am Ophthalmol Soc **87**: 598-618.(1989).

22. M.Katavisto "The diurnal variations of ocular tension in glaucoma." Acta Ophthalmol (Copenh) **78**(suppl 1).(1964).

23. W.M. Grant (1955),Clinical aspects of the outflow of the aqueous humour. In Glaucoma, a symposium, Oxon, (126-146).

24. W.M.Grant "Tonographic method for measuring the facility and rate of aqueous flow in human eyes." Arch Ophthalmol **44**: 204-214.(1950).

25. H.Zachary, A.K.Gupta, et al. "Ultrasensitive Biomems Sensors Based on Microcantilevers Patterned with Environmentally Responsive Hydrogels." Bio- medical Microdevices, Kluwer Academic Publishers. **5**(3): 177-184.(2003).

26. M.Yang, X.Zhang, et al. "Modeling and Optimal Design of High Sensitivity Piezoresistive Microcantilevers Within Flow channels for Biosensing Applications." Bio-medical Microdevices, Kluwer Academic Publishers. **5**(4):323-332.(2003).

27. P.Rai-Choudury (2000). MEMS and MOEMS technology and applications, Bellingham and Walsh :SPIE Optical Engineering Press.

28. N.Najafi and A.Ludomirsky "Initial Animal studies of a Wireless,Batteryless,MEMS Implant for Cardiovascular Applications." Bio-medical Microdevices, Kluwer Academic Publishers. **6**(1): 61-65.(2004).

29. D.Sparks, R.Smith, et al.(Oct 2003). A Portable MEMS Coriolis Mass Flow Sensor. IEEE Sensors Conference, Toronto, Canada No.8.4,p.90

30. N.Maluf (2000). An introduction to microelectromechanical systems engineering. Boston ; London, Artech House.

31. The American Heritage Stedman's Medical Dictionary,2nd ed. Houghton Mifflin Company.(2004)

32. P.A.Chandler and W. M. Grant (1965). Lectures on Glaucoma. Philadelphia, Lea and Febgier.

33. A.Azuara-Blanco, V.P. Costa, et al. (2002.). Handbook of glaucoma. London, Martin Dunitz.

34. C.D.Phelps and G.K.Phelps "Measurement of intracoular pressure:A study of its reproducibility." Graefes Arch Clin Exp Opthalmol **198**(39).(1976).

35. R.Collins and T. J. V. d. Werf (1980). Mathematical Models for the Dynamics of the Human Eye. New York, Springer-Verlag.

36. J.Draeger (1966). Tonometry: Physical fundamentals,development of methods and clinical applications. Basel, Karger.

37. J.S.Kaiden, T.J.Zimmerman, et al. "Hand held tonometers." Arch Opthalmol **89**(110).(1973).

38. R.F.Brubaker "Computer assisted instruction of current concepts in Aqueous humor dynamics." Am J Opthalmol **82**(59).(1976).

39. Medtronic Opthalmics,Products <http://www.medtronicophthalmics.com/products-tonopen-overview.html> <http://www.takagi-j.com/seihin_e/katarogu_e/at1_e.html>,viewed 25 October 2005.

40. A.E.Kolker and J.Heatherington (1976). Becker-Schaeffer's Diagnosis and therapy of the glaucomas, 4th ed. St.Louis, C.V.Mosby Co.

41. H.E.Kauffman "Pressure Measurement ;Which tonometer?" Invest Opthamol **11**(80).(1972).

42. J.S.Friedenwald "Tonometer Calibration: An attempt to remove Discrepancies found in the 1954 calibration scale for Schiotz tonometers." Trans Am.Acad.Opthalmol Otolaryngol **61**: 108-123.(1957).

43. R.A.Moses "The Goldmann Applanation tonometer." Am J Opthalmol **46**: 865.(1958).

44. T.Krupin (1942). The Glaucomas, St. Louis : Mosby.ed (1989)

45. R.A.Moses, E.Marg, et al. "Evaluation of the basic validity and clinical usefulness of the Mackay-Marg tonometer." Invest Opthalmol **1**: 78-85.(1962).

46. C.C.Collins "Miniature Pressure Trans sensor for implanting in the eye." IEEE ,Transactions on Biomedical Engineering **BME -14**: 74-83.(1967).

47. F.Bertoncini, R.Gianetti, et al. A Magnetic sensors Feasibility Investiagtion for continuous Intraocular Pressure Monitoring. Sensors for Industry conference, Houston,Texas, USA.(2002).

48. S.K.Alam, D.W.Richards, et al. "Detection of Intraocular PressureChange in a Human Eye model usingSonoelastic Doppler Ultrasound." Ultrasonics Symposium **1057**: 1057-1060.(1992).

49. L.Leonardi A Soft Contact Lens with a MEMS strain gauge embedded for intraocular pressure monitoring. 12th International Conference on Solid State Sensors,Actuators and Microsystems, Boston, June 8-12(2003).

50. U.Schankenberg, P.Walter, et al. Basic Investigations on a system for measuring Intraocular Pressure. 12th European Conference on Solid State Transducers, Den hague ,The Nertherlands.(September 12-15,1999).

51. C.denBesten and P.Bergveld A New Tonometer based on the Application of Micro- Mechanical Sensors. Microelectromechanical systems, MEMS '93, Proceedings 'An Investigation of Micro Structures, Sensors, Actuators, Machines and Systems,IEEE.(7-10 February,1993).

52. A.L.Coleman, R.Hill, et al. "Initial clinical experience with the Ahmed Glaucoma Valve implant." Am J Ophthalmol **120**(1): 23-31.(July 1995).

53. H.Miyamoto, Y.Ogura, et al. "Biodegradable scleral implant for intravitreal controlled release of fluconazole." Curr Eye Res **16**(9): 930-935.(September 1997).

54. GLEAMS "Glaucoma Valve implants." Glaucoma Research Foundation Newsletter **18**(3).(January 2001).

55. C.R.Neagu A Medical Microactuator based on an Electrochemical Principle. MESA Research Institute, ,s. Enschede, The Netherland, University of Twente**:** 162.(1998).

56. K.Stangel, S.Kolsnberg, et al. "A Programmable Intraocular CMOS Pressure Sensor System Implant." IEEE Journal of Solid-State Circuits **36**(7): 1094-1099.(2001).

57. R.Chomiak "An Approach to designing an Implantable Intraocular Pressure sensor." IEEE: 154-155.(2003).

58. C.Heirold, B.Clasbrummel, et al. Implantable low power integrated pressure sensor system for minimal invasive telemetric patient monitoring. The Eleventh Annual International Workshop on Micro ElectroMechanical Systems, 1998. 25-29 January, 1998 Page(s):568-573.

59. L.Leonardi, P.Leuenberger, et al. A Soft Contact Lens with a MEMS strain gauge embedded for intraocular pressure monitoring. 12th International Conference on Solid State Sensors,Actuators and Microsystems, Boston.(2003).

60. M.H.Bao (2000). Handbook of Sensors and Actuators. Netherlands, Elsevier.

61. M.Suster, D.J.Young, et al. Micro-Power Wireless Transmitter for MEMS Sensing and Communication Applications. The Fifteenth IEEE International

Conference on Micro Electro Mechanical Systems,(20-24 January 2002) Pages 641-644.

62. B.Ziaie and K.Najafi "An implantable Microsystem for Tonometric Blood Pressure Measurement." Bio-medical Microdevices, Kluwer Academic Publishers. **3**(4): 285-292.(2001).

63. P.A.Chandler and W.M.Grant (1896). Chandler and Grant's Glaucoma. Philadelphia, Lea and Febiger.9th ed.(1986).

64. C.C.Mow "Theoretical Model of the cornea for use in Studies of Tonometry." Bulletin of Mathematical Biophysics **30**: 437-453.(1968).

65. W.Lotmar "Theoretical Eye model with Aspherics." Journal of the Optical Society of America **61**(11): 1522-1529.(November 1971).

66. C.R.Canning and M.J.Greaney "Fluid Flow in the Anterior Chamber of a Human Eye." IMA Journal of Mathematics applied in Medicinie and Biology **19**: 31- 60.(2002).

67. J.J.Heys, V.H.Barocas, et al. "Modeling Passive Mechanical Interaction Between Aqueous Humor and Iris." Transactions of the ASME **123**: 540-547.(2001).

68. K.P.Scherer, H.Eggert, et al. Biomechanical Simulations for refractive corneal surgery. Karlsrhue ,Germany, Institute For Applied Computer Science.(1996)

69. J.O.Hjortdal "Regional Elastic Performance of the Human Cornea." J.Biomechanics **29**(7): 931-942.(1996).

70. J.W.Mclaren, N.Ziai, et al. A Simple Three-compartment Model of Anterior Segment Kinetics. Rochester,M.N,U.S.A, Department of Opthalmology, Mayo Clinic,**:** 355-366.(1993)

71. A.B.Friedland "A Hydrodynamic Model of Aqueous Flow in the Posterior Chamber of the Eye." Bulletin of Mathematical Biology **40**: 223-235.(1978).

72. F.Vacherand New Emerging Technologies for Contactless Microsystems. Smart objects and Ambient Intelligence (sOc- EUSAI), Grenoble, France.(October 12- 14,2005).

73. C.P.Townsend, S.W.Arms, et al. Remotely powered,multichannel,microprocessor based telemetry systems for a smart implantable total knee implant. 294 N Winooski Ave, Burlington,VT 05041-USA, Microstrain Inc.

74. C.S.Smith "Piezoresistance effect in germanium and silicon." Phys,Rev., **94**: 42-49.(1954).

75. S.D.Senturia (2001). Microsystem Design. Massachusetts, Kluwer Academic Publishers.

76. B.Gordon and M.Andrew, Improving The MEMS Pressure Sensor, Motorola Semiconductor products,Sensor products Division**:** Sensors online webpage. (July2000).

77. Datasheet- Mouser Electronics (2005 May-July), 1261 DATASHEET Piezoresistive Pressure Sensor.

78. Datasheet-Motorola Semiconductor Technical data (2002),MPXM2053 series. Freescale Semicontor .Inc

79. Microsystems, S. I. SM5108 Ultra Low Cost OEM Pressure Die. Milipitas, CA, USA, Silicon Microstructures.Inc.(2005)

80. Microsystems, S. I. SM5430 LowCost Packaged Pressure Sensors Milipitas, C.A, USA, Silicon Microstructures .Inc.(2005)

81. K.Anderson, A.El-Sheikh, et al. "Application of structural Analysis to the mechanical behaviour of the cornea." J.R.Soc.Lond Interface **1**: 1-13.(2004).

82. L.Lin, H.Chu, et al. "A Simulation Program for the Sensitivity and Linearity of Piezoresistive Presure Sensors." Journal of Microelectromechanical Systems **8**(4): 514-523.(1999).

83. S.Timoshenko, Theory of Elasticity. (3rd Edition) New York, Mc-graw Hill. (1969, c1970).

84. S.Timoshenko and S.Woinowsky-Kreiger, Theory of Plates and Shells,) 2nd Edition, NewYork, McGraw-Hill Book Company(1959).

85. J.Y.Pan, P. P. Lin, et al. Verification of FEM analysis of load-deflection methods for measuring mechanical properties of thin films. Solid-State Sensor and Actuator Workshop, 1990. 4th Technical Digest., IEEE.(4-7 June 1990).

86. R.Sudarshan Modelling and Analysis of a Silicon Piezoresistive Pressure Sensor.High Temperature Materials Laboratory, School of Mechanical Engineering, Purdue University,West Lafayette.

87. H.Kim and K.Chun 1997, Integrated MEMS for Pressure Transponder. International Conference on Solid-State Sensors and Actuators, Chicago, June 16-19, 1997 pp. 1011-1014.

88. W.Menz and T.Fukuda (1998). Micro mechanical systems : principles and technology. Amsterdam ; New York, Elsevier.

89. Z.A.Strong, A.W.Wang, et al. "Hydrogel-Actuated Capacitive Transducer for Wireless Biosensors." Bio-medical Microdevices, Kluwer Academic Publishers. **4**(2): 97-103.(2002).

90. M.K.Jain and C.A.Grimes "A Wireless Magnetoelastic Micro-Sensor Array for Simultaneous Measurement of Temperature and Pressure." IEEE Transactions on Magnetics **37**(4): 2022-2024.(2001).

91. T.Eggers, C.Marschner, et al. Advanced Hybrid Integrated Low-power Telemetric Pressure Monitoing System For Bio-medical Applicatons. Bremen, Germany, Institute for Micro-sensors,-actuators and -systems (IMSAS), University of Bremen.(2000)

92. K.J.Kim and M.Shahinpoor "Ionic polymer- metal composites -2 . Manufacturing techniques." Smart Materials and Structures **12**: 65-79.(2003).

93. K.J.Kim and M.Shahinpoor "Ionic polymer-metal composites: 4. Industrial and Medical Applications." Smart Materials and Structures **14**: 197-214.(2005).

94. X.Bao, Y.Bar-Cohen, et al. Measurements and Macro Models of Ionomeric Polymer-Metal composites (IPMC). proceedingd of the SPIE Smart Struc tures and Materials Symposium,EAPD Conference., San-Diego, CA, SPIE.(March 18-21,2002).

95. S.Sherrit and Y.Bar-Cohen "Methods and Testing Charchterisation, Electroactive Polymer (EAP) Actuators as Artificial Muscles- Reality , Potential and Challenges." SPIE Press **PM98**: 405-453.(2001).

96. K.Bhattacharya, J.Li, et al. "Electro-mechanical models for optimal design and effective behaviour, Electroactive Polymer (EAP) Actuators as Artificial Muscles- Reality,Potentials and Challenges." SPIE Press **PM98**: 309-330.(2001).

97. J.Mohr, P.Bley, et al. "Microactuators fabricated by the LIGA process." J.Micromech.Microeng **2**: 234-241.(1992).

98. J.Mohr, C.Burbaum, et al. Movable microstructures manufactured by the LIGA Process as basic elements for microsystems. Microsystems Technologies 90. H.Reichl. Berlin**:** 529--537.(1990)

99. M.Madou (1997). Fundamentals of Microfabrication. New York, CRC Press LLC.

100. J.Michopoulos Computational Modelling of Multi-field Ionic Continuum Systems. M.Bubak. Berlin, Special projects group, Code 6303, Naval Research Laboratory, U.S.A.(2004)

101. T.Shing Analysis of Anodic Bonding and Packaging Efects in Micro Sensors. Taiwan, Materia Research Lab, Industrial Technology Research Institute.

102. N.K.S.Lee, S.R.Goentillike, et al. "A Flexible encapsulated MEMS pressure sensor system for Biomechanical applications." Microsystem Technologies **7**: 55- 62.(2001).

103. L.L.Fry "Postoperative intraocular pressure rises: a comparison of Healon, Amvisc and Viscoat." J cataract Refract Surg **15**: 415-420.(1989).

104. T.Tanaka, H.Inoue, et al. "Relationship between postoperative intraocular pressure elevation and residual sodium hyaluronate following phacoemulsification and aspiration." J cataract Refract Surg: 284-288.(1997).

105. www.calcoastophthalmic.com,http://images.google.co.in/images?hl=en&q=tonopen%20image&btnG=Google+Search&ie=UTF-8&oe=UTF-8&sa=N&tab=wi>,viewed 8th December 2006.

APPENDIX

A pressure conversion table from mmHg to kPa is provided here in the appendix for the convenience of the reader as the unit of IOP has been taken as kPa in the simulations and calculations in chapter 5.

Pressure Conversion table		
IOP		**IOP**
mmHg		**kPa**
1		0.1333224
5		0.666612
10		1.3332239
15		1.9998359
20		2.6664478
25		3.3330598
30		3.9996717
35		4.6662837
40		5.3328956
45		5.9995076
50		6.6661195

Table A1 Pressure Conversion Table

Paper Published as part of the Proceedings of the SPIE International Symposium for Micro and Nano Materials, held at the University of Technology in Sydney, from 11-15, December 2004.

Development of a M E M S device to monitor Glaucoma

Smitha Shankar, J.P. Chaffey
School of Electrical and Computer Engineering
RMIT University, GPO box 2476V
Melbourne, Victoria 3001, Australia.

ABSTRACT

Glaucoma is one of the leading causes of blindness affecting millions of people worldwide. Regular monitoring of intra ocular pressure (IOP) in the eyes is an important component in the treatment of this affliction. Current manual measurements do not give room for continuous indication of the progression of the disease. Microelectromechanical System (MEMS) technology lends itself to the development of devices capable of in-situ monitoring of the phenomenon that occur at the micro and nano scales, inside the human body. The paper reports on the complex flow and pressure relationships in the eye and the current methods of monitoring Glaucoma. The comparison highlights the requirements of an implantable miniature device that can indicate the changes leading to an increase of IOP inside the eye. An analysis of the pressures in the anterior chamber of the eye was undertaken to estimate the out put voltages that could be obtained from a micro structure implanted in the eye.

Key words- Microelectromechanical systems (MEMS), Glaucoma, Intra ocular pressure, anterior chamber, human eye, aqueous humor, pressure sensor, Finite element method (FEM) analyses.

1. INTRODUCTION

Glaucoma is one of the leading causes of blindness in the world. It is estimated that 6.7 million people, are blind from glaucoma and about 70 million are suffering from the disease worldwide[1]. The disease occurs when the fluid (aqueous humor) flowing continuously in the anterior chamber of the eye gets blocked, due to various pathological, reasons[2]. Once the flow gets blocked, intra ocular pressure (IOP) begins to rise steadily [2]. Figure 1, below illustrates the point of entry of the fluid into the anterior chamber, from its site of production. The fluid enters through the pupil, circulates through the anterior chamber, nourishing all the intra ocular contents . It then exits at the angles where the cornea meets the iris via numerous exit channels, filters through a porous tissue called the trabecular meshwork and finally drains back into the venous system.

Smart Structures, Devices, and Systems II, edited by Said F. Al-Sarawi,
Proceedings of SPIE Vol. 5649 (SPIE, Bellingham, WA, 2005)
0277-786X/05/$15 · doi: 10.1117/12.582263

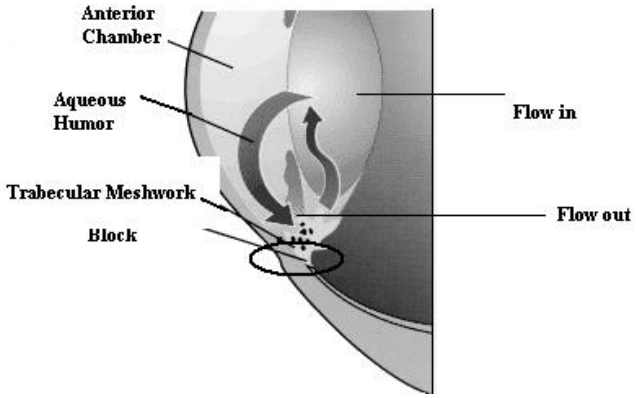

Fig1. [3] Illustration of the flows in the Eye

1.1Flows in the Eye

There exists a delicate, but complex equilibrium between the fluid flow and pressures associated with eye[4]. The flow rates into and out of the eye are balanced and maintained at 2.5-3 μl/min. IOP in the eye is measured at 15 mmHg (1999Pa) normally[3]. When the flows into or out of the eye are obstructed, then the equilibrium is disturbed and the pressures inside the eye begin to rise steadily, up to 40mmHg (3999 Pa). IOP, the pressure head in the anterior chamber of the eye[4], is the tissue pressure of the intra ocular contents also responsible for maintaining the shape of the eyeball. A rise in IOP levels causes damage to the optic nerve resulting in blindness. Thus a shift in the complex flow pressure equilibrium thus in high IOP. All the parameters relevant to glaucoma and high IOP are linked to one another as shown in Fig 2.

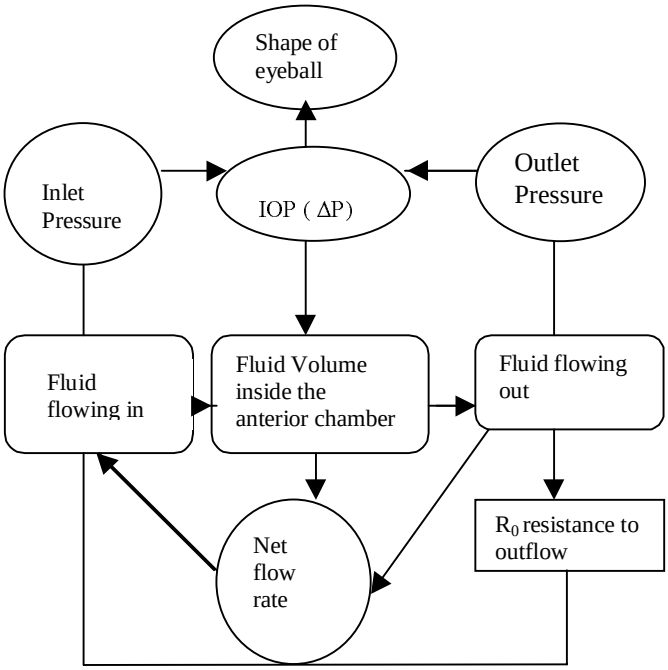

Fig2. Inter-dependence of key factors in the Eye

1.2 Key parameters in Glaucoma

The key parameters, for indication of glaucoma conditions are:

F_{in} = Flow into the eye (micro litres/min)

F_{out} = Flow out of the eye (micro litres/min)

ΔP (IOP) = Intra ocular Pressure (mm/Hg) (pressure head in the anterior chamber)

P inlet = Pressure at inlet (mm/Hg)

P outlet = Pressure at outlet (mm/Hg)

$R_0 = 1/c$ = Resistance to outflow/Outflow Facility (micro litre/ min/mmHg)

These key parameters, are related to IOP as shown in fig3.

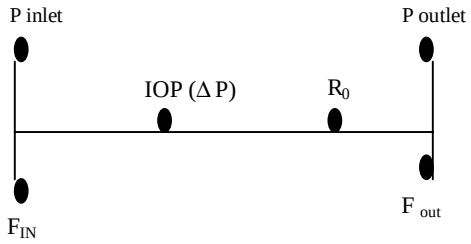

Fig3. IOP and the key parameters for glaucoma indication.

According to Adler's text[4] glaucoma is signified by an increase in the parameter, $R_{o,}$ the resistance to outflow, measured in µl /min/mmHg. An increase in R_0 is accompanied by a decrease in the outflow (F_{out}) of fluid. A decrease in outflow triggers a simultaneous increase in both IOP, (ΔP), and fluid production in order to maintain the net flow rate between 2.5-3 µl/min. The phenomenon of glaucoma is illustrated by referring to the graphs in fig4 adapted from[4].

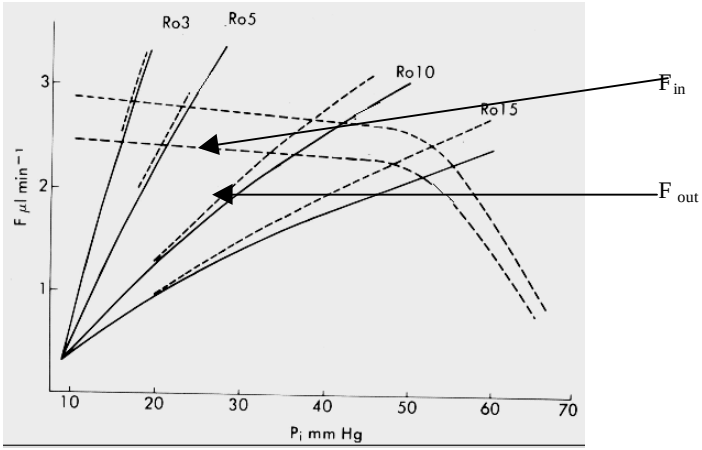

Fig4 [4] Effect of the key parameters in Glaucoma on each other

From experiments and studies performed on enucleated human eyes reported in literature[5,6,7], it is seen that during the normal operation of the eye, the fluid inflow rate is estimated to be around, 2.5µl/min. The dashed curves falling to the right in fig 4, represent fluid inflow rates. The resistance to outflow is measured to be 0.16µl/min/mmHg (R_o = 3 in fig 4). The solid lines in the figure, rising from the origin represent the resistance to outflow (R_o) range. When Glaucoma sets in the resistance to outflow (R_0 =5, 6, 7 etc. in fig4), and the inflow rate increase (3µl/min in fig4). The outflow rates are represented by the dashed lines rising from the origin in the figure. They fluctuate with change in resistance to outflow. These set of curves represent the complex equilibrium in the eye. A steady rise in IOP, accompanies these phenomenon. Currently, glaucoma is monitored; by measuring, IOP alone , from time to time (normally intervals of 3-6 months). Treatment is directed at the reduction of pressures in order to bring down the risk of optic nerve damage and blindness. Since the frequency of monitoring pressure is low, a person with glaucoma has no indication of the likely advancement of the disease, due to changes associated with the other key phenomenon relevant to the condition.

1.3 Current external methods of monitoring Glaucoma.

The current external methods of monitoring glaucoma, adopted clinically are discussed in this section. Once diagnosed with glaucoma, the pressure levels and the extent of blockage in the eyes are assessed at regular intervals[2] . Table1, below categorises the types and functions of the different external methods adopted to monitor glaucoma, universally[6,7].

METHOD	SENSOR	RANGE	TYPES	ACTION	FUNCTION
Applanation Tonometry	Pressure Sensor	0-40mm Hg	A Goldmann, Mackay Marg Tonometer B. Malakoff & Posner Tonometers C. Automated Handheld Tonometers	Force required to flatten a constant area on the CORNEA measured.	Assess extent of block and measure IOP
Indentation Tonometry	Pressure Sensor	0-50 mm Hg	Schiotz Tonometer.	Constant force applied on cornea and depth of indentation due to pressure inside measured	Assess extent of block and measure IOP

Table 1. Current external methods of monitoring Glaucoma.

The extent of the block to fluid flow and the steady state IOP level in the eye are determined by tonometry. Eyes with glaucoma, are treated by either suppressing the increased fluid production or decreasing the pressure at the outlet channels of the eye[2]. Tonometers are, external probe like instruments impressed upon the eye, to artificially raise the volume of fluid and pressure inside the eye and measure the time taken by the eye, to remove that extra fluid and pressure. The rate of fall of pressure is measured as a decay of pressure over time and linked directly to the extent of the block at the outlet channels[6,7]. When the time taken for the pressure to decay is in excess of 25%/min, then it is confirmed that glaucoma has set in[7] . Efforts are under way to eliminate these laboratory type measurements for glaucoma, which are discontinuous and sometimes painful, as they might require local anaesthesia[6] . However, it is observed that these

methods may not able to indicate the onset of glaucoma in the eye and only aid in an assessment of the condition to check further advancement.

2. OBJECTIVE

The present research is aimed at developing an implantable device, capable of indicating the onset of a block to the fluid flow. The device requires to be placed in the anterior chamber of the eye to monitor the conditions leading to glaucoma. In order to this, the device would have to be miniature in size so that it can operate within a fluid volume of 250-260 μl^5, and IOP ranging between (12-30 mmHg). The device will have to able to alert the patient to an imbalance in flow rates, a rise in (R_0), resistance to outflow, and a subsequent rise in IOP which are all the key parameters in glaucoma diagnosis and treatment. An indication of this kind will enable the patient to take steps towards management of the disease. Though an indication of this kind is currently unavailable to the patient, recent developments in micro electro mechanical systems (MEMS) technology has given room for the development of miniature, medical devices that can replace external measurements and provide continuous indications of internal biological activity[8]. MEMS, technology allows for the sensing, actuating, and signal processing electronics to be available on the same implantable chip. Therefore, the development of an implantable miniature device, capable of continuously monitoring glaucoma is undertaken using the advancement in this technology.

2.2 MEMS IOP sensors reported in literature

MEMS IOP sensors have been reported in literature from 1999, based on the pioneering work of Collins in 1969[9]. Table 2 below compares the type s and functions of these sensors[8,10,11,12,13]

SENSOR-MECHANISM	DATA TRANSMISSION	REFERENCE PRESSURE	RANGE	TYPE OF IMPLANT &SIZE	FUNCTION
Diaphragm movement Capacitive element	RF transmission with on chip antenna	Absolute (measured against vacuum as reference pressure).	50-150 KPa	Implantable in the Lens. 6.76mm^2	Measurement of IOP
Diaphragm movement-Capacitive element	RF transmission with on chip antenna	Absolute	50-150 KPa	Implantable in Lens-with a silicone coating 6.25mm^2	Measurement of IOP
Diaphragm movement Capacitive and Piezo resistive elements.	Not specified	Absolute	Not specified	Not specified	Measurement of IOP
Diaphragm movement-Capacitive Sensing	On Chip-Frequency transmission	Absolute	14-220 KPa	Not Specified.	Measurement of IOP
Strain Gauge based sensing	RF transmission with on chip antenna	None		Strain gauge sensors built onto a contact lens	Measurement of IOP

Table 2. Type & Function of MEMS IOP sensors reported in literature.

The sensors listed in table 2, have been designed to measure IOP, (ΔP) alone. They are not able to indicate the extent of blockage in glaucoma or indicate the onset of a block as possible in the external methods for monitoring glaucoma. The sensors[8,10,11, 12] are designed to be, lens implants. On comparing the average size of the lens implants (6-8mm) and the size of the human les (3-4mm transverse and 9mm,equatorial)[14] it is seen that the reported implants is nearly the size of the human lens and might obstruct the vision of the wearer. Thus, the reported miniature IOP sensors can monitor changes in the pressures in glaucoma successfully but are not capable of indicating an imbalance in flow rates or an increase in resistance to the outflow of fluid in the eye.

3. PRESSURE SENSOR ANALYSIS

In developing an integrated system, capable of comprehensively monitoring glaucoma, an analysis was performed on the pressures that occur in the anterior chamber of the eye. The range of pressures that would be encountered by a microstructure if it were to be place in a section of the anterior chamber, was, considered for this analysis. The range and pattern of the stresses that these pressures would create in a microstructure were calculated. A sensing technology such as the piezo resistive sensing technology was then applied to determine the sensitivities that could be obtained from these pressures. The magnitude and range of stresses, which the normal and glaucoma pressures will impart on a microstructure, are presented in this section. The theoretical calculations were supported with finite element method (FEM) software (ANSYS) to visualise the stress contours, and compute the regions of maximum stress. A microstructure having dimensions 2*2*0.001 mm was considered for the pressure analysis.

3.1 Stresses

ANSYS, a finite element method (FEM) software, was used to calculate the longitudinal and transverse stresses on the surface of a microstructure. A 10 node, 3 dimensional solid FEM model was used for the analysis, which provided very accurate results. The results were found to be consistent with the theoretical calculations in[15]. The pressures were applied as loads, along the (-z)-axis of the microstructure. The simulations showed that the stresses were maximum at the edge centres and minimum at the centre of the plate. The stress components along the x and y axes of the microstructure, between its centre (0, 0), see fig.5, and the edges of the diaphragm were then calculated for the entire range of pressures. The stresses obtained were, symmetrical on both the perpendicular, axes.

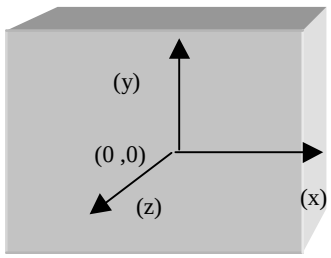

Fig.5 Microstructure with centre (0, 0), and direction of load application.

Fig 6 depicts the stress contours obtained on a microstructure when subjected to IOP loads. The stresses varied uniformly across the entire surface of the structure.

Here, σ_{xx} = Longitudinal Stress, and σ_{yy} = Transverse Stress.

A half of the surface, from the centre (0,0) to the edge, of the microstructure was considered along both, x and y directions, to charchterise the stress pattern. Several nodes were picked at equal intervals, along both

axes (x,y)on the surface of the micro structure. Table 3, lists pattern of the transverse and longitudinal stresses on the surface of a microstructure for and a normal IOP load (15 mmHg/1999 Pa/203.926 kg/m^2).

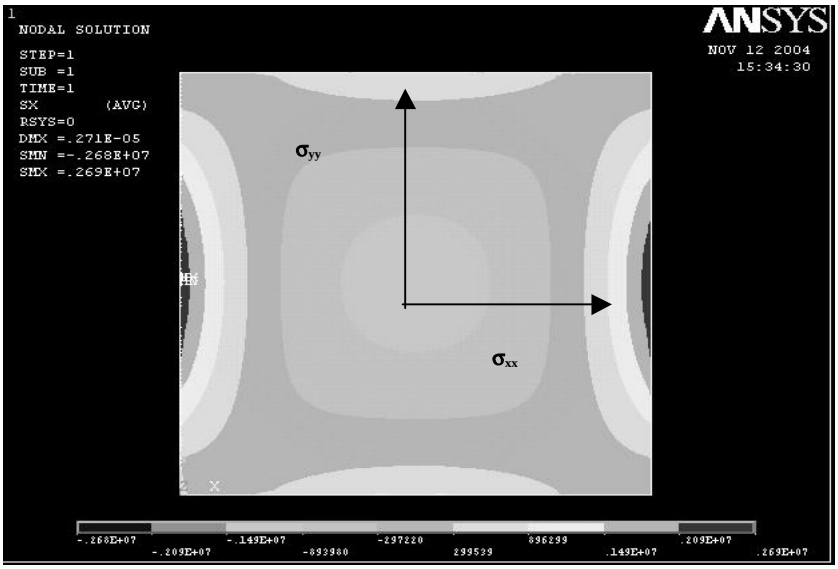

Fig 6: Stress contours obtained for IOP loads

Length (m)	σ_{xx} (kg/m^2)	σ_{yy} (kg/m^2)
.001	0.10984E7	0.11019E7
.0012	0.10007E7	0.10148E7
.0014	0.744E6	0.74163E6
.0016	0.1620E6	0.18738E6
.0018	-0.8525E6	-0.58933E6
.002	-0.22649E7	-0.25228E7

Table 3: Stress values along surface of a microstructure, for a normal IOP load

On observing the pattern of the stresses in table 3, it can be seen that the magnitude, of the stresses, increased from 0.10984E7, at the centre up to 0.22649E7 at the edges along both the axes, considered. A similar pattern was obtained when higher, IOP belonging to the Glaucoma regime were applied as loads. The values of the stresses were similar on both axes for the entire range of IOP.

Figure 7, shows a linear increase in the magnitude of the maximum longitudinal and transverse stresses, estimated to be obtained along the edge centres of a microstructure, subjected to IOP. The values were calculated from formulas 1 and 2 given in [16].

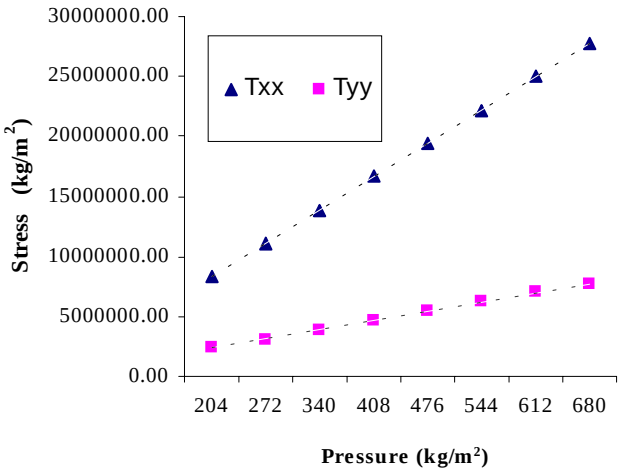

.

Fig 7: $\sigma_{xx\,max} = T_{xx}$ & $\sigma_{yy\,max} = T_{yy}$ for IOP

3.2 Piezo Resistive Sensing

The piezo resistive theory, for pressure sensing could be applied to estimate the range of output voltages that could be obtained from normal and glaucomatous, IOP. In order to do this the regions that depicted maximum stress on the surface on application of the pressure loads were calculated theoretically using the formulas 1 and 2, provided by Bao [16]. The values obtained were similar to the values obtained from ANSYS simulations in the previous section.

$$\sigma_{xx}\max = 1.02 * p * (a/h)^2 \qquad (1)$$

$$\sigma_{yy}\max = 1.02 * p * \nu * (a/h)^2 \qquad (2)$$

The regions that showed maximum stress due to the loads applied would be chosen for the location of resistors. The differential movement of the resistors, in the longitudinal and transverse, on being subjected to loads would yield in an output voltage that could be used to detect the pressures that caused them. Thus it would be possible to estimate the range of electrical outputs that could be obtained from the intra ocular pressures. The symbols used for the calculations are as follows,

$\Delta R/R)l$ = Piezo resistance perpendicular to edge of diaphragm

$(\Delta R/R)t$ = Piezo resistance parallel to the edge of diaphragm

$\sigma_{xx\ max}$ = Maximum edge centre stresses along x axis

$\sigma_{yy\ max}$ = Maximum edge centre stresses along y axis

Π_{44} is a function of the doping level of the resistors, assumed to be = 81.574 x10^{-12} kg/m^2

The piezo resistors were chosen to be perpendicular to 2 of the edges and parallel to the other 2 edges of the micro structure, in the regions which showed maximum stress. They were assumed to be in the <110 plane>. The resistors would have to be located where; the differential movement in the longitudinal and transverse directions would be equal.

$$(\Delta R/R)l = (\Delta R/R)t \tag{3}$$

The formulas used to calculate the piezo resistive coefficients for the resistors that would be positioned perpendicular to 2 of the edges was, given by formula 4 in [16]

$$(\Delta R/R)l = 0.5 * \Pi_{44} * 1.02 * p * (a/h)^2 * (1-v) \tag{4}$$

A similar formula (5) [16] was used to compute the piezo resistive coefficients for the resistors that would be positioned parallel to the other 2 edges of the microstructure.

$$(\Delta R/R)t = -0.5 * \Pi_{44} * 1.02 * p * (a/h)^2 * (1-v) \tag{5}$$

Table 4, lists the values of the piezo resistive coefficients for the resistors located near the edge centres of a microstructure, subjected to IOP.

Pressure (mmHg)	Pressure (kg/m^2)	(ΔR/R) *l*	(ΔR/R) *t*
15	203.926	0.000244337	-0.00024434
20	271.902	0.000325782	-0.00032578
25	339.877	0.000407227	-0.00040723
30	407.853	0.000488673	-0.00048867
35	475.828	0.000570118	-0.00057012
40	543.804	0.000651564	-0.00065156
45	611.779	0.000733009	-0.00073301
50	679.755	0.000814455	-0.00081445

Table 4 Piezo resistive coefficients that will be obtained for IOP loads

Thus the piezo resistive coefficients for the resistors, that would be placed parallel and perpendicular to the edges of the microstructure, when subjected to all the IOP, were calculated. The values were similar to one another but differed in magnitude owing to the difference in orientation of the resistors.

3.3 Sensitivities

The sensitivity of a Wheatstone bridge was then calculated for the range of intra ocular pressure that will be encountered inside the anterior chamber of the eye. The output voltages that would be obtained as a result of the stresses created by the pressures were calculated using formula 6 [16].

$$V_{out} = 0.51*(1-\nu)*p*(a/h)^2 * \Pi_{44} * V_s \quad (6)$$

Where,

Π_{44} is a function of the doping level of the resistors, assumed to be = 81.574x10^{-12} kg/m^2

p = Range of intra ocular pressures applied (203.926kg/m^2 - 679.7550 kg/m^2

a = 0.002m

h = 0.00001m and

ν = Poisson's ratio = 0.28 for Si.

V_s = assumed to be 5 volts.

Pressure (mmHg)	Pressure (kg/m^2)	dV/V (mV/V)
15	203.926	0.00122
20	271.902	0.00163
25	339.877	0.00204
30	407.853	0.00244
35	475.828	0.00285
40	543.804	0.00326
45	611.779	0.00367
50	679.755	0.00407

Table5. Estimated output voltages for IOP

The IOP, inside the anterior chamber of the eye, would yield output voltages between 1 mV and 4 mV if piezo resistors were embedded onto a microstructure. The output voltages could be linearly increased, by functionalising the microstructure, to be more sensitive to the intra ocular pressures.

4. CONCLUSION

The initial efforts towards the development of a miniature, implantable glaucoma indicator, have been presented. The piezo resistive pressure sensing mechanism yielded output voltages between 1mV and 4mV, to detect IOP on a microstructure to be placed in the anterior chamber of the eye. The next step in the research will focus on developing a mechanism to indicate a shift in the complex flow-pressure equilibrium in the eye to monitor glaucoma conditions. The practical issues concerning the powering and fabrication of such a device will also be analysed. The development of a device with these capabilities will indicate to a patient, any changes in the condition of glaucoma and enable him/her to take steps towards better management of the disease.

ACKNOWLEDGEMENTS

The author wishes to thank Dr. Jason Chaffey, supervisor, Prof. Ian Bates, director and the team at the AECM micro systems technology centre, RMIT University, Melbourne, Australia, for all their guidance and support.

REFERENCES

1.Nathan A. Congdon, David S. Friedman, Important causes of visual impairment in the world today, The Journal of the American Medical Association 2003; 290:2057-2060

2.Becker and Shaffer, Diagnosis and therapy of the Glaucomas, St. Louis 19

3. http://www.glaucoma.org.au/whatis.htm

4. Adler's Physiology of the eye: clinical application/edited by William M.Hart, Jr. – 9th Ed.

5. R.collins, T.J. Van der Werf, Mathematical models of the dynamics of the human eye, Springer Verlag 1980

6. Transactions of the Third Conference on Glaucoma 1958,Princeton,N.J

7. Glaucoma Symposium in Tut zing August 5-10,1966

8. Wilfred Mokwa and Uwe Schnakenberg, Micro-Transponder Systems for Medical applications, IEEE Transactions on instrumentation and Measurement, vol.50, no.6, December 2001.

9. C. Collins, Miniature Passive Pressure Tran sensor for implanting in the eye, IEEE transactions in Biomedical Engineering, Vol BME-14. pp. 74-83, 1967

10. K .Stangel, A programmable Intraocular CMOS Pressure Sensor System Implant, IEEE journal of solid state Circuits, vol. 36 , No.& ,July 2001.

11. R. Chomiak, An approach to designing an Implanatable Intraocular Pressure Sensor, IEEE 2003.

12. Michael Suster, Darrin J.Young, Wen H.Ko, Micro power wireless transmitter for MEMS sensing and Communication Applications, IEEE 2002

13. M.Leonardi,P Leunberger,D Bertrand, A soft contact lens with a MEMS strain gage embedded for Intraocular pressure monitoring, Transducers '03,12th International Conference on sensors and actuators, Boston,June 8-12,2003.

14. B.R Masters, Three Dimensional microscopic tomographic imaging of the cataract in a human lens in-vivo, Optics Express, October 1998,Vol 3,no.9.332.

15. S. Timoshenko, Theory of Plates and Shells. New York :McGraw-Hill, 1959.

16. M.H. Bao, Micromechanical transducers, Pressure sensors, gyroscopes and accelerometers, Elsevier, vol 8,2000.

17. K.P Scherer, H Eeggert, H. Guth, P. Stiller, Application of simulation techniques in human eye corneal surgery, 13th International Conference of the Society for Medical Innovation and Technology, SMIT@CARS,Berlin,June 27-30,2001.

18. Jeffrey Heys, Victor. H. Barocas, Michael.J.Taravella, Modelling Passive mechanical interaction of the aqueous humor and iris, J. Bio.Mech engg, vol 123 December 2001.